DIELECTRIC MEASUREMENTS USING AN OPEN RESONATOR

A thesis submitted to the University of London

for the Degree of Doctor of Philosophy

by

Ping Kong Yu

Department of Electronic and Electrical Engineering

University College London

ABSTRACT

This thesis describes a new method of measuring dielectric constants and loss tangents using an open resonator. The dielectric constant measurement method consists basically of perturbing the resonant frequency of an open resonator by placing a dielectric sample at the centre of the resonator normal to its axis. By measuring the resonant frequency of a symmetrical mode and of the adjacent lower-frequency asymmetrical mode, the dielectric constant can be determined.

Based on the Gaussian beam theory, a pair of transcendental equations, one for each mode, are derived by assuming first the surfaces of the dielectric sample are spherical and coincident with the phase fronts of the resonator modes. These equations can easily be solved for the refractive index n, by using a computer. When sample in sheet form is measured, the results can be corrected to account for the error so introduced. The formula giving this correction is derived by using the perturbational technique.

From these two equations, two sets of approximate formulas are also derived for the determination of the dielectric constant. An important feature of these formulas is that they are algebraic expressions, but reduction in their accuracy occurs if the sample is nearly a multiple of half wavelengths thick.

The loss tangent is determined by the measurements of Q of the perturbed and the unperturbed resonator. Based on the usual definition of Q, an algebraic expression is derived relating the loss tangent to the experimentally measurable quantities.

Measurements of dielectric constants and loss tangents of polystyrene and perspex have been made at X-band frequencies and the results are presented. It is on these results that the accuracy of ±0.25% for measuring dielectric constant is claimed. The accuracy of the loss tangent measurement is estimated to be about ±10%. The method is applicable to the measurements of both low-loss and high-loss materials, and becomes more accurate at shorter wavelengths.

CONTENTS

ACKNOWLEDGEMENT

The work described in this thesis was done under the supervision of Professor A. L. Cullen, Head of the Department of Electronic and Electrical Engineering at University College London, to whom the author is deeply grateful for his valuable advice and guidance.

Thanks are also due to Mr. M. Effemey for his assistance in designing, and to Mr. F. W. Rason and his colleagues in the Departmental Workshop for constructing the open resonator.

The author is indebted to the University of Hong Kong for granting him the study leave.

LIST OF SYMBOLS

The following list contains those symbols most frequently used throughout the thesis.

a_m radius of the mirrors

a_o radius of the coupling apertures

A_l amplitude factor

c velocity of light

d distance from the dielectric sample to the mirror

D distance of separation between the mirrors

f resonant frequency

f_a resonant frequency of the asymmetrical mode

f_s resonant frequency of the symmetrical mode

$H_m(x)$ Hermite polynomial

k propagation constant in free space

$k_a = 2\pi f_a/c$ propagation constant for asymmetrical mode

$k_s = 2\pi f_s/c$ propagation constant for symmetrical mode

$L_p^{\ell}(x)$ generalized Laguerre polynomial

n refractive index

N Fresnel number

Q_o quality factor of the empty resonator

Q_L quality factor of the resonator when the dielectric is inserted

R radius of curvature of the phase front

R_s surface resistance

R_o radius of curvature of the mirrors

R_l radius of curvature of the phase front inside the dielectric

R_2 radius of curvature of the phase front outside the dielectric

t half thickness of the dielectric sample

w radius of the beam

w_m beam radius at the mirrors

$w_t = w_1(t) = w_2(t)$ beam radius at the interfaces

w_o radius of the beam waist

w_1 beam radius inside the dielectric

w_2 beam radius outside the dielectric

X_s surface reactance

Z_o intrinsic impedance of free space

Z_s surface impedance

ϵ_r relative permittivity

λ wavelength

Φ additional phase shift

$\Phi_t = \Phi_1(t)$ value of Φ at the interface

$\Phi_d = \Phi_2(d + t) - \Phi_2(t)$

Φ_1 additional phase shift inside the dielectric

Φ_2 additional phase shift outside the dielectric

ψ a slowly varying complex function

$\omega = 2\pi f$ angular frequency

CHAPTER 1

INTRODUCTION

The dielectric properties of materials employed in microwave devices can be measured by means of conventional cavity-resonator or waveguide techniques. However, at millimetric and submillimetric wavelengths, these techniques become increasingly difficult to use and inaccurate because of the small physical size of the cavity or waveguide involved. Open resonator techniques are inherently suited for measurements of low loss materials at wavelengths of below one centimetre, but with proper precautions they can also be used at centimetre wavelengths when dielectric materials in sheet form are measured. As there are no side walls, no opening and closing of the resonant structure for the insertion or removal of the dielectric is necessary and a closely fit sample to the cross-section of the resonator is not required.

Several open resonator methods employing spherical mirrors have been proposed.[1-4] The first three are resonator length variation methods in which the separation between the mirrors is varied to bring the resonant frequency back to its original value when the sample is removed from the resonator. While the theories are quite simple by using plane wave approximation, in actual practice it is troublesome to restore the resonant frequency precisely by tuning the mirror and the accurate measurement of the small mirror movement is rather difficult. The fourth one is a frequency variation method. However, the sample is required to be placed at the Brewster angle which is not known in advance and has to

be found experimentally. This complicates the experimental procedures and eventually leads to errors in the measurements. More details of these methods will be discussed in the next chapter.

Since frequency can be measured much more accurately than displacement, it is obvious that a simple measuring scheme, involving only the measurements of the resonant frequencies and the Q of the resonator,is advantageous and desirable. The method described in this thesis has the merit of being simple and quite accurate. Placing the sample symmetrically between two fixed mirrors of equal curvature, the dielectric constant and the loss tangent can be related to the resonant frequencies and the Q of the resonator measured with and without the dielectric. The analysis is based on the Gaussian beam theory by Kogelnik and Li[5] where the spherical phase front and the additional phase shift of the beam wave have been taken into account. Assuming first that the dielectric sample has two spherical surfaces coincident with the phase fronts of the resonator modes, the formulas for ε_r and $\tan\delta$ can be derived. When samples in sheet form are to be measured, the measured dielectric constant and loss tangent can be corrected by applying corrections to the measured resonant frequencies to account for the errors introduced by the plane dielectric surfaces.

CHAPTER 2

USUAL METHODS OF DIELECTRIC MEASUREMENT

This chapter surveys the existing methods of measuring dielectric properties of materials. The number of such methods and variations which exist are, however, so numerous that is is virtually impossible to treat all of them here. The following more useful methods are consequently emphasized: waveguide methods, cavity methods and open resonator methods.

Free-wave methods are sometimes employed in the measurement of dielectric constants and loss tangents of materials in sheet form. In the majority of cases, free-wave methods are less satisfactory than guided-wave methods, because the former ones involve a lot of special problems, such as the suppression of unwanted reflections, the launching of a plane wave in a limited space, and diffraction from the edges of the sample.

The microwave bridge methods rely on measurements of phase and attenuation at different points along the axis of the waveguide which contains the sample. This can be achieved by the use of a precision rotary phase shifter and rotary attenuator. However, these methods are not widely used since the range of dielectric constants which can be measured by their use substantially duplicates the range afforded by the methods given, while calibration and instrumentation problems usually increase with their use.

2.1 Waveguide Methods[6, 7]

The dielectric properties of materials can be determined from the results of measurements on a length of waveguide within which is a sample of that material. Two types of measurement have been found useful for this purpose. The first type is for those depending on the standing-wave pattern in the guide when terminated by a known impedance, usually a short or an open circuit. The second type is for those in which the absorption of waves passing through the sample is the main object of interest.

Two distinct observations must be made in order to obtain full information concerning the dielectric properties of the sample as there are two independent quantities, the relative permittivity and the loss tangent, to be determined. Typical examples of these observations are the propagation constant including the attenuation and phase constant, and the complex wave impedance or admittance of the sample-filled waveguide. Other methods combine in different ways the measurements described by the above two types.

The properties of gases may be determined by the technique described by Hershberger.[8, 9] A section of a waveguide is sealed off by gas tight mica windows. Measurements can then be made when the sealed section of the guide is evacuated and when it is filled with the gas to be measured.

Measurements on liquids and solids are complicated by the fact that the relative dielectric constant no longer approximates to unity, and reflections at the boundary with the surrounding air cannot be neglected. Under such circumstances the method given by Roberts and

and Von Hippel[10] may be used. The input impedance of a short-circuited waveguide is measured with and without the sample and a transcendental equation must be solved. Unless the approximate dielectric constant is known, two such measurements must be carried out with samples of different lengths.

A method, requiring two reactive terminals and only one sample, has been used.[11, 12] Generally, it is not as accurate as the above method because sample length cannot be properly optimized for both terminations simultaneously, but it involves a simple solution. When for some reason the length or the location of the sample cannot be evaluated properly, the techniques described by Oliner and Altschuler[13] can be applied. Since these are predicated on network representations, any one of the many available impedance measurement methods for two ports is applicable.

When a dielectric material has a very high loss tangent, it becomes difficult to measure it satisfactorily with the methods usually applied to low and medium loss materials. In such cases, a simple waveguide method can be carried out by considering the sample to be of infinite length. It requires the determination of essentially only the normalized input impedance at the sample face.

The method for the measurement of the relative permittivity of low-loss dielectric rod[14] which is mounted on the axis of a circular waveguide with one end contacting a short-circuit plate has the advantage that the samples do not have to fit the waveguide cross-section, but the loss tangent cannot be determined from the measurements without considerable computational effort.

An unconventional waveguide method has been proposed by Bell and Rupprecht[15] for the measurement of small dielectric losses in materials of high permittivity. This utilizes a sample large enough to support a dielectric resonance, but small compared with the dimensions of the waveguide in which it is suspended. The dielectric loss of $SrTiO_3$ was measured at a frequency range from 3 GHz to 37 GHz. Due to the large variation of permittivity with temperature, there are many temperatures at which the sample is resonant, and the loss tangent can then be determined.

Waveguide methods have been widely used and are versatile, but they have the very serious disadvantage that for wavelengths below 4 mm the very small waveguide size used gives rise to practical difficulties.

2.2 Cavity Methods

In resonant cavity methods, the resonant frequency and Q-factor of a resonant cavity are measured with and without a suitably shaped dielectric sample. A variety of methods using resonant cavities to measure the dielectric properties of materials have been developed. Three types of methods are commonly used in different situations and are as follows:

(i) Completely filled cavity of arbitrary shape[7, 16, 17]

(ii) Partially filled cavity[18-21]

(iii) Cavity perturbation methods.[7, 22, 23]

A measurement method in (i) has been derived from Maxwell's equations without reference to cavity shape or mode. It involves a cavity which is completely filled with a reference material (or a vacuum) with known dielectric constant and loss tangent, and which

resonates in an arbitrary but fixed mode. The reference material is replaced by the sample which must also fill the cavity completely, and then a second measurement is made with the cavity again resonating in the same mode. This method finds its application in the measurement of gases and low loss liquids. A variation of this method, which is often considered preferable, employs two identical cavities, one containing the reference material, the other containing the sample.

In the case of measurements on liquids and solids, much larger changes in resonant frequency and Q will normally be experienced, if the sample completely fills the resonator. Since large frequency excursions, while theoretically permissible, actually tend to lead to error, it is desirable to fill the cavity partially.

Samples of dielectric used for partial filling often take the form of a disc, a rectilinear body or an axial rod. Frequency or cavity length can be adjusted to resonate the cavity with and without the sample or for different lengths of the sample. These methods are particularly suited for measurements on low-loss materials, but usually require that the dielectric sample should be an accurate fit with respect to one or two of the cavity dimensions. Another disadvantage is that the mathematical analysis becomes much more complicated and, in general, the numerical or graphical solution of a transcendental equation is involved.

Cavity perturbation methods involve approximations in their formulation which lead to acceptable results only under very restricted conditions: The sample must be very small compared with the cavity itself, so that a frequency shift which is small compared with the resonant frequency of the empty cavity, is produced by the insertion of

the sample. Moreover, since the fields assumed in the sample are usually the solutions of static problems, certain sample dimensions must be small compared with wave length, or the unperturbed field in the sample region must be uniform. Cavity perturbation measurements can be highly accurate and are particularly advantageous in measuring relatively lossy materials. Perturbation techniques also permit the measurement of small dielectric samples of various shapes.

Like the waveguide methods, resonant cavity methods have been found to be capable of high accuracy, but the problem of physical size and increased metal losses at short wavelengths remains.

2.3 Open Resonator Methods

It has become increasingly difficult to use the conventional waveguide and microwave cavity resonator methods for measuring the permittivity of materials at the lower millimetric or shorter wavelengths. Thus development of new methods is necessary to overcome the difficulties of small cavity dimensions and the increased metal losses. In order to obtain accuracy in the measurements, a resonator of high Q-factor at short wavelength is desirable and recent development has been concentrated on more suitable types of resonator.

The work of Hakki and Coleman[24] is an interesting development. Here the measuring structure is a resonator made up of a right circular cylindrical dielectric rod placed between two parallel conducting plates. The problem of physical size is avoided to some extent, and metal losses are reduced. However, the modes of interest are restricted to the $TE_{on\ell}$ which form a small portion of all the possible modes of operation, and a highly selective method of excitation is rather difficult to obtain.

Difficulties also arise in the determination of the mode indexes, and the method would become more difficult to apply at very short wavelengths.

The application of a Fabry-Perot interferometer with plane mirrors for the measurement of the permittivities and loss tangents of materials at millimetric and sub-millimetric wavelengths has been considered by Culshaw and Anderson.[25] Permittivities are deduced from the change in the plate spacing for resonance when the sheet is inserted. This involves the solution of a transcendental equation. The measurement of loss tangent depends on measurements of the Q-factor with and without the dielectric sheet in the interferometer. However, the Q-factor of the empty interferometer, which is limited by the relatively high diffraction losses, is not particularly high to give accurate tanδ measurements of low-loss materials, and the assumption of constant diffraction losses may lead to errors in the results.

A method of measuring dielectric constants of materials in sheet form by insertion in a Fabry-Perot confocal resonator has been described by Degenford and Coleman.[1] By tilting the dielectric sheet at a small angle with respect to the system axis, the reflected wave can be eliminated. The working formula for determining the dielectric constant then reduces to a simple linear relation involving the ratio of the mirror motion required to restore resonance to the thickness of the dielectric. This method has a drawback that tilting the dielectric sheet at an angle of more than 5^{o} reduces drastically the Q-factor of the resonator. This increases the difficulty of an accurate measurement of the resonant frequency. Sometimes the Q-factor becomes so low that the output is undetectable even before the reflected wave is completely

eliminated. The above has been verified by an experiment carried out by using the resonator described in this thesis. It was found that the measured dielectric constant of a 6.96 mm thick polystyrene sheet varied from 2.542 to 2.659 for a tilt angle ranging from 5^{o} to 7^{o}. At 8^{o} the output was hardly detectable.

This method has been extended to the measurements of dielectric loss tangent.[2] The technique basically consists of perturbing a microwave confocal resonator with a dielectric sheet placed normal to the axis of the resonator. The change in Q and the change in cavity length necessary to restore resonance can then be related to the loss tangent of the dielectric.

A technique similar to the foregoing has been developed for use with a semiconfocal resonator.[3] The advantage of this technique is that it allows the simultaneous measurements of dielectric constant and loss tangent. Also, in applying this technique the sample is mounted against the flat mirror in the semiconfocal system, thus eliminating any uncertainty in the angular position of the sample.

The above three are length variation methods which involve the adjustment of the mirror spacing to restore the resonant frequency when the sample is removed from the resonator. The accuracy of these methods depends on the precision of the mirror adjustment and the measurement of of the small displacement of the mirror.

Measurement of complex dielectric constant using a Fabry-Perot resonator by installing the dielectric sample at Brewster angle has been carried out by Yuba et al.[4] Results are derived from application of computations on the transmission and reflection coefficients with

respect to a plane wave incident obliquely upon the dielectric sheet. But tilting of the sample at large angle causes misalignment of the mirrors and it is difficult to find the Brewster angle accurately which is not known in advance.

CHAPTER 3

THEORY OF THE OPEN RESONATOR

Dick,[26] Prokhorov,[27] and Schawlow and Townes[28] were first to suggest the use of a Fabry-Perot interferometer as a resonator operating at infrared or optical frequencies. Theoretical studies of the modes of an open resonator, as determined by diffraction effect, were made by Fox and Li.[29] Boyd and Gordon,[30] and Boyd and Kogelnik[31] developed a theory for resonators with spherical mirrors and approximated the modes by wave beams. The concept of electromagnetic wave beams was also introduced by Goubau and Schwering[32] who studied the guided transmission of reiterative beams. In this chapter, we consider the mode theory of spherical mirror resonators based on the analysis by Kogelnik and Li.[5] Diffraction losses, resonant conditions and mode patterns are also discussed.

3.1 The Travelling Beam Modes

Two methods have been used to find the transverse modes. One is to seek simple solutions to Maxwell's equations which take the form of wave beams. The other method is to use the scalar formulation of Huygen's principle to determine the mode patterns and the actual diffraction losses.

Let us consider the approximate solutions to the scalar wave equation[5]

$$\nabla^2 E + k^2 E = 0 \tag{3.1}$$

where E is a field component and $k = 2\pi/\lambda$, the propagation constant in the medium.

For beam waves travelling in the z direction, we can write

$$E = \psi(x, y, z) \exp(-jkz) \tag{3.2}$$

where ψ is a complex function varying so slowly with z that it is assumed its second derivative $\frac{\partial^2\psi}{\partial z^2}$ can be neglected (see Appendix I). Substitution of (3.2) into (3.1) then gives

$$\frac{\partial^2\psi}{\partial x^2} + \frac{\partial^2\psi}{\partial y^2} - 2jk\frac{\partial\psi}{\partial z} = 0 \tag{3.3}$$

3.1.1 Fundamental Mode

A solution of (3.3) is

$$\psi(r, z) = \frac{w_o}{w} \exp\{-\frac{r^2}{w^2} + j(\Phi - \frac{kr^2}{2R})\} \tag{3.4}$$

Substituting (3.4) into (3.2), the fundamental Gaussian beam can be written in the form

$$E(r, z) = \frac{w_o}{w} \exp\{-j(kz - \Phi) - r^2(\frac{1}{w^2} + \frac{jk}{2R})\} \tag{3.5}$$

where r measures the distance from the z-axis and $\Phi(z)$ indicates an additional phase shift due to the geometry of the beam. The radius of the beam is w(z) at which the field amplitude falls to 1/e, and the radius of curvature of the phase front at z is R(z).

As shown in Fig. 3.1, the Gaussian beam has a minimum diameter $2w_o$ at the beam waist at z = 0 where the phase front is plane. As the beam propagates it expands according to a hyperbolic law. The expansion of the beam is given by

$$w^2 = w_o^2\{1 + (\frac{z}{z_o})^2\} \tag{3.6}$$

where $z_o = \pi w_o^2/\lambda$, the mirror spacing of the equivalent confocal resonator.

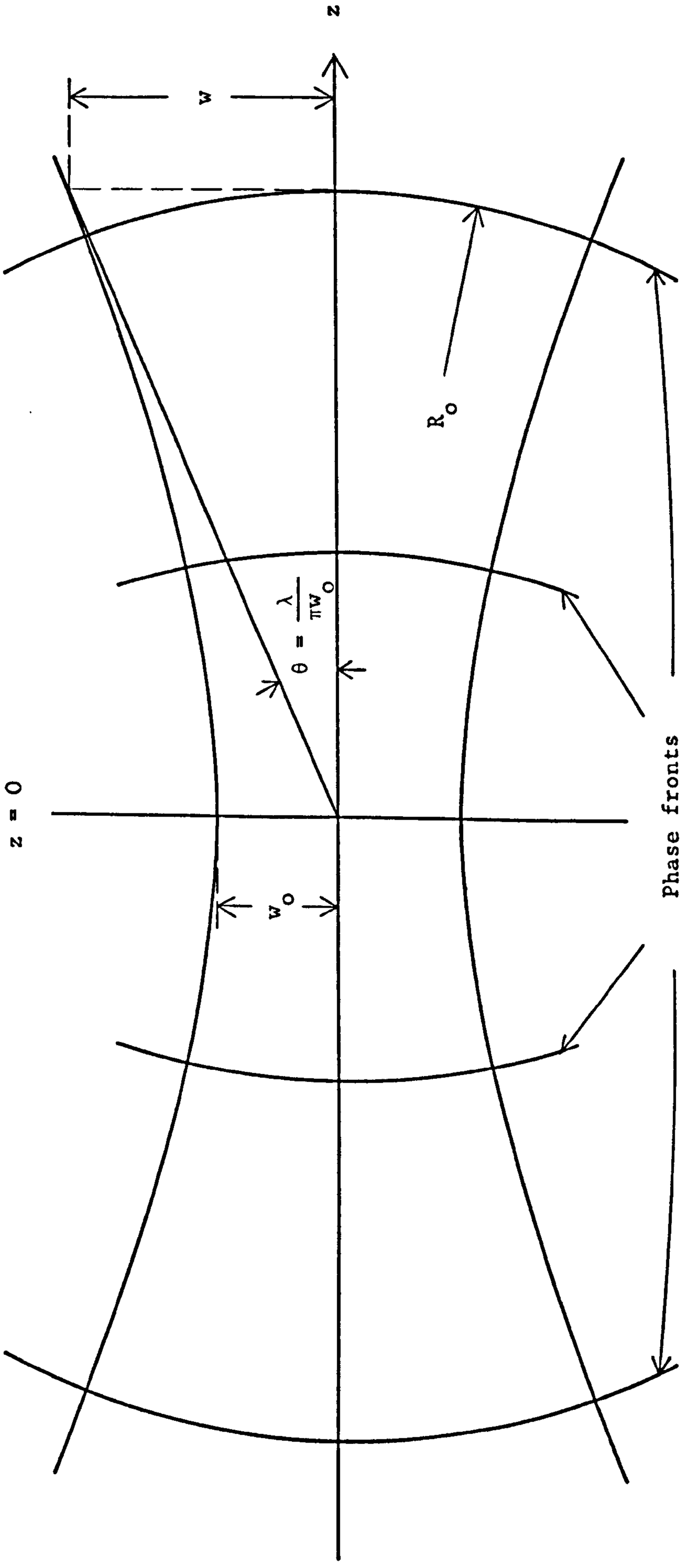

FIG. 3.1 Beam contour

The radius of curvature of the phase front is given by

$$R = z\left[1 + \left(\frac{z_o}{z}\right)^2\right] \tag{3.7}$$

and the additional phase shift is

$$\Phi = \tan^{-1}\left(\frac{z}{z_o}\right) \tag{3.8}$$

Dividing (3.7) by (3.5), we have

$$\frac{\lambda z}{\pi w_o^2} = \frac{\pi w^2}{\lambda R} \tag{3.9}$$

which is a very useful relation.

If we assume that E_x is the only component of the electric field and let

$$g = \frac{1}{w^2} + \frac{jk}{2R} \tag{3.10}$$

equation (3.5) can be written as

$$E_x = \frac{w_o}{w} \exp\left[-j(kz - \Phi) - gr^2\right] \tag{3.11}$$

From Maxwell's equations, the magnetic field has the form (see Appendix I)

$$H_y = \frac{j}{\omega\mu_o}\frac{\partial E_x}{\partial z} = \frac{k}{\omega\mu_o}\left[1 + \frac{2}{k^2}(g^2r^2 - g)\right]E_x \tag{3.12}$$

The last two terms inside the square bracket when comparing with 1 are of the same order of magnitude as the term neglected when deriving (3.11) and, therefore, are negligible. Equation (3.12) then becomes

$$H_y = \frac{k}{\omega\mu_o} E_x \tag{3.13}$$

This is a very good approximation as long as $k^2 w_o^2 >> 1$.

3.1.1 Higher Order Modes

In addition to the solution discussed in the preceding section there are other solutions of (3.3) with similar properties. They are called higher order modes which form a complete and orthogonal set of functions. These modes are distinguished by their mode numbers, which are m, n and q for rectangular geometries and p, ℓ and q for cylindrical geometries. The mode number q measures the number of field zeros of the standing wave pattern along the z-axis.

(i) Modes in Cartesian Coordinates: For a system with a rectangular geometry the solution has the form

$$E = H_m(\sqrt{2}\,\frac{x}{w})H_n(\sqrt{2}\,\frac{y}{w})\,\exp\{-j\,[kz - \Phi(m,\,n;\,z)] - (x^2 + y^2)(\frac{1}{w^2} + \frac{jk}{2R})\} \qquad (3.14)$$

where H_m and H_n are Hermite polynomials of order m and n which measure the field nodes in the x and y direction respectively, and the phase shift $\Phi(m, n; z)$ is now given by

$$\Phi(m,\,n;\,z) = (m + n + 1)\,\tan^{-1}(\frac{z}{z_o}) \qquad (3.15)$$

Some Hermite polynomials of low order are

$$H_o(x) = 1$$

$$H_1(x) = x$$

$$H_2(x) = 4x^2 - 2 \qquad (3.16)$$

(ii) Modes in Cylindrical Coordinates: For a system with cylindrical (r, ϕ, z) geometry the solution of (3.3) has the form

$$E = (\sqrt{2}\,\frac{r}{w})^{\ell} L_p^{\ell}(2\,\frac{r^2}{w^2})\,\exp\{-j\{kz - \Phi(p,\,\ell;\,z) + \ell\phi\} - r^2(\frac{1}{w^2} + \frac{jk}{2R})\} \qquad (3.17)$$

where the L_p^{ℓ} are the generalized Laguerre polynomials, and p and ℓ are radial and angular mode numbers. The phase shift $\Phi(p, \ell; z)$ is now given by

$$\Phi(p,\,\ell;\,z) = (2p + \ell + 1)\,\tan^{-1}(\frac{z}{z_o}) \qquad (3.18)$$

The beam parameter R(z) is the same for all modes.

Some polynomials of low order are

$$L_o^{\ell}(x) = 1$$

$$L_1^{\ell}(x) = \ell + 1 - x$$

$$L_2^{\ell}(x) = \tfrac{1}{2}(\ell + 1)(\ell + 2) - (\ell + 2)x + \tfrac{1}{2}x^2 \qquad (3.19)$$

Since we are more interested in cylindrical geometries, some linearly polarized mode configurations are shown in Fig. 3.2.

3.2 Open Resonator

Given the beam modes discussed in the preceding section, we can insert two mirrors which match two of the spherical surfaces defined by (3.7) to form a resonator. Alternatively, given two mirrors with spherical curvature and some distance of separation, the position and the radius of the beam waist can be adjusted so that the mirrors coincide with two such surfaces. The present discussion applies to resonators with mirror apertures that are large compared to the size of the beam.

Consider an open resonator with mirrors of equal curvature. Let D be the distance of separation and R_o be the radius of curvature of

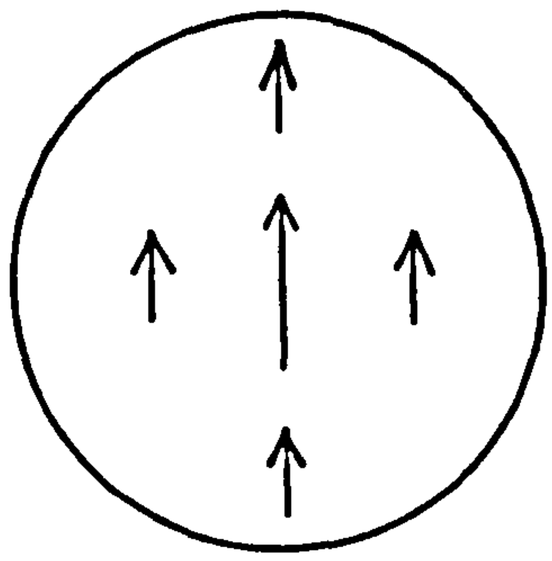

TEM_{oo}

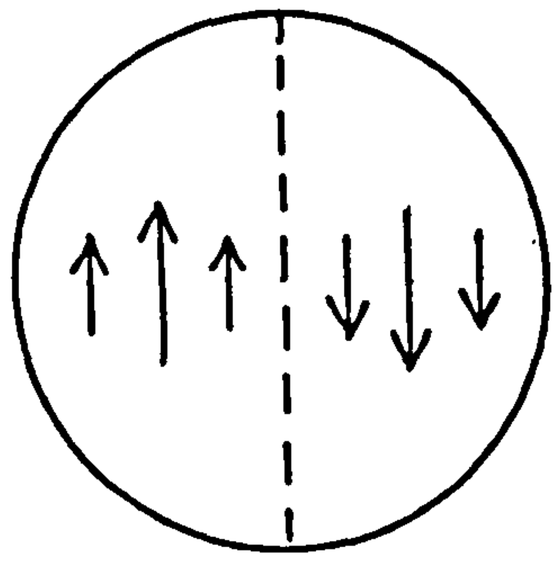

TEM_{o1}

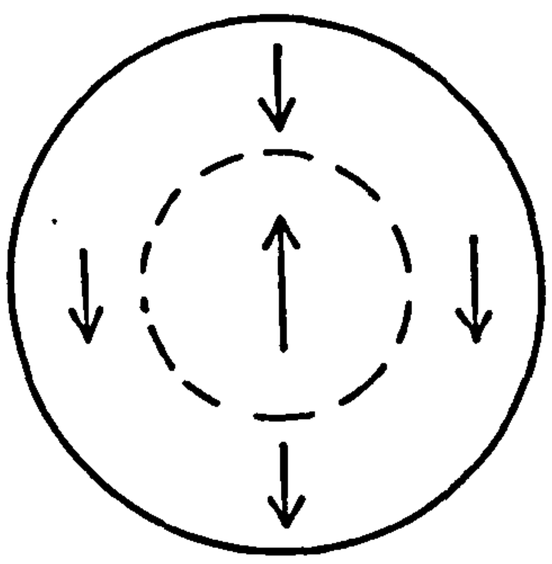

TEM_{1o}

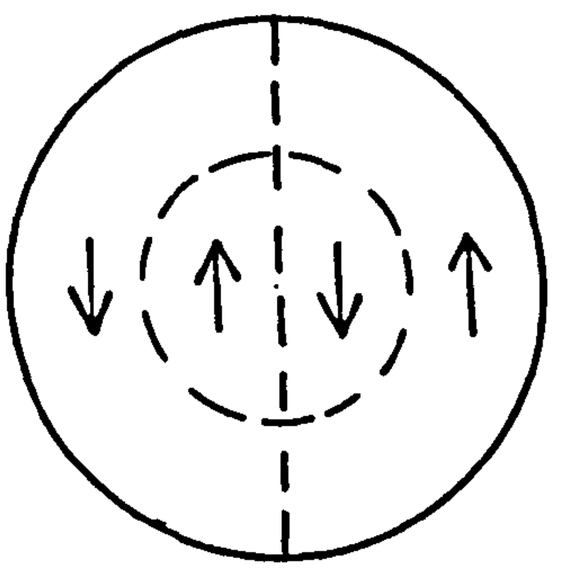

TEM_{11}

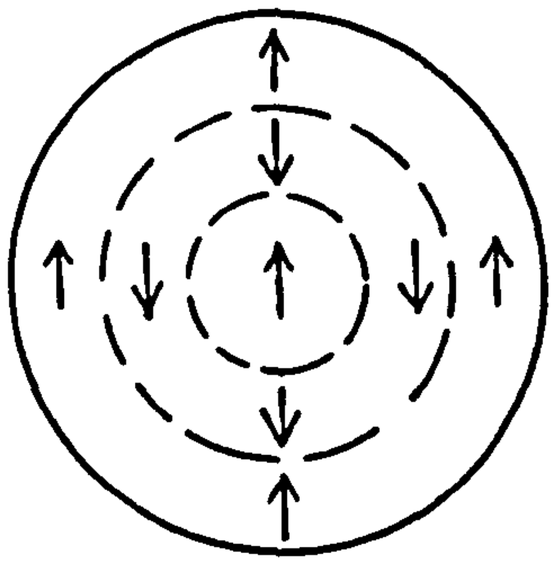

TEM_{2o}

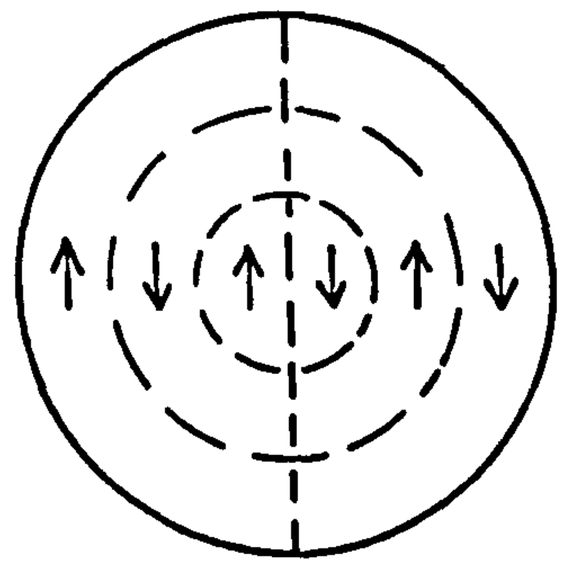

TEM_{21}

FIG. 3.2 $TEM_{p\ell}$ mode configurations for circular mirrors

the mirrors. From (3.7) with $z = D/2$, the beam waist w_o in the centre of the resonator is given by

$$w_o^2 = \frac{\lambda}{2\pi}\sqrt{D(2R_o - D)} \tag{3.20}$$

Using (3.9) and (3.20), the beam radius at the mirrors can be written as

$$w^2 = \frac{\lambda R}{\pi}\sqrt{\frac{D}{2R_o - D}} \tag{3.21}$$

Fig. 3.3 shows how the beam radii vary with the distance of separation between two given mirrors, w_{oc} being the beam waist when the resonator is confocal.

For modes of circular geometry, resonance occurs when the phase shift from one mirror to the other is a multiple of π. From (3.17) and (3.18), this condition can be written as

$$kD - 2(2p + \ell + 1)\tan^{-1}(\frac{z}{z_o}) = (q + 1)\pi \tag{3.22}$$

where $(q + 1)$ is the number of half wavelengths of the axial standing wave pattern.

The frequency spacing of longitudinal modes is

$$f_o = \frac{c}{2D} \tag{3.23}$$

where c is the velocity of light. Combination of (3.20), (3.22) and (3.23) yields the resonant frequency of a mode

$$\frac{f}{f_o} = (q + 1) + \frac{1}{\pi}(2p + \ell + 1)\cos^{-1}(1 - \frac{D}{R_o}) \tag{3.24}$$

where $\frac{f_o}{\pi}\cos^{-1}(1 - \frac{D}{R_o})$ is the frequency separation between adjacent azimuthal modes.

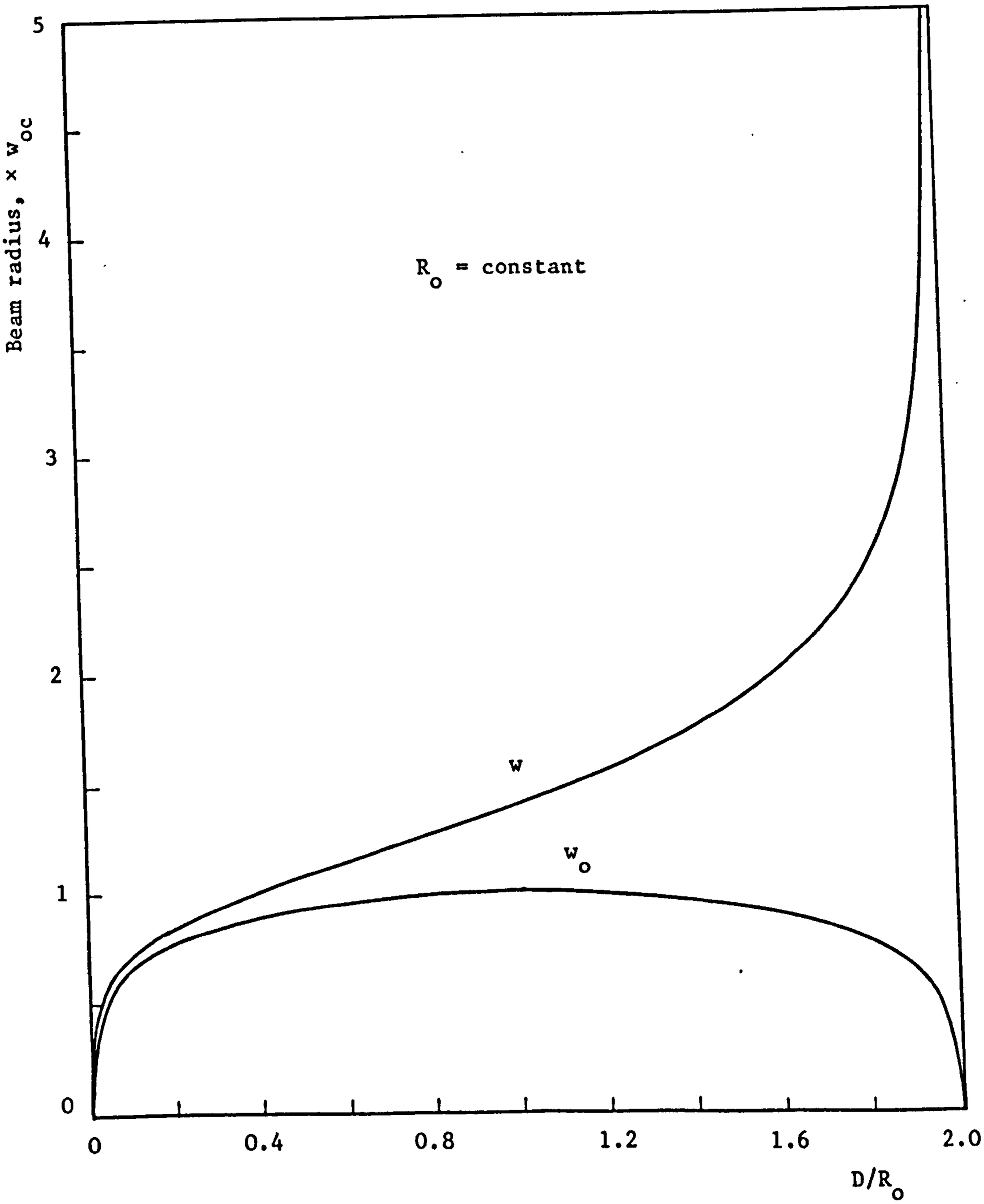

FIG. 3.3 Variation of beam radius with distance of separation

It is clear that for a given q, all modes with $2p + \ell$ = constant are degenerate. If the the resonator is confocal, then D = R and (3.24) becomes

$$\frac{f}{f_o} = (q + 1) + \tfrac{1}{2}(2p + \ell + 1) \qquad (3.25)$$

and all the modes with the same $(2q + 2p + \ell)$ are thus degenerate.

3.3 Diffraction Losses

In practical resonator systems the losses due to diffraction spillover are usually small compared with the other losses such as metal losses suffered at the resonator mirrors and coupling losses. Knowledge of the amount of loss is, however, desirable whenever one wishes to design a resonator operating in the fundamental mode only.

The loss is a fucntion of the radius of curvature R_o of the mirrors, the mirror spacing D, and the size and shape of the mirrors. An important loss parameter is the Fresnel number $N = \frac{a_m^2}{D\lambda}$, where for round mirrors a_m is the mirror radius and for strip or rectangular mirrors $2a_m$ is the mirror width.

The results of theoretical calculation of the diffraction losses for low-loss modes of a confocal resonator with circular mirrors are shown in Fig. 3.4.[33] For non-confocal resonators, diffraction losses can be obtained by finding first the corresponding equivalent confocal systems.

The open resonators with either plane or spherical mirrors are inherently multimode devices. In general the systems resonate in several modes at the corresponding resonant frequencies. However, because of the Gaussian-Laguerre transverse field distribution, the diffraction losses are higher for higher-order modes for a given system. By a proper choice of

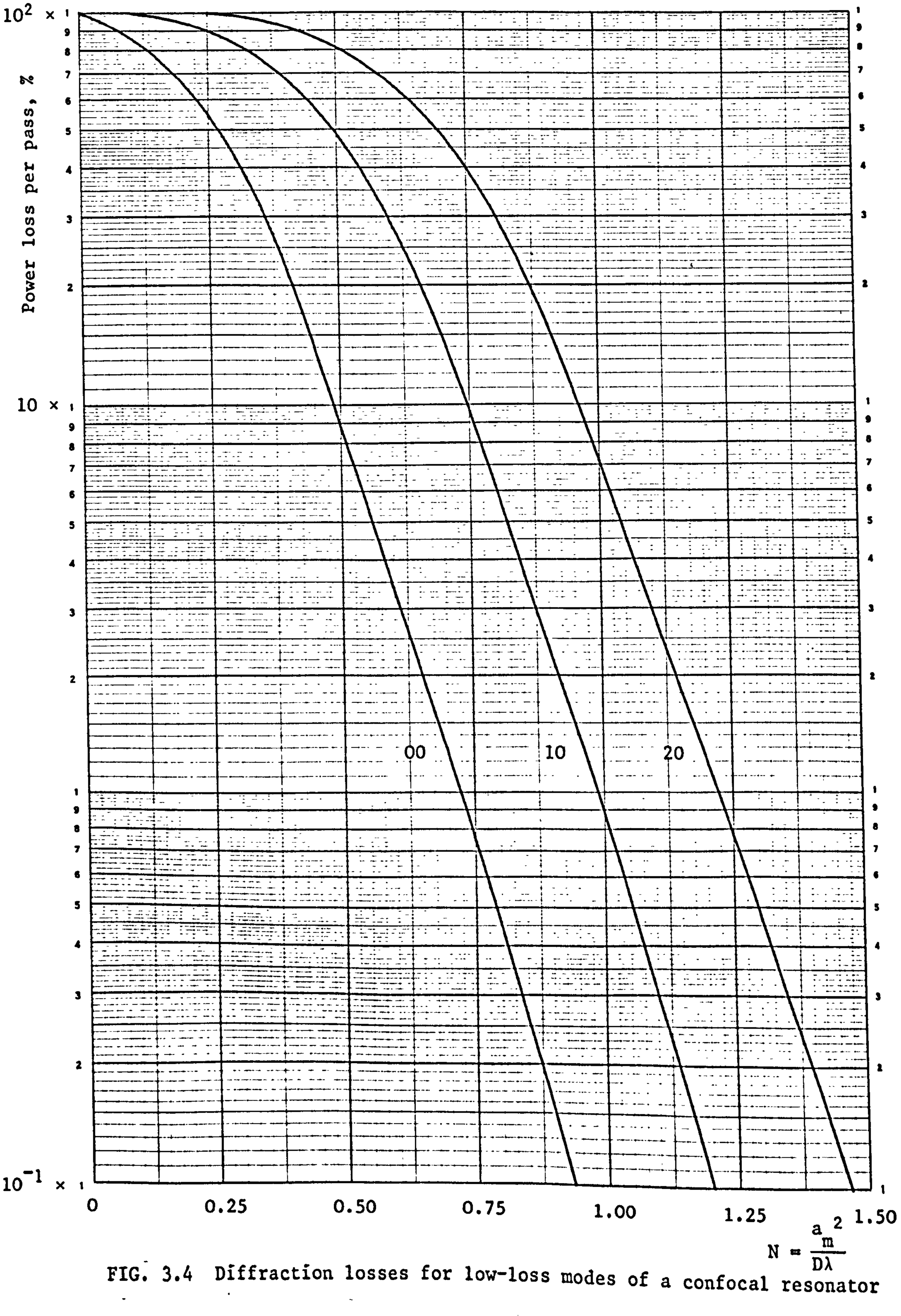

FIG. 3.4 Diffraction losses for low-loss modes of a confocal resonator

of the parameter N, we can thus discriminate against higher-order modes by increasing their losses relative to that of the fundamental mode.

In addition to diffraction losses, there are losses due to coupling, absorption, scattering and other effects. If the total loss is small the Q of the resonator can be approximated by

$$Q = \frac{2\pi D}{\lambda \alpha_t} \tag{3.26}$$

where α_t is the total loss.

CHAPTER 4

MEASUREMENT OF DIELECTRIC CONSTANT

4.1 Method of Measurement

The dielectric sample of thickness 2t is placed symmetrically at the centre of the resonator formed by two spherical mirrors of equal curvature as shown in Fig. 4.1. For the moment these mirrors will be regarded as having infinite aperture, and the dielectric sample will be assumed to have zero loss and to be slightly convex on both sides so that they are coincident with the phase fronts of the resonator modes.

In considering the axial standing-wave electric field patterns in the resonator and with the axial mode number q measuring the number of zeros between the mirrors, the mode is symmetrical when q is even or an antinode is at the centre, and the mode is asymmetrical when q is odd or a node is at the centre. As shown in Fig. 4.2, the mode spectrum of an empty resonator comprises a set of equispaced resonances while the resonant frequencies of a resonator with a dielectric sample inserted are unevenly spaced. The shift in the resonant frequency is proportional to the electric energy increased by the insertion of the dielectric.

The proposed method of measurement is very simple. It consists of measuring the resonant frequency of a symmetrical mode and of the adjacent lower-frequency asymmetrical mode. From these two frequencies the dielectric constant can be determined without the need to solve a transcendental equation, so long as $\lambda << d$. The dielectric constant can also be found by using a computer to solve the two transcendental equations relating the refractive index to these frequencies.

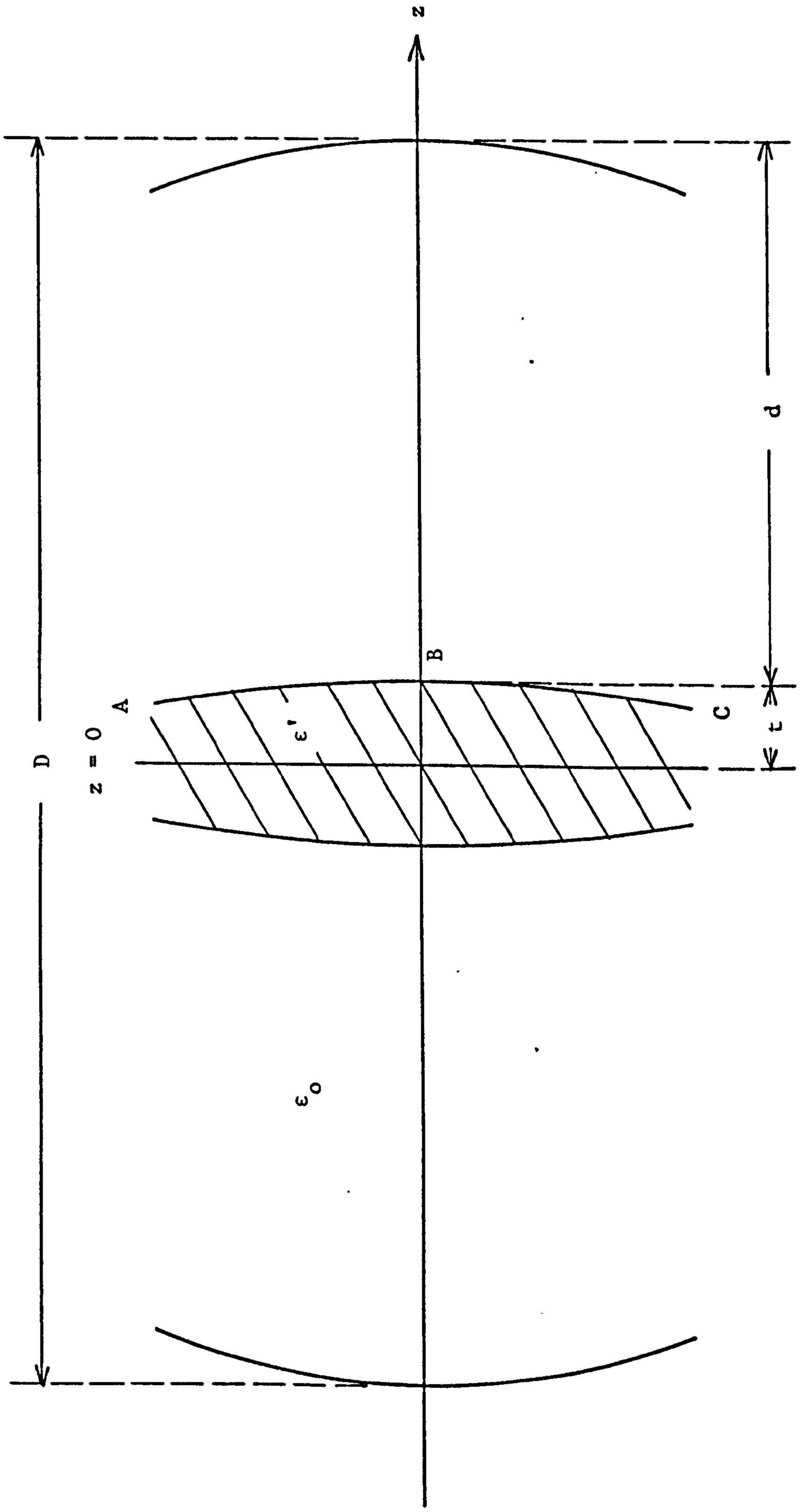

FIG. 4.1 Open resonator with dielectric sample

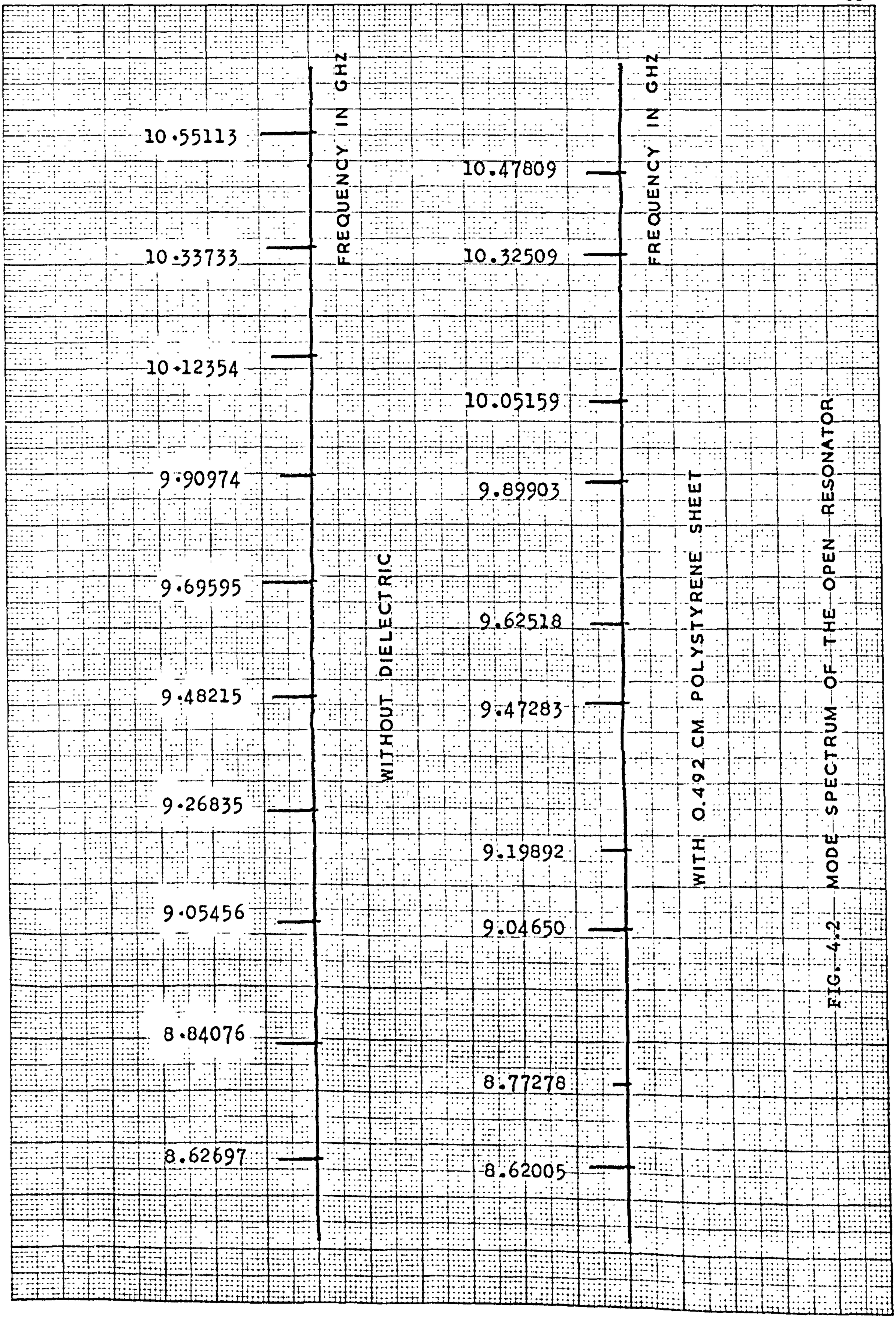

FIG.-4.2— MODE SPECTRUM OF THE OPEN—RESONATOR

4.2 Fields of the Resonator with the Dielectric Sample at the Centre

Fig. 4.1 shows the arrangement to be considered with the dielectric sample at the centre between the mirrors. The mirror separation is D, the thickness of the sample is 2t, and the distance from the sample to the mirror is d. It is assumed that the electromagnetic field inside the resonator is of the TEM_{oo} mode, and that the electric and the magnetic fields have only x and y components respectively. The assumption of no longitudinal component is a very good approximation if $k^2w_o^2 \gg 1$ or when the region of interest is near the centre of the resonator where the wave front is almost plane.

Because of the symmetry about the plane z = 0, it is sufficient to consider only half of the resonator, i.e. a resonator with an open circuit for symmetrical mode and a short circuit for asymmetrical mode at z = 0, and a short circuit at the mirror intercepting the axis at z = t + d. Let subscripts 1 and 2 indicate fields and beam parameters inside and outside the dielectric respectively. From (3.5) and (3.13), the fields in the two regions may be written as

$$\left.\begin{aligned} E_1 &= \frac{A_1 w_o}{w_1} \exp\left(-\frac{r^2}{w_1^2}\right) \begin{matrix}\cos\\ \sin\end{matrix}\left[nkz - \Phi_1(z) + \frac{nkr^2}{2R_1(z)}\right] \\ Z_1 H_1 &= \mp \frac{jA_1 w_o}{w_1} \exp\left(-\frac{r^2}{w_1^2}\right) \begin{matrix}\sin\\ \cos\end{matrix}\left[nkz - \Phi_1(z) + \frac{nkr^2}{2R_1(z)}\right] \end{aligned}\right\} 0 \leqslant z \leqslant t \qquad (4.1)$$

$$\left.\begin{aligned} E_2 &= \frac{w_o'}{w_2} \exp\left(-\frac{r^2}{w_2^2}\right) \sin\left[kz - \Phi_2(z) + \frac{kr^2}{2R_2(z)} + \alpha\right] \\ Z_o H_2 &= \frac{jw_o'}{w_2} \exp\left(-\frac{r^2}{w_2^2}\right) \cos\left[kz - \Phi_2(z) + \frac{kr^2}{2R_2(z)} + \alpha\right] \end{aligned}\right\} t \leqslant z \leqslant t + d \qquad (4.2)$$

where A_1 is the amplitude factor, $k = 2\pi/\lambda_o$, the propagation constant in free space, $Z = \sqrt{\mu/\epsilon}$, the intrinsic impedance, and $Z_o/Z_1 = n$, the refractive index of the dielectric. The upper trigonometric functions are for the symmetrical mode and the lower ones are for the asymmetrical mode. From (3.6), (3.7) and (3.8), the beam parameters and the additional phase shift in region 1 can be written as

$$\left.\begin{aligned} w_1^2(z) &= w_o^2\left[1 + \left(\frac{2z}{nkw_o^2}\right)^2\right] \\ R_1(z) &= z\left[1 + \left(\frac{nkw_o^2}{2z}\right)^2\right] \\ \Phi_1(z) &= \tan^{-1}(2z/nkw_o^2) \end{aligned}\right\} \quad 0 \leqslant z \leqslant t \qquad (4.3)$$

where w_o is the beam radius at $z = 0$.

Applying the boundary condition that $E_2 = 0$ at the mirror, we have

$$\alpha = -k(d + t) + \Phi_2(d + t) \qquad (4.4)$$

Substitution of (4.4) into (4.2) gives

$$\left.\begin{aligned} E_2 &= \frac{w_o'}{w_2}\exp\left(-\frac{r^2}{w_2^2}\right)\sin\left[k(z - d - t) + \Phi_2(d + t) - \Phi_2(z) + \frac{kr^2}{2R_2(z)}\right] \\ Z_o H_2 &= \frac{jw_o'}{w_2}\exp\left(-\frac{r^2}{w_2^2}\right)\cos\left[k(z - d - t) + \Phi_2(d + t) - \Phi_2(z) + \frac{kr^2}{2R_2(z)}\right] \end{aligned}\right\} \quad t \leqslant z \leqslant t+d \qquad (4.5)$$

Expressions for $\Phi_2(z)$, $w_2(z)$ and $R_2(z)$ can be found by matching the beam parameters at the interface.

4.3 Matching of Beam Parameters

As illustrated in Fig. 4.3, the beam in the region $t \leqslant z \leqslant t + d$ can be considered as coming from the beam waist w_o' of an equivalent empty resonator formed by the spherical mirror at $z = t + d$ and a plane mirror at $z = f$. Under such circumstances, the beam radius and the radius of curvature of the wave front in region 2 can be written as

$$\left.\begin{aligned} w_2^2(z) &= w_o'^2\left[1 + \left(\frac{2(z - f)}{kw_o'^2}\right)^2\right] \\ R_2(z) &= (z - f)\left[1 + \left(\frac{kw_o'^2}{2(z - f)}\right)^2\right] \end{aligned}\right\} \quad t \leqslant z \leqslant t + d \qquad (4.6)$$

The matching of amplitude and radius of curvature of the wave front at the interface requires $w_1(t) = w_2(t)$ and $R_1(t) = R_2(t)$. Combination of (4.3) and (4.6) yields

$$w_o^2\left[1 + \left(\frac{2t}{nkw_o^2}\right)^2\right] = w_o'^2\left[1 + \left(\frac{2(t - f)}{kw_o'^2}\right)^2\right] \qquad (4.7)$$

$$t\left[1 + \left(\frac{nkw_o^2}{2t}\right)^2\right] = (t - f)\left[1 + \left(\frac{kw_o'^2}{2(t - f)}\right)^2\right] \qquad (4.8)$$

Dividing (4.7) by (4.8), we have

$$\frac{4t}{n^2k^2w_o^2} = \frac{4(t - f)}{k^2w_o'^2}$$

Hence

$$f = t - \frac{tw_o'^2}{n^2w_o^2} \qquad (4.9)$$

Substitution of (4.9) into (4.7) yields

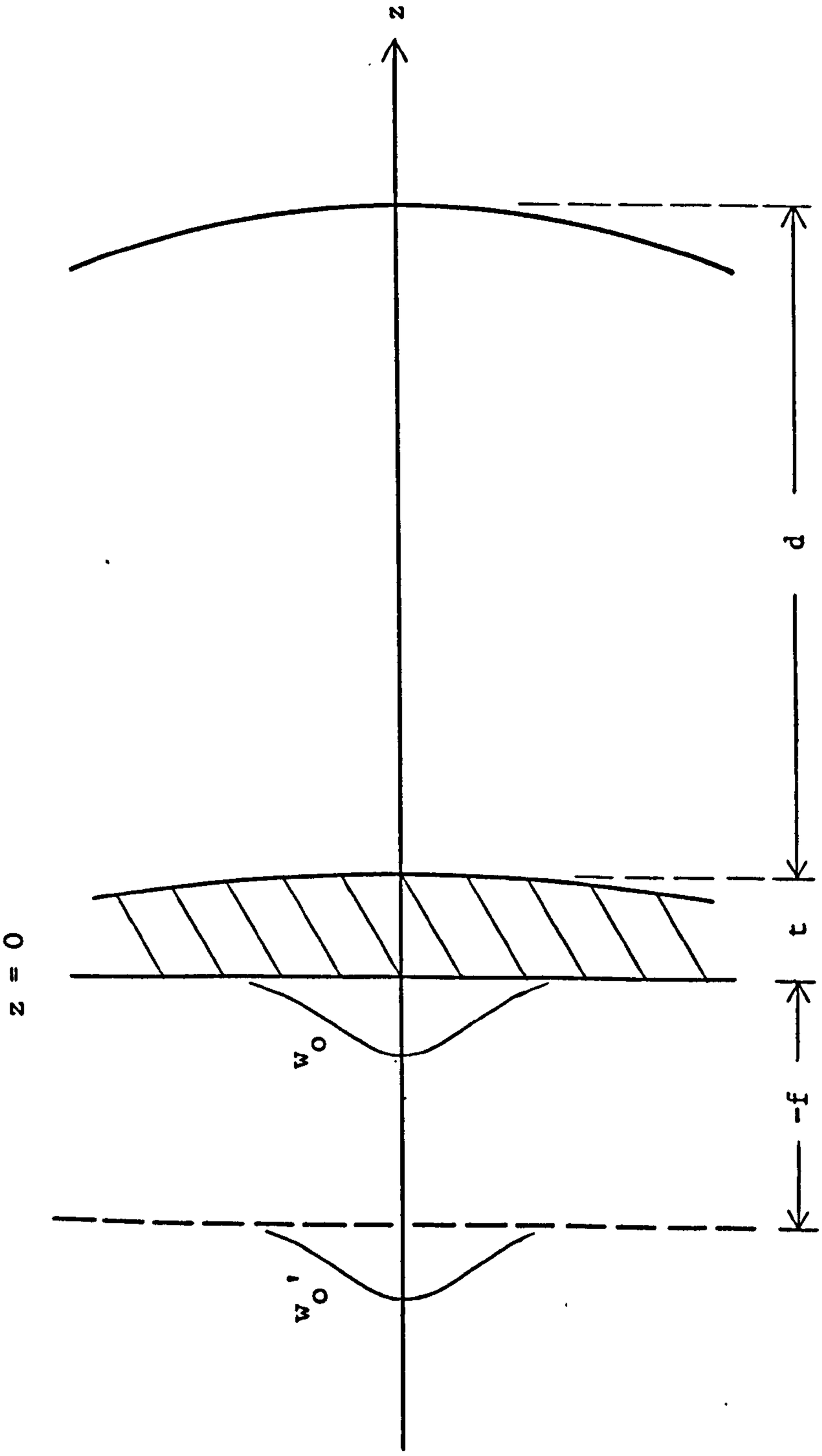

FIG. 4.3 Matching of beam parameters

$$\frac{w_o'^2}{w_o^2} = \frac{1 + \left(\frac{2t}{nkw_o^2}\right)^2}{1 + \left(\frac{2t}{n^2kw_o^2}\right)^2} \tag{4.10}$$

The right-hand side of (4.10), when $k^2w_o^2 >> 1$, can be approximated by 1 with very little error. Equation (4.9) then becomes

$$f = t - \frac{t}{n^2} \tag{4.11}$$

Using (4.11), the beam parameters in (4.6) may be written as

$$\left.\begin{aligned} w_2^2(z) &= w_o^2\left[1 + \left(\frac{2}{kw_o^2}(z - t + \frac{t}{n^2})\right)^2\right] \\ R_2(z) &= (z - t + \frac{t}{n^2})\left[1 + \left(\frac{kw_o^2}{2(z - t + t/n^2)}\right)^2\right] \end{aligned}\right\} t \leq z \leq t + d \tag{4.12}$$

and the additional phase shift in region 2 is

$$\phi_2(z) = \tan^{-1}\left[\frac{2(z - f)}{kw_o^2}\right] = \tan^{-1}\left[\frac{2}{kw_o^2}(z - t + \frac{t}{n^2})\right] \tag{4.13}$$

At $z = t + d$, the wave front of the resonant mode is coincident with the mirror surface. From (4.12), the radius of curvature of the mirrors is given by

$$R_o = (d + \frac{t}{n^2})\left[1 + \left(\frac{kw_o^2}{2(d + t/n^2)}\right)^2\right] \tag{4.14}$$

For a pair of mirrors of known equal curvature, the beam radius w_o in the centre of the resonator with the dielectric sample inserted can be calculated by means of (4.14) as

$$w_o^2 = \frac{2}{k}\sqrt{(d + t/n^2)(R_o - d - t/n^2)} \tag{4.15}$$

4.4 Transcendental Equations

On an equiphase surface intersecting the axis at z, (4.1) and (4.5) reduce to

$$\left.\begin{aligned} E_1 &= \frac{A_1 w_o}{w_1} \exp\left(-\frac{r^2}{w_1^2}\right) \begin{matrix}\cos\\ \sin\end{matrix}\left[nkz - \Phi_1(z)\right] \\ Z_1 H_1 &= \mp \frac{jA_1 w_o}{w_1} \exp\left(-\frac{r^2}{w_1^2}\right) \begin{matrix}\sin\\ \cos\end{matrix}\left[nkz - \Phi_1(z)\right] \end{aligned}\right\} \quad 0 \leqslant z \leqslant t \qquad (4.16)$$

$$\left.\begin{aligned} E_2 &= \frac{w_o}{w_2} \exp\left(-\frac{r^2}{w_2^2}\right) \sin\left[k(z - d - t) + \Phi_2(d + t) - \Phi_2(z)\right] \\ Z_o H_2 &= \frac{jw_o}{w_2} \exp\left(-\frac{r^2}{w_2^2}\right) \cos\left[k(z - d - t) + \Phi_2(d + t) - \Phi_2(z)\right] \end{aligned}\right\} \quad t \leqslant z \leqslant t + d \qquad (4.17)$$

where it has been assumed that w is constant over the surface.

For the symmetrical mode, E_1 has a maximum at z = 0. At the interface ABC (Fig. 4.1), the wave impedance looking to the left is

$$Z_s = -\frac{E_1}{H_1} = -jZ_1 \cot\left[nk_s t - \Phi_1(t)\right] \qquad (4.18)$$

where $k_s = 2 f_s/c$, f_s being the resonant frequency of the symmetrical mode.

For the asymmetrical mode

$$Z_a = jZ_1 \tan\left[nk_a t - \Phi_1(t)\right] \qquad (4.19)$$

The impedance looking to the right at ABC is

$$Z_{s_a}' = jZ_o \tan\left[k_{s_a} d - \Phi_2(t + d) + \Phi_2(t)\right] \qquad (4.20)$$

Applying the resonance condition $Z + Z' = 0$, we find

$$-\frac{1}{n}\cot\left[nk_s t - \Phi_1(t)\right] + \tan\left[k_s d - \Phi_2(t + d) + \Phi_2(t)\right] = 0 \qquad (4.21)$$

$$\frac{1}{n}\tan\left[nk_a t - \Phi_1(t)\right] + \tan\left[k_a d - \Phi_2(t + d) + \Phi_2(t)\right] = 0 \qquad (4.22)$$

where

$$\Phi_1(t) = \tan^{-1}\left(\frac{2t}{nkw_o^2}\right) \qquad (4.23)$$

$$\Phi_2(t) = \tan^{-1}\left(\frac{2t}{n^2 kw_o^2}\right) \qquad (4.24)$$

$$\Phi_2(t + d) = \tan^{-1}\left[\frac{2}{kw_o^2}\left(d + \frac{t}{n^2}\right)\right] \qquad (4.25)$$

$$kw_o^2 = 2\sqrt{(d + t/n^2)(R_o - d - t/n^2)} \qquad (4.15)$$

which are the same for both symmetrical and asymmetrical modes.

Let

$$\Phi_t = \Phi_1(t)$$

$$\Phi_d = \Phi_2(t + d) - \Phi_2(t) \qquad (4.26)$$

Equations (4.21) and (4.22) can be written as

$$-\frac{1}{n}\cot(nk_s t - \Phi_t) + \tan(k_s d - \Phi_d) = 0 \qquad (4.27)$$

$$\frac{1}{n}\tan(nk_a t - \Phi_t) + \tan(k_a d - \Phi_d) = 0 \qquad (4.28)$$

The dielectric constant can be found by solving these two equations for n using either a numerical method or an approximate method.

4.5 Computer Solutions for the Transcendental Equations

Equations (4.27) and (4.28) can easily be solved for the refraction index n by using a computer. If d, t and f_s (or f_a) are known values obtained from the measurements, both equations can be written in the form

$$f(n) = 0 \tag{4.29}$$

which can be solved numerically by means of Mueller's iteration scheme of successive bisection and inverse parabolic interpolation. A computer programme, in which a standard subroutine RTMI[34] is called to solve the transcendental equation using this iteration scheme, has been written to find ε_r and is included in Appendix II. In addition to input data on d, t and f, input values which specify the initial left and right bounds of the root n and the upper bound of the resultant error have to be entered into the programme when it is used.

Experimental procedures can be greatly simplified if the dielectric constant of a sample of known thickness can be determined from the measured values of f_s and f_a only, without the knowledge of d. In this case, (4.27) and (4.28) can be written in the form

$$\begin{aligned} f(n, d) &= 0 \\ g(n, d) &= 0 \end{aligned} \tag{4.30}$$

and can be solved simultaneously for both n and d using the method of minimization. In this method, solving the pair of equation in (4.30) is equivalent to minimizing

$$S(n, d) = \{f(n, d)\}^2 + \{g(n, d)\}^2 \tag{4.31}$$

A standard subroutine $VA_{04}A$ for finding the minimum of a function of several variables[35] can be used for this purpose. This forms a part of the programme for the determination of ε_r by solving (4.27) and (4.28) simultaneously. This programme is also included in Appendix II.

In view of the periodic nature of the tangent function, there exists an infinite number of solutions for ε_r. It is consequently either necessary to know ε_r approximately in order to pick the right solution, or to perform a second identical experiment with a sample of different thickness. In the former case, an approximate value of ε_r can be obtained using the formulas derived in the following section. The proper solution in the latter case is the one common to the two sets of solutions. Graphically this is an intersection point as shown in Fig. 4.4 for a particular case.

4.6 Approximate Solutions for the Transcendental Equations

4.6.1 First Approximation

If $\lambda << d$, the frequency change from k_a to k_s will be relatively small, and we may assume that

$$k_a = k_s - k_1 \tag{4.32}$$

$$nk_1t << 1 \tag{4.33}$$

By applying Taylor's expansion to the left-hand side, (4.28) can be written as

$$\frac{1}{n}\tan(nk_st - \Phi_t) - k_1t\sec^2(nk_st - \Phi_t) = -\tan(k_ad - \Phi_d) \tag{4.34}$$

where the higher order terms in nk_1t has been neglected.

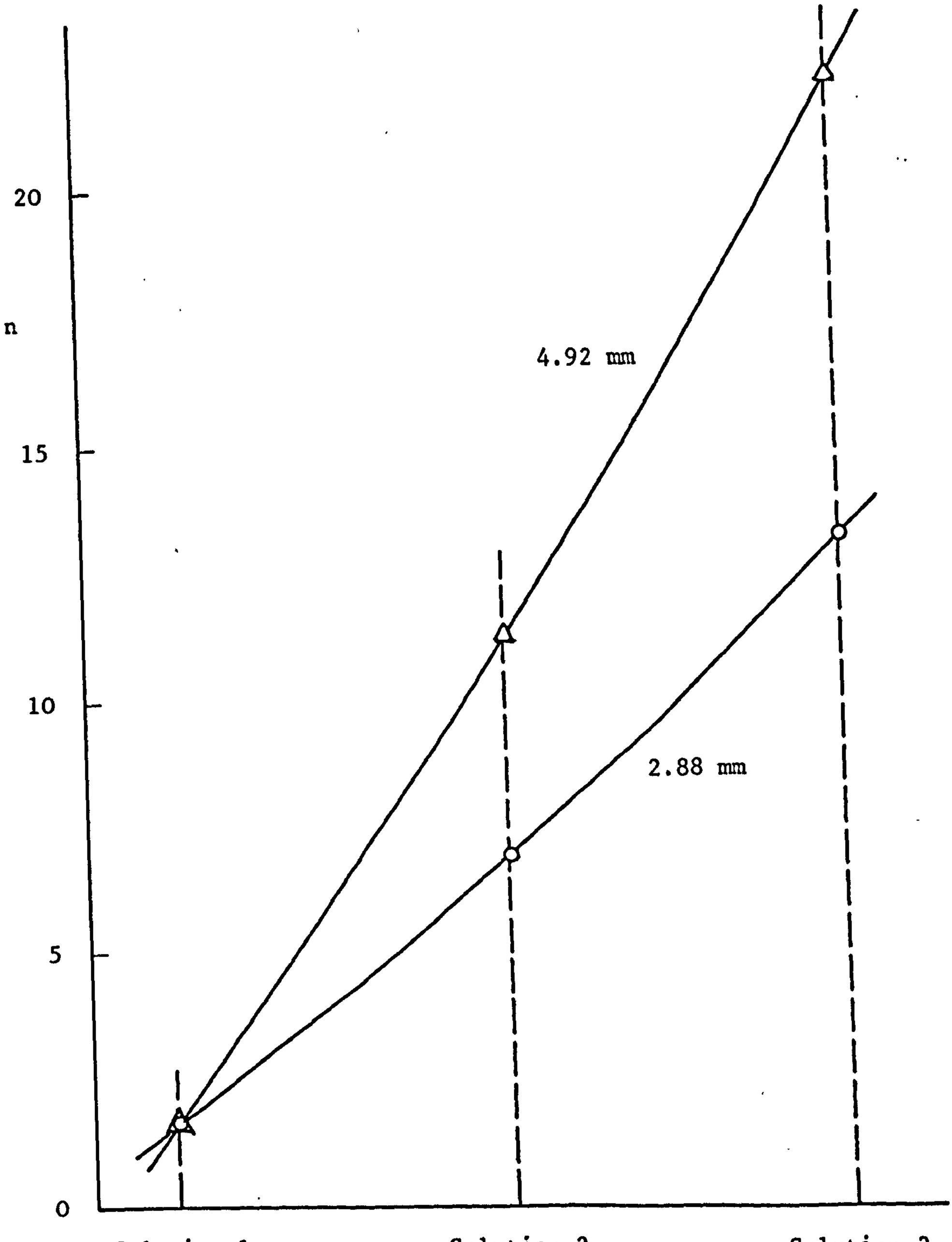

FIG. 4.4 Solution for n obtained from the measurement of two sample of different thickness

From (4.27)

$$\tan(nk_s t - \Phi_t) = \frac{1}{n} \cot(k_s d - \Phi_d) \tag{4.35}$$

Substitution of (4.35) into (4.34) gives

$$\frac{1}{n^2} \cot(k_s d - \Phi_d) - k_1 t\{1 + \frac{1}{n^2} \cot^2(k_s d - \Phi_d)\} = -\tan(k_a d - \Phi_d) \tag{4.36}$$

Solving this equation for n^2, we have

$$\varepsilon_r = - \frac{\cot(k_s d - \Phi_d) - k_1 t \cot^2(k_s d - \Phi_d)}{\tan(k_a d - \Phi_d) - k_1 t} \tag{4.37}$$

Since higher order terms in $\tan(nk_s t - \Phi_t)$ have been neglected in the Taylor's expansion, (4.37) can be used if

$$|\tan(nk_s t - \Phi_t)| \leqslant 1 \tag{4.38}$$

or, from (4.35)

$$|\cot(k_s d - \Phi_d)| \leqslant n \tag{4.39}$$

By similar operations expanding (4.27), a complementary formula for ε_r can be obtained as

$$\varepsilon_r = - \frac{\cot(k_a d - \Phi_d) + k_1 t \cot^2(k_a d - \Phi_d)}{\tan(k_s d - \Phi_d) + k_1 t} \tag{4.40}$$

which can be used if

$$|\cot(nk_a t - \Phi_t)| \leqslant 1 \tag{4.41}$$

or

$$|\cot(k_a d - \Phi_d)| \leqslant n \tag{4.42}$$

Strictly speaking, Φ_d is a function of n and, from (4.26), (4.24), (4.25) and (4.15), can be written as

$$\Phi_d = \tan^{-1}\left[\frac{2}{kw_o^2}(d + \frac{t}{n^2})\right] - \tan^{-1}(\frac{2t}{n\ kw_o^2})$$

$$= \tan^{-1}\left[\frac{d}{R_o - d}\sqrt{\frac{R_o}{d + t/n^2} - 1}\right] \qquad (4.43)$$

The term involving n in (4.43) can frequently be neglected with very little error. This can be done by using a large mirror spacing when comparing with the thickness of the dielectric sample. Equation (4.43) then becomes

$$\Phi_d = \tan^{-1}\sqrt{\frac{d}{R_o - d}} \qquad (4.44)$$

If the condition $d >> t/n^2$ can not be fulfilled and the error involved in neglecting this term is found to be large, then an iterative procedure can be followed to find ε_r. First, an approximate value for ε_r can be calculated from (4.37) and (4.44). This value of ε_r can be used to calculate Φ_d from (4.43). Knowing Φ_d, a more accurate ε_r can be found from (4.37).

4.6.2 Second Approximation

The accuracy of the formula (4.37) can be improved by including second order terms in the expansion of (4.28) as

$$\frac{1}{n}\tan(nk_st - \Phi_t) - k_1t\sec^2(nk_st - \Phi_t) - nk_1^2t^2\tan(nk_st - \Phi_t)\sec^2(nk_st - \Phi_t)$$

$$= -\tan(k_ad - \Phi_d) \qquad (4.45)$$

Substituting (4.35) into (4.45) and solving for n^2, we find

$$\varepsilon_r = -\frac{\cot(k_sd - \Phi_d) - k_1t\cot^2(k_sd - \Phi_d) - k_1^2t^2\cot^3(k_sd - \Phi_d)}{\tan(k_ad - \Phi_d) - k_1t - k_1^2t^2\cot(k_sd - \Phi_d)} \qquad (4.46)$$

As before, this formula can be used if $|\cot(k_sd - \Phi_d)| \leq n$.

In the same way, by including second order terms, (4.40) can be replaced by

$$\varepsilon_r = - \frac{\cot(k_a d - \Phi_d) + k_1 t \cot^2(k_a d - \Phi_d) + k_1^2 t^2 \cot^3(k_a d - \Phi_d)}{\tan(k_s d - \Phi_d) + k_1 t + k_1^2 t^2 \cot(k_a d - \Phi_d)} \quad (4.47)$$

which can be used if $|\cot(k_a d - \Phi_d)| \leq n$.

4.6.3 Accuracy of the Approximate Formulas

The accuracy of formulas (4.37) and (4.40) can be studied by comparing with those including second order terms. Considering (4.37) and (4.46) first, we have

$$\varepsilon_{r1} = - \frac{\cot S - k_1 t \cot^2 S}{\tan A - k_1 t} \quad (4.48)$$

$$\varepsilon_{r2} = - \frac{\cot S - k_1 t \cot^2 S - k_1^2 t^2 \cot^3 S}{\tan A - k_1 t - k_1^2 t^2 \cot S} \quad (4.49)$$

where

$$S = k_s d - \Phi_d$$
$$A = k_a d - \Phi_d \quad (4.50)$$

The error $\delta\varepsilon_r$ is given by

$$\delta\varepsilon_r = \varepsilon_{r2} - \varepsilon_{r1} \quad (4.51)$$

Maximum error due to the approximation occurs under the limiting conditions

$$\cot S \approx \pm n$$
$$\tan A \approx \pm n \quad (4.52)$$

Combining (4.48), (4.49), (4.50) and (4.52), and dividing the resulting equation by n , we have

$$\frac{\delta\varepsilon_r}{\varepsilon_r} \leqslant \frac{2n^2k_1{}^2t^2}{(1 \pm nk_1t)(1 \pm nk_1t + n^2k_1{}^2t^2)} \tag{4.53}$$

Similarly, from (4.40) and (4.47), we find

$$\frac{\delta\varepsilon_r}{\varepsilon_r} \leqslant \frac{-2n^2k_1{}^2t^2}{(1 \pm nk_1t)(1 \pm nk_1t - n^2k_1{}^2t^2)} \tag{4.54}$$

When $nk_1t \ll 1$ both (4.53) and (4.54) can be approximated by

$$\left|\frac{\delta\varepsilon_r}{\varepsilon_r}\right| \leqslant 2n^2k_1{}^2t^2 \tag{4.55}$$

This sets an error limit to (4.37) and (4.40) due to the approximations made.

4.7 Correction for Plane Dielectric Surfaces

It has so far been assumed that the sample surfaces are spherical and coincident with the equiphase surfaces forming a perfectly matched system. This condition, however, is very difficult to fulfil in practice, and dielectric sheet sample having two parallel flat surfaces is usually used. The measured dielectric constant can be corrected by applying corrections to the resonant frequencies to account for the error so introduced. These corrections can be derived using perturbation theory.

Let $\bar{E}$, $\bar{H}$, ω represent the field and resonant frequency of the resonator with dielectric sample of spherical surfaces at the centre, and let $\bar{E} + \bar{E}'$, $\bar{H} + \bar{H}'$, $\omega + \delta\omega$ represent the corresponding quantities of the perturbed resonator having plane dielectric surfaces. In both cases, the Maxwell's equations must be satisfied, that is

$$\nabla \times \bar{E} = -j\omega\bar{B} \tag{4.56}$$

$$\nabla \times \bar{H} = j\omega\bar{D} \tag{4.57}$$

$$\nabla \times (\bar{E} + \bar{E}') = -j(\omega + \delta\omega)(\bar{B} + \bar{B}') \tag{4.58}$$

$$\nabla \times (\bar{H} + \bar{H}') = j(\omega + \delta\omega)(\bar{D} + \bar{D}') \tag{4.59}$$

Here
$$\bar{D}' = \varepsilon_o\{\varepsilon_r(\bar{E} + \bar{E}') - \bar{E}\}$$
$$\bar{B}' = \mu_o\bar{H}' \tag{4.60}$$

inside the volume $2V_1$ bounded by the plane and the original spherical dielectric surfaces as shown in Fig. 4.5, and

$$\bar{B} = \mu_o\bar{H} \qquad \bar{D} = \varepsilon\bar{E}$$
$$\bar{B}' = \mu_o\bar{H}' \qquad \bar{D}' = \varepsilon\bar{E}' \tag{4.61}$$

outside $2V_1$, ε being a function of position.

Subtracting (4.56) from (4.58), we have

$$\nabla \times \bar{E}' = -j\{\omega\bar{B}' + \delta\omega(\bar{B} + \bar{B}')\} \tag{4.62}$$

Scalarly multiplying (4.57) by $\bar{E}'$ and (4.62) by $\bar{H}$, we obtain

$$\bar{E}'\cdot\nabla \times \bar{H} = j\omega\bar{E}'\cdot\bar{D} \tag{4.63}$$

$$\bar{H}\cdot\nabla \times \bar{E}' = -j\omega\bar{H}\cdot\bar{B}' - j\delta\omega(\bar{H}\cdot\bar{B} + \bar{H}\cdot\bar{B}') \tag{4.64}$$

Subtracting and applying the identity

$$\nabla\cdot(\bar{A} \times \bar{B}) = \bar{B}\cdot\nabla \times \bar{A} - \bar{A}\cdot\nabla \times \bar{B}$$

we have

$$\nabla\cdot(\bar{H} \times \bar{E}') = j\omega(\bar{E}'\cdot\bar{D} + \bar{H}\cdot\bar{B}') + j\delta\omega(\bar{H}\cdot\bar{B} + \bar{H}\cdot\bar{B}') \tag{4.65}$$

Similarly, from (4.57) and (4.59), we find

$$\nabla\cdot(\bar{E} \times \bar{H}') = -j\omega(\bar{H}'\cdot\bar{B} + \bar{E}\cdot\bar{D}') - j\delta\omega(\bar{E}\cdot\bar{D} + \bar{E}\cdot\bar{D}') \qquad (4.66)$$

The sum of the last two equations is integrated over the volume of the resonator $2V_o$ bounded by the mirrors and a hyperbolic surface S_h, and the divergence theorem is applied to the left-hand terms. The left-hand terms then vanish, because both $\hat{n} \times \bar{E} = 0$ and $\hat{n} \times \bar{E}' = 0$ on the boundary surfaces (see Section 5.3). The resulting equation is

$$0 = j\omega\int_{2V_o} (\bar{E}'\cdot\bar{D} - \bar{E}\cdot\bar{D}')dV + j\delta\omega\int_{2V_o} \{(\bar{H}\cdot\bar{B} - \bar{E}\cdot\bar{D}) + (\bar{H}\cdot\bar{B}' - \bar{E}\cdot\bar{D}')\}dV \qquad (4.67)$$

In the region $2V_o - 2V_1$, the contribution to the first term cancels with that to the second term in the first integral. Thus we only require the contribution to this integral from the region $2V_1$. Neglecting $\bar{D}'$ and $\bar{B}'$ in comparison with $\bar{D}$ and $\bar{B}$ in the second integral, (4.67) becomes

$$\frac{\delta\omega}{\omega} = \frac{\int_{2V_1} (\bar{E}'\cdot\bar{D} - \bar{E}\cdot\bar{D}')dV}{\int_{2V_o} (\bar{E}\cdot\bar{D} - \bar{H}\cdot\bar{B})dV} \qquad (4.68)$$

Assuming that the additional field E' is so small that it can be neglected in comparison with E, (4.68) then becomes

$$\frac{\delta\omega}{\omega} = -\frac{\int_{2V_1} \bar{E}\cdot\bar{D}'dV}{\int_{2V_o} (\bar{E}\cdot\bar{D} - \bar{H}\cdot\bar{B})dV} \qquad (4.69)$$

where $$\bar{D}' = \varepsilon_o(\varepsilon_r - 1)\bar{E} \qquad (4.70)$$

In the perturbed volume, the field has very little variation with z and the electric field can be written as

$$E = \frac{w_o}{w_t} \exp(-\frac{r^2}{w_t^2}) \sin(kd - \Phi_d) \qquad (4.71)$$

where $w_t = w_1(t) = w_2(t)$, being the beam radius at the interfaces.

Let the elementary volume be $dV = \frac{\pi r^3}{R_t} dr$ (Fig. 4.5), where $R_t = R(t)$, the radius of curvature of the phase front intersecting the z-axis at z = t. The numerator on the left-hand side of (4.69) can be written as

$$\int_{2V_1} \bar{E}\cdot\bar{D}'dV = \frac{2\pi w_o^2 \varepsilon_o}{R_t w_t^2} (\varepsilon_r - 1)\sin^2(kd - \Phi_d)\int_o^\infty r^3 \exp(-\frac{2r^2}{w_t^2})dr \qquad (4.72)$$

Since

$$\int_o^\infty r^3 \exp(-\frac{2r^2}{w_t^2})dr = \frac{w_t^4}{8} \qquad (4.73)$$

using (4.73) and (3.9), (4.72) becomes

$$\int_{2V_1} \bar{E}\cdot\bar{D}'dV = \frac{\pi t \varepsilon_o}{\varepsilon_r k^2} (\varepsilon_r - 1)\sin^2(kd - \Phi_d) \qquad (4.74)$$

Let W be the total energy stored in the unperturbed resonator. We have

$$\int_{2V_o} (\bar{E}\cdot\bar{D} - \bar{H}\cdot\bar{B})dV = 4W \qquad (4.75)$$

Substituting (4.72) and (4.75) into (4.69), and using (5.39) for W, we obtain

$$\frac{\delta\omega}{\omega} = -\frac{t(\varepsilon_r - 1)\sin^2(kd - \Phi_d)}{\varepsilon_r k^2 w_o^2 (\Delta t + d)} \qquad (4.76)$$

This gives the amount of frequency shift due to small perturbations of the interfaces, and can be applied to both symmetrical and asymmetrical modes.

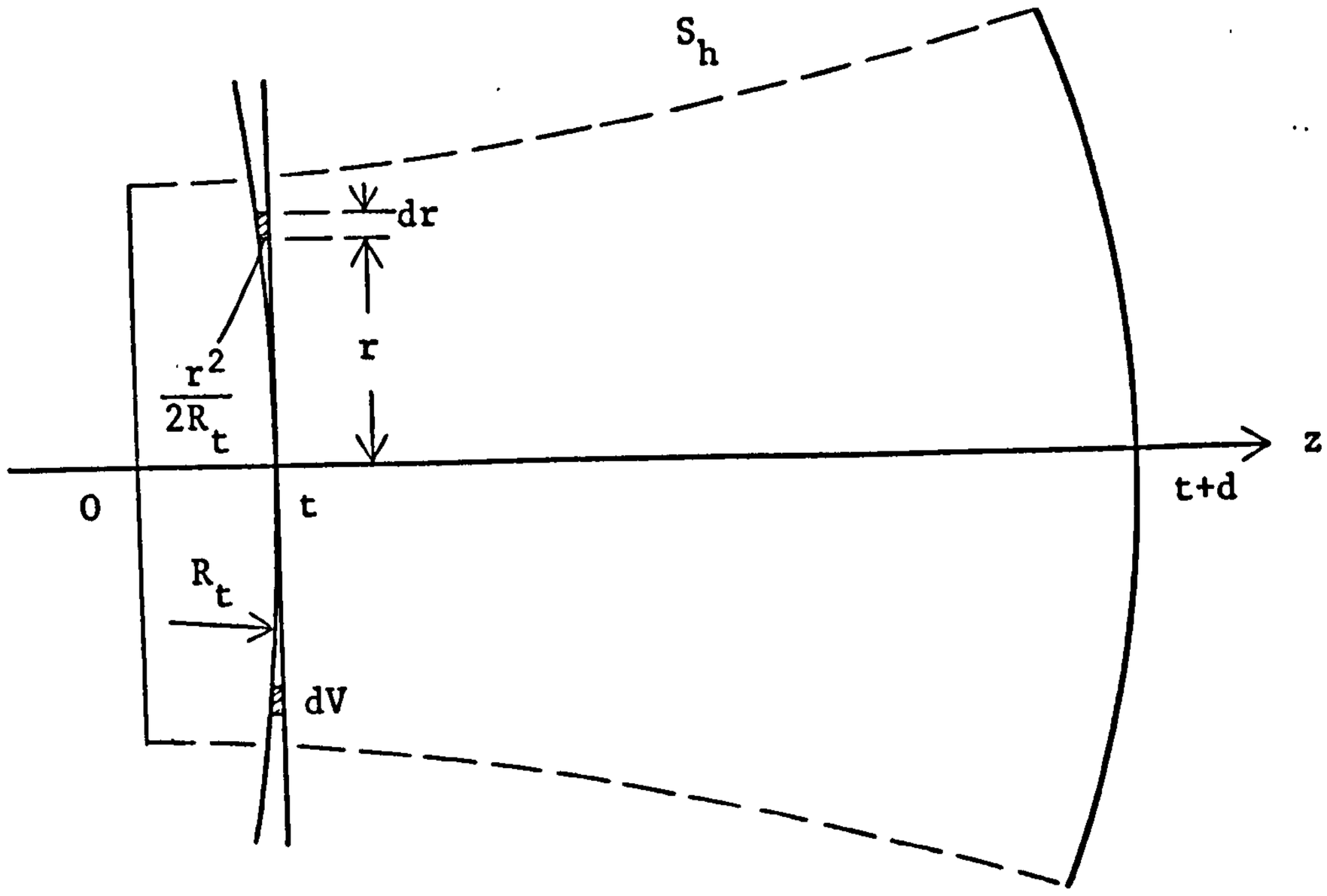

FIG. 4.5 Element of volume

CHAPTER 5

MEASUREMENT OF LOSS TANGENT

5.1 Energy Stored in an Open Resonator

The Q-factor of the resonator may be defined in the usual way as

$$Q = \frac{\omega \times \text{energy stored}}{\text{power lost}} \tag{5.1}$$

Since the loss tangent is determined by measurements of Q with and without the dielectric sample in the resonator, a knowledge of the energy stored in an open resonator is essential before we derive a formula for the calculation of loss tangent.

5.1.1 Without Dielectric Sample

The electric field inside an empty resonator can be written as

$$E_x = \frac{w_o}{w} \exp(-\frac{r^2}{w^2}) \begin{matrix}\cos\\ \sin\end{matrix}(kz - \Phi - \frac{kr^2}{2R}) \tag{5.2}$$

where the cosine and the sine functions are for symmetrical and asymmetrical modes respectively, and w, R and Φ are given by (3.6), (3.7), and (3.8).

Let
$$z' = z - \frac{r^2}{2R} \tag{5.3}$$

Using (3.9), this can be written as

$$z' = z\left(1 - \frac{2r^2}{k^2 w_o^2 w^2}\right) \tag{5.4}$$

Then

$$z = \frac{z'}{1 - \frac{2r^2}{k^2 w_o^2 w^2}} \tag{5.5}$$

Substituting (5.5) into (3.6), w can be approximated by

$$w^2 = w'^2 + \frac{4r^2}{k^2 w_o^4 w^2} \tag{5.6}$$

where

$$w'^2 = w_o^2\left[1 + \left(\frac{2z'}{kw_o^2}\right)^2\right] \tag{5.7}$$

When $r < a_m$, the second term on the right-hand side of (5.6) can be neglected with very little error.

Similarly, Φ can be approximated by Φ' where

$$\Phi' = \tan^{-1}\left(\frac{2z'}{kw_o^2}\right) \tag{5.8}$$

Equation (5.1) then becomes

$$E_x = \frac{w_o}{w'}\exp\left(-\frac{r^2}{w'^2}\right)\begin{matrix}\cos\\ \sin\end{matrix}(kz' - \Phi') \tag{5.9}$$

As shown in Fig. 5.1 where ABC is an equiphase surface, the elementary volume will be taken as the ring

$$dV = 2\pi r\, dr\, dz' \tag{5.10}$$

At resonance the time-average electric and magnetic energy stored in the resonator are equal. The average stored electric energy is given by

$$W_e = \frac{\varepsilon_o}{4}\int_V |E_x|^2 dV$$

$$= \pi w_o^2 \varepsilon_o \int_o^{D/2}\int_o^{\infty} \frac{r}{w'^2}\exp\left(-\frac{2r^2}{w'^2}\right)\begin{matrix}\cos^2\\ \sin^2\end{matrix}(kz' - \Phi')dr\, dz' \tag{5.11}$$

The upper limit of the r-integration is taken as infinity sine the field is negligible when r is larger than the radius of the mirrors.

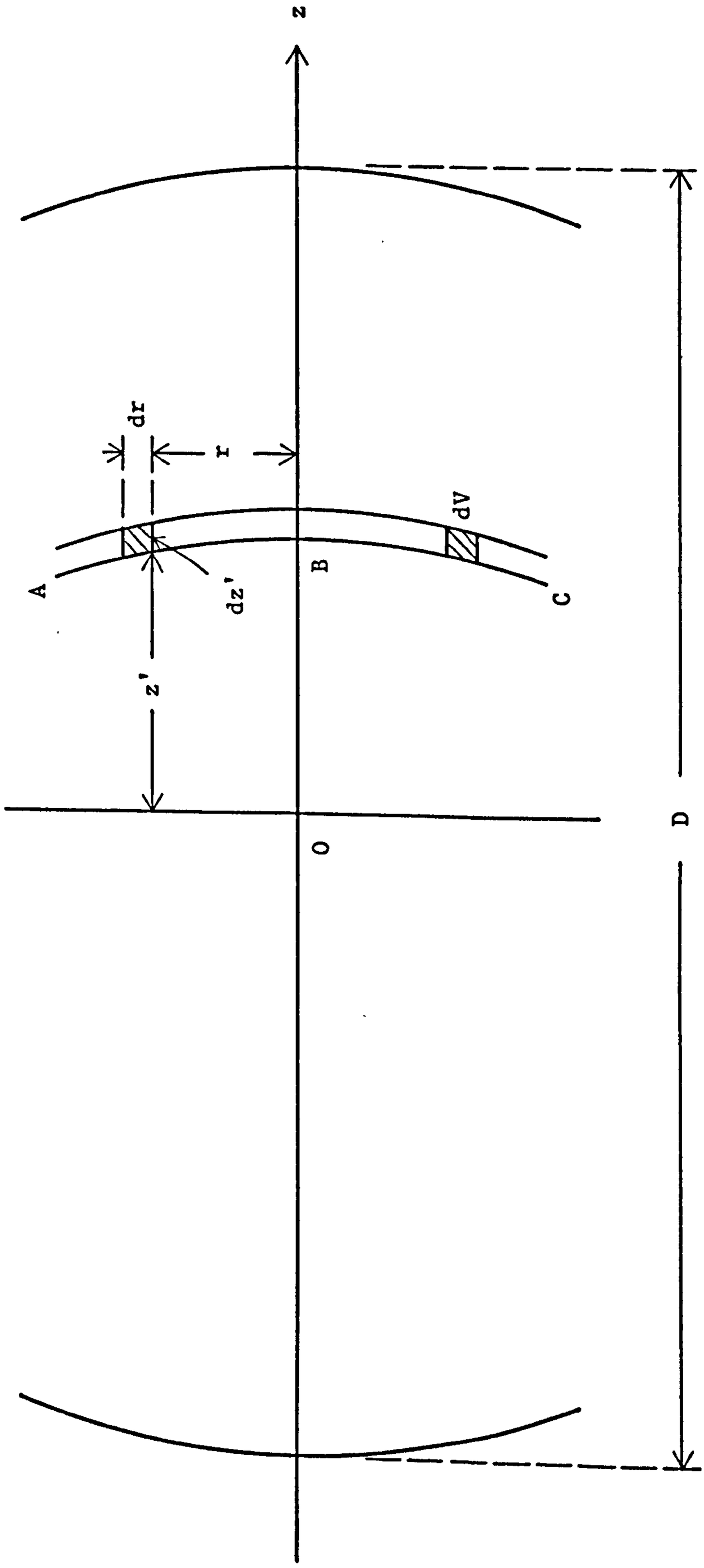

FIG. 5.1 Element of volume in an open resonator

Since the variable of intergration in a definite integral is of no importance, (5.11) can be written as

$$W_e = \pi w_o^2 \varepsilon_o \int_0^{D/2} \int_0^{\infty} \frac{r}{w^2} \exp(-\frac{2r^2}{w^2}) \sin^2(kz - \Phi) dr\, dz \qquad (5.12)$$

Integrating with respect to r from zero to infinity, we have

$$W_e = \frac{\pi w_o^2 \varepsilon_o}{4} \int_0^{D/2} \cos^2 \sin^2(kz - \Phi) dz$$

$$= \frac{\pi w_o^2 \varepsilon_o}{8} \int_0^{D/2} \{1 \pm \cos 2(kz - \phi)\} dz \qquad (5.13)$$

Let us consider the integral

$$I = \int_0^{D/2} \cos 2(kz - \Phi) dz$$

$$= \int_0^{D/2} \frac{1}{2(k - 2/kw^2)} d\sin 2(kz - \Phi) \qquad (5.14)$$

Integrating by parts, this becomes

$$I = \frac{\sin\{kD - 2\Phi(D/2)\}}{2\{k - 2/kw^2(D/2)\}} - \int_0^{D/2} \frac{2\sin 2(kz - \phi)}{Rkw^2(k - 2/kw^2)^2} dz \qquad (5.15)$$

Since $kD - 2\Phi(D/2) = \pi(q + 1)$ where $q = 0, 1, 2, 3...$, the first term on the right-hand side of (5.15) vanishes. The integral becomes

$$I = -\int_0^{D/2} \frac{I}{Rkw^2(k - 2/kw^2)^3} d\cos 2(kz - \Phi) \qquad (5.16)$$

Integrating by parts again, we obtain

$$I = \frac{1}{R_o kw^2(D/2)\{k - 2/kw^2(D/2)\}^3} + \int_0^{D/2} \cos 2(kz - \Phi)\, d\left[\frac{1}{Rkw^2(k - 2/kw^2)^3}\right] \qquad (5.17)$$

If we continue this operation, the integral in (5.17) will yield a series of terms that are very small in comparison with D/2 and can be neglected.

Substitution of (5.13) into (5.17) yields

$$W_e = \frac{\pi w_o^2 \varepsilon_o}{8}\left[\frac{D}{2} \pm \frac{1}{R_o kw^2(D/2)\{k - 2/kw^2(D/2)\}^3}\right] \qquad (5.18)$$

Hence the total energy stored in the resonator is given by

$$W = 2W_e = \frac{\pi w_o^2 \varepsilon_o D}{8}\left[1 \pm \frac{2}{R_o kw^2(D/2)\{k - 2/kw^2(D/2)\}^3}\right] \qquad (5.19)$$

where

$$R_o = R(D/2) = \frac{D}{2}\left[1 + \left(\frac{kw_o^2}{D}\right)^2\right]$$
$$w^2(D/2) = w_o^2\left[1 + \left(\frac{D}{kw_o^2}\right)^2\right] \qquad (5.20)$$

being the radius of curvature of the mirrors and the beam radius at the mirrors respectively. The plus sign in (5.19) is for symmetrical mode and the minus sign is for asymmetrical mode. If $k^2w_o^2 >> 1$, the second term on the left-hand side of (5.19) is much smaller than 1, and can usually be neglected.

5.1.2 With Dielectric Sample

Electric fields in a resonator with the dielectric sample at the centre can be written as

$$E_1 = \frac{A_1 w_o}{w_1}\exp(-\frac{r^2}{w_1^2}) \begin{matrix}\cos\\ \sin\end{matrix}\{nkz - \Phi_1(z)\}, \qquad 0 \leqslant z \leqslant t \qquad (4.16)$$

$$E_2 = \frac{w_o}{w_2}\exp(-\frac{r^2}{w_2^2})\sin\{k(z - t - d) - \Phi_2(z) + \Phi_2(t + d)\}, \quad t \leqslant z \leqslant t + d \qquad (4.17)$$

where for symmetrical mode, the amplitude factor A_1 has the value

$$A_{1s} = - \frac{\sin(k_s d - \Phi_d)}{\cos(nk_s t - \Phi_t)} \tag{5.21}$$

and for asymmetrical mode, it has the value

$$A_{1a} = - \frac{\sin(k_a d - \Phi_d)}{\sin(nk_a t - \Phi_t)} \tag{5.22}$$

If the lossy dielectric material has a permittivity $\varepsilon = \varepsilon' - j\varepsilon''$, the time-average electric energy stored in the resonator is given by

$$W_e = \frac{\varepsilon'}{4} \int_{2V_1} |E_1|^2 dV + \frac{\varepsilon_o}{4} \int_{2V_2} |E_2|^2 dV \tag{5.23}$$

where $2V_1$ and $2V_2$ are the volume in regions 1 and 2 of the resonator respectively.

Consider first the integral

$$I_1 = \int_{2V_1} |E_1|^2 dV \tag{5.24}$$

Taking an element of volume $dV = 2\pi r\, dr\, dz'$ and following similar procedures as those in the previous section, we have

$$I_1 = 4\pi w_o^2 |A_1|^2 \int_0^t \int_0^\infty \frac{r}{w_1^2} \exp(-\frac{2r^2}{w_1^2}) \cos^2 \sin^2\{nkz - \Phi_1(z)\} dr\, dz$$

$$\simeq \frac{\pi w_o^2 |A_1|^2}{2} \left[t \pm \frac{\sin 2(nkt - \Phi_t)}{2(nk - 2/nkw_t^2)} \right] \tag{5.25}$$

where $\Phi_t = \Phi_1(t)$ and $w_t = w_1(t) = w_2(t)$ being the additional phase shift and the beam radius at the interfaces.

In the same way, the second integral in (5.21) can be written as

$$I_2 = \int_{2V_2} |E_2|^2 dV$$

$$= 4\pi w_o^2 \int_t^{t+d} \int_o^{\infty} \frac{r}{w_2^2} \exp(-\frac{2r^2}{w_2^2}) \sin^2\{k(z - t - d) - \Phi_2(z) + \Phi_2(t + d)\} dr\, dz \quad (5.26)$$

Integrating by parts and neglecting small terms, we have

$$I_2 \simeq \frac{\pi w_o^2}{2} \left[d - \frac{\sin 2(kd - \Phi_d)}{2(k - 2/kw_t^2)} \right] \quad (5.27)$$

From (5.23), (5.26) and (5.27), the total energy stored in the resonator with the dielectric sample at the centre is

$$W = \frac{\pi w_o^2 \varepsilon_o}{4} \left\{ \varepsilon_r |A_1|^2 \left[t \pm \frac{\sin 2(nkt - \Phi_t)}{2(nk - 2/nkw_t^2)} \right] + \left[d - \frac{\sin 2(kd - \Phi_d)}{2(k - 2/kw_t^2)} \right] \right\} \quad (5.28)$$

where the positive sign in the first square bracket is for symmetrical mode and the negative sign is for asymmetrical mode.

Now let us consider

$$\cot(nk_s t - \Phi_t) = n \tan(k_s d - \Phi_d) \quad (4.27)$$

$$\tan(nk_a t - \Phi_t) = -n \tan(k_a d - \Phi_d) \quad (4.28)$$

Squaring and adding 1 to both sides of (4.27), we have

$$\cot^2(nk_s t - \Phi_t) + 1 = n^2 \tan^2(k_s d - \Phi_d) + 1 \quad (5.29)$$

Hence

$$\sin^2(nk_s t - \Phi_t) = \frac{1}{\Delta_s} \cos^2(k_s d - \Phi_d) \quad (5.30)$$

$$\cos^2(nk_s t - \Phi_t) = \frac{n}{\Delta_s} \sin^2(k_s d - \Phi_d) \quad (5.31)$$

$$\sin 2(nk_s t - \Phi_t) = 2n \sin^2(nk_s t - \Phi_t) \tan(k_s d - \Phi_d)$$

$$= \frac{n}{\Delta_s} \sin 2(k_s d - \Phi_d) \quad (5.32)$$

where $$\Delta_s = n^2\sin^2(k_s d - \Phi_d) + \cos^2(k_s d - \Phi_d)$$

$$= \frac{n^2}{n^2\sin^2(nk_s t - \Phi_t) + \cos^2(nk_s t - \Phi_t)} \tag{5.33}$$

Similarly, from (4.28), we obtain

$$\sin^2(nk_a t - \Phi_t) = \frac{n^2}{\Delta_a}\sin^2(k_a d - \Phi_d) \tag{5.34}$$

$$\cos^2(nk_a t - \Phi_t) = \frac{1}{\Delta_a}\cos^2(k_a d - \Phi_d) \tag{5.35}$$

$$\sin2(nk_a t - \Phi_t) = -\frac{n}{\Delta_a}\sin2(k_a d - \Phi_d) \tag{5.36}$$

where $$\Delta_a = n^2\sin^2(k_a d - \Phi_d) + \cos^2(k_a d - \Phi_d)$$

$$= \frac{n^2}{n^2\cos^2(nk_a t - \Phi_t) + \sin^2(nk_a t - \Phi_t)} \tag{5.37}$$

Using (5.31) and (5.34), (5.21)and (5.22) can be written as

$$|A_1|^2 = \frac{\Delta}{n^2} \tag{5.38}$$

where $A_1 = A_{1_s^a}$ and $\Delta = \Delta_s^a$. Let $\theta_s^a = nk_s^a t - \Phi_t$. Then the variation of $|A_1|^2$ with θ_s^a can be plotted as shown in Fig. 5.2. From these curves, it can be seen that $|A_1|^2$ has a value between 1 and $1/\varepsilon_r$ when the thickness of the dielectric sample varies from 0 to $\lambda/2$.

Substitution of (5.32), (5.36) and (5.38) into (5.28) yields

$$W = \frac{\pi w_o^2 \varepsilon_o}{4}\left[\Delta t + \frac{\sin2(kd - \Phi_d)}{2k(1 - 2/n^2k^2w_t^2)} + d - \frac{\sin2(kd - \Phi_d)}{2k(1 - 2/k^2w_t^2)}\right] \tag{5.39}$$

When $k^2w_o^2 >> 1$, (5.39) can be approximated by

$$W = \frac{\pi w_o^2 \varepsilon_o}{4}(\Delta t + d) \tag{5.40}$$

with very little error.

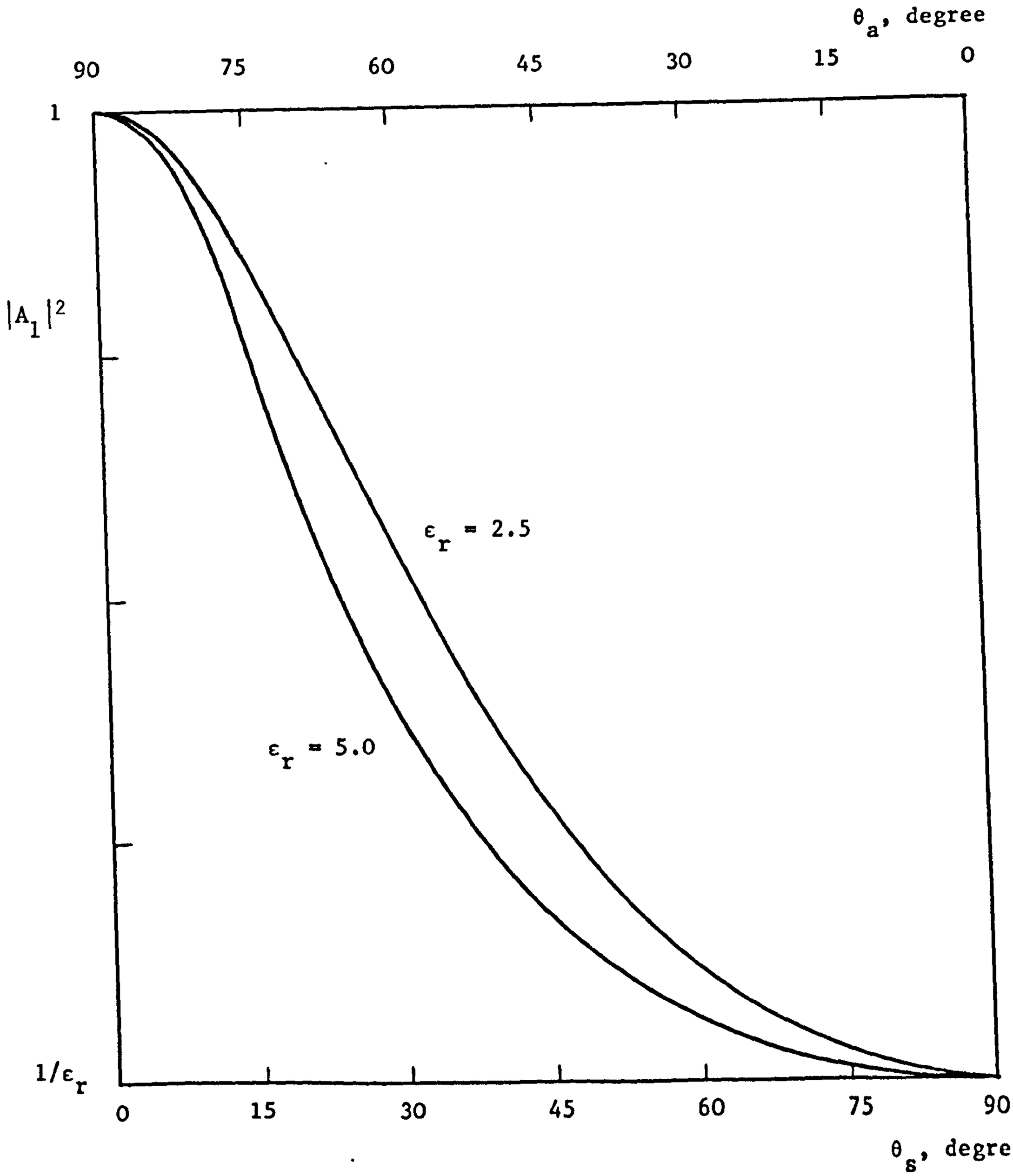

FIG. 5.2 Variation of $|A_1|^2$ with θ_a^s

5.2 Determination of Loss Tangent

Keeping the same resonator arrangement as shown in Fig. 4.1, the loss tangent measurement takes the form of Q-factor measurements with and without the dielectric sample. Let Q_o be the Q of the empty resonator, Q_L be the Q after insertion of the dielectric sample, and Q_ε be the Q due to the dielectric loss only. These three factors are related by

$$\frac{1}{Q_\varepsilon} = \frac{1}{Q_L} - \frac{1}{Q_o} \tag{5.41}$$

where it has been assumed that the energy stored, the diffraction losses and the coupling losses are approximately constant in the measurements.

The lossy dielectric material, of which the permittivity can be written as $\varepsilon = \varepsilon' - j\varepsilon''$, has an effective conductivity $\omega\varepsilon''$. Hence the power loss in the dielectric is

$$P = \frac{\omega\varepsilon''}{2} \int_{2V_1} |E_1|^2 dV = \frac{\omega\varepsilon' \tan\delta}{2} \int_{2V_1} |E_1|^2 dV \tag{5.42}$$

With the use of (5.1), we find that Q_ε is given by

$$Q = \frac{2\omega W_e}{P_\varepsilon} \tag{5.43}$$

Substitution of (5.23) and (5.42) into (5.43) yields

$$Q_\varepsilon = \frac{\int_{2V_1} |E_1|^2 dV + \frac{1}{\varepsilon_r} \int_{2V_2} |E_2|^2 dV}{\tan\delta \int_{2V_1} |E_1|^2 dV} \tag{5.44}$$

Using (5.25), (5.32), (5.36) and (5.39), this becomes

$$\tan\delta = \frac{1}{Q_\varepsilon}\left[\frac{\Delta t + d}{\Delta t + \sin 2(kd - \Phi_d) \,/\, 2k(1 - 2/n^2k^2w_t^2)}\right] \tag{5.45}$$

This is the required expression relating tanδ to the various measurable quantities, and is valid for both symmetrical and asymmetrical modes. The value of Δ can be calculated from (5.33) and (5.37) or obtained from a graph similar to those shown in Fig. 5.2.

5.3 Effect of Plane Interfaces on the Measurement of Loss Tangent

Equation (5.45) has been derived assuming that the interfaces are spherical forming a perfectly matched system with no reflection loss. If dielectric materical in sheet form is to be measured, the system is perturbed by the small volume of dielectric bounded by the plane and the original spherical interfaces. It can be considered that a polarization current $\bar{J}$ is induced in this small volume of which the effect on the measurement of loss tangent can be seen by considering the field excited by this current and the external source.

Let $\bar{E}_a$, $\bar{H}_a$ be the actual field in the resonator with excitation, and $\bar{E}_b$, $\bar{H}_b$ be the test field which exists when the mirrors are perfectly conducting, the dielectric surfaces are spherical, and there is no coupling aperture. Assuming the dielectric loss is negligible, we have for the actual field

$$\nabla \times \bar{E}_a = -j\omega\mu_o \bar{H}_a \tag{5.46}$$

$$\nabla \times \bar{H}_a = j\omega\epsilon \bar{E}_a + \bar{J} \tag{5.47}$$

and for the test field

$$\nabla \times \bar{E}_b = -j\omega_o\mu_o \bar{H}_b \tag{5.48}$$

$$\nabla \times \bar{H}_b = j\omega_o\epsilon \bar{E}_b \tag{5.49}$$

Multiplying (5.46) by $\bar{H}_b$ and (5.48) by $\bar{E}_a$ and subtract the second resulting equation from the first. This gives

$$\nabla\cdot(\bar{E}_a \times \bar{H}_b) = -j\omega\mu_o\bar{H}_a\cdot\bar{H}_b - j\omega_o\varepsilon\bar{E}_a\cdot\bar{E}_b \tag{5.50}$$

Similarly, from (5.47) and (5.48), we have

$$\nabla\cdot(\bar{E}_b \times \bar{H}_a) = -j\omega_o\mu_o\bar{H}_a\cdot\bar{H}_b - j\omega\varepsilon\bar{E}_a\cdot\bar{E}_b - \bar{E}_b\cdot\bar{J} \tag{5.51}$$

Dividing (5.50) by ω_o and (5.51) by ω and subtract the latter resulting equation from the former. We obtain

$$\frac{1}{\omega_o}\nabla\cdot(\bar{E}_a \times \bar{H}_b) - \frac{1}{\omega}\nabla\cdot(\bar{E}_b \times \bar{H}_a) = -j\mu_o\left(\frac{\omega}{\omega_o} - \frac{\omega_o}{\omega}\right)\bar{H}_a\cdot\bar{H}_b + \frac{1}{\omega}\bar{E}_b\cdot\bar{J} \tag{5.52}$$

Integration over the volume of the resonator V and application of the divergence theorem gives

$$\int_S\left\{\frac{1}{\omega_o}(\bar{E}_a \times \bar{H}_b)\cdot\hat{n} - \frac{1}{\omega}(\bar{E}_b \times \bar{H}_a)\cdot\hat{n}\right\}dS = -j\mu_o\left(\frac{\omega}{\omega_o} - \frac{\omega_o}{\omega}\right)\int_V\bar{H}_a\cdot\bar{H}_b dV + \frac{1}{\omega}\int_V\bar{E}_b\cdot\bar{J}\, dV \tag{5.53}$$

As shown in Fig. 5.3, the surface S can be devided up as: $2S_m$, the total surface of the two mirrors, S_h, a hyperbolic surface on which the surface integral vanishes since $\bar{E}_a \times \bar{H}_b$ and $\bar{E}_b \times \bar{H}_a$ are both parallel to the surface, and S_a, S_b the coupling apertures. Since E_b is zero on S_m, S_a and S_b, and the current $\bar{J} = j\omega\varepsilon_o(\varepsilon_r - 1)\bar{E}_a$ exists only within the volume 2V', (5.53) becomes

$$\int_{2S_m+S_a+S_b}(\bar{E}_a \times \bar{H}_b)\cdot\hat{n}\, dS = -j\omega_o\mu_o\left(\frac{\omega}{\omega_o} - \frac{\omega_o}{\omega}\right)\int_V\bar{H}_a\cdot\bar{H}_b dV + j\omega_o\varepsilon_o(\varepsilon_r - 1)\int_{2V'}\bar{E}_a\cdot\bar{E}_b dV \tag{5.54}$$

We next define $\bar{E}_a$ on the three surfaces. On the surfaces of the mirrors

$$\bar{E}_a = -Z_m\hat{n} \times \bar{H}_a \tag{5.55}$$

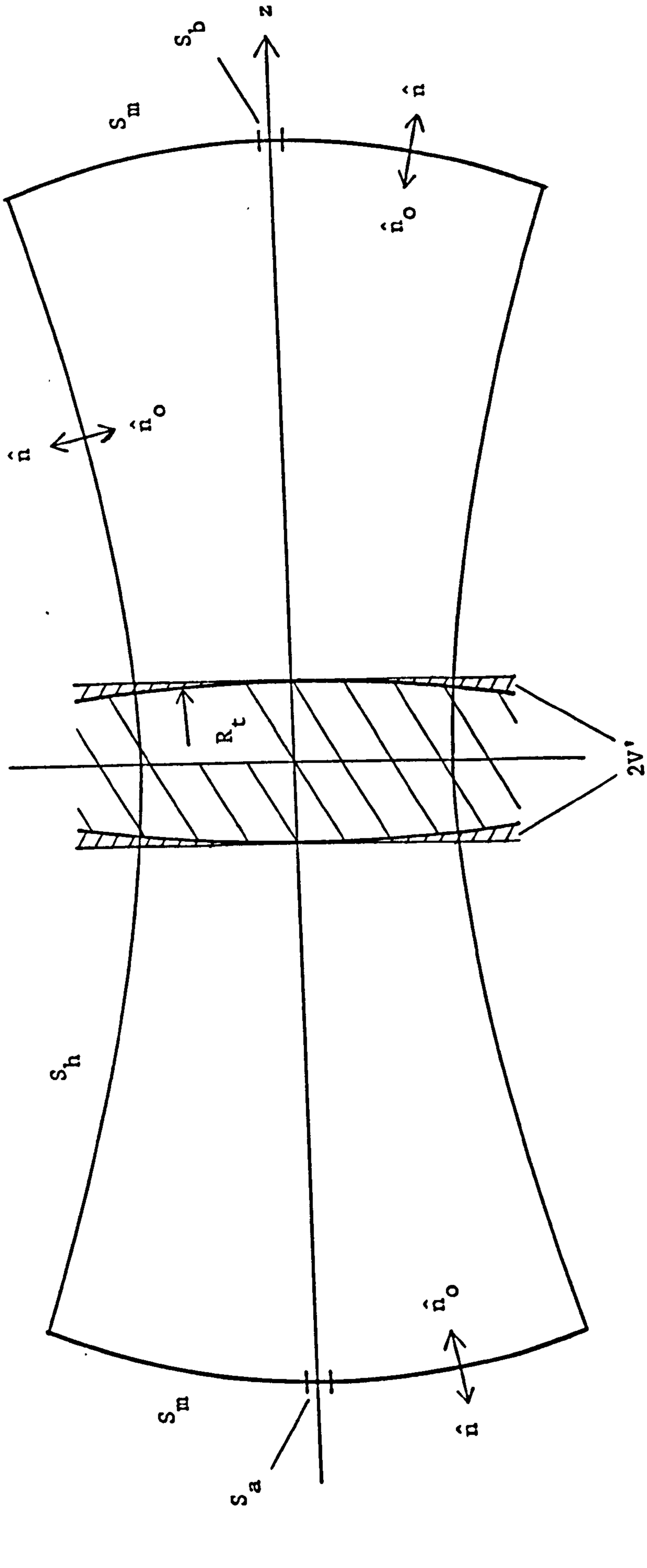

FIG. 5.3 Excitation of the open resonator

where $Z_m = \sqrt{j\omega\mu_o/\sigma}$, the surface impedance of the metal. The integrand on the left-hand side of (5.54) can be written as

$$(\bar{E}_a \times \bar{H}_b)\cdot\hat{n} = \hat{n}\cdot(\bar{E}_a \times \bar{H}_b) = \hat{n} \times \bar{E}_a \cdot \bar{H}_b$$

$$= -Z_m \hat{n} \times \hat{n} \times \bar{H}_a \cdot \bar{H}_b = Z_m \bar{H}_a \cdot \bar{H}_b \qquad (5.56)$$

On S_b, the output coupling aperture

$$\bar{E}_a = -Z_b \hat{n} \times \bar{H}_a \qquad (5.57)$$

where Z_b is the wave impedance presented by the detector to the output coupling aperture. The integrand becomes

$$(\bar{E}_a \times \bar{H}_b)\cdot\hat{n} = Z_b \bar{H}_a \cdot \bar{H}_b \qquad (5.58)$$

On S_a, the input coupling aperture

$$\bar{E}_a = \bar{E}_o \qquad (5.59)$$

This is the external excitation, and is assumed known.

Substitution of (5.56), (5.58) and (5.59) into (5.54) gives

$$\int_{S_a} (\bar{E}_o \times \bar{H}_b)\cdot\hat{n}\, dS = -2Z_m \int_{S_m} \bar{H}_a \cdot \bar{H}_b dS - Z_b \int_{S_b} \bar{H}_a \cdot \bar{H}_b dS - j\omega_o\mu_o\left(\frac{\omega}{\omega_o} - \frac{\omega_o}{\omega}\right)\int_V \bar{H}_a \cdot \bar{H}_b dV$$

$$+ j\omega_o\varepsilon_o(\varepsilon_r - 1)\int_{2V'} \bar{E}_a \cdot \bar{E}_b dV \qquad (5.60)$$

In the evaluation of the integral over S_m, the surface element may be written as $dS = 2\pi r\, dr$ and the surface integral becomes

$$2\pi \int_o^\infty \bar{H}_a \cdot \bar{H}_b r\, dr \qquad (5.61)$$

Strictly the coupling apertures, holes of radius a_o should be excluded, and the curvature of the mirrors should be taken into consideration. However, if $a_o << w_o$ and $R_o >> w_o$, then the error in the evaluation due to including the coupling aperture and neglecting the curvature of the mirrors will be very small. Also the upper limit of the integration is taken as infinity since the field is negligible when $r > a_m$. The integration is thereby simplified.

The mode most likely to be excited are those having circular symmetry, i.e. $\ell = 0$. For such modes, neglecting longitudinal component the magnetic field $\bar{H}_b = \hat{j}H_{yb}$ outside the dielectric may be written as

$$H_{yb} = \frac{w_o}{w_2} L^o_{p_b}\left(\frac{2r^2}{w_2^2}\right)\exp\left(-\frac{r^2}{w_2^2}\right)\cos\{kz - (2p_b + 1)\Phi_2 + \alpha\} \qquad (5.62)$$

At the mirrors, the field has the special value

$$H_{ybm} = \frac{w_o}{w_2} L^o_{p_b}\left(\frac{2r^2}{w_2^2}\right)\exp\left(-\frac{r^2}{w_2^2}\right) \qquad (5.63)$$

The magnetic field $\bar{H}_a = \hat{j}H_{ya}$ is assumed to be very closely that given by (5.62) with p_a replacing p_b, and with an amplitude factor A_o. Thus

$$H_{ya} = \frac{A_o w_o}{w_2} L^o_{p_a}\left(\frac{2r^2}{w_2^2}\right)\exp\left(-\frac{r^2}{w_2^2}\right)\cos\{kz - (2p_a + 1)\Phi_2 + \alpha\} \qquad (5.64)$$

Similarly

$$H_{yam} = \frac{A_o w_o}{w_2} L^o_{p_a}\left(\frac{2r^2}{w_2^2}\right)\exp\left(-\frac{r^2}{w_2^2}\right) \qquad (5.65)$$

Consider first the integral over S_m in (5.60) using (5.61), (5.63) and (5.65). We have

$$\int_{S_m} \bar{H}_a \cdot \bar{H}_b dS = 2\pi A_o \int_o^\infty \left(\frac{w_o}{w_2}\right)^2 L^o_{p_a}\left(\frac{2r^2}{w_2^2}\right) L^o_{p_b}\left(\frac{2r^2}{w_2^2}\right)\exp\left(-\frac{2r^2}{w_2^2}\right) r\, dr \qquad (5.66)$$

Let $$u = \frac{2r^2}{w_2^2} \tag{5.67}$$

$$du = \frac{4r\ dr}{w_2^2}$$

The integral becomes

$$\int_{S_m} \bar{H}_a \cdot \bar{H}_b dS = \frac{\pi w_o^{\ 2} A_o^{\ o}}{2} \int_o^\infty L_{p_a}^o(u) L_{p_b}^o(u) \exp(-u)\ du \tag{5.68}$$

This is a standard form[36] and yields

$$\int_{S_m} \bar{H}_a \cdot \bar{H}_b dS = \frac{\pi w_o^{\ 2} A_o^{\ o}}{2} \{\Gamma(p+1)\}^2 \tag{5.69}$$

where the test field and the actual field have the same value of p.

Otherwise the integral is zero.

Let us for the moment assume that there is no output aperture.

Using the fact that $Z_m = \sqrt{j\omega\mu_o/\sigma} = R_m + jX_m$ where $R_m = X_m = \sqrt{\omega\mu_o/2\sigma}$,

and that the Q-factor of the resonator

$$Q = \frac{\omega\mu_o \int_V \bar{H}_a \cdot \bar{H}_b dV}{2R_m \int_{S_m} \bar{H}_a \cdot \bar{H}_b dS} \tag{5.70}$$

equation (5.60) then becomes

$$-\int_{S_a} (\bar{E}_o \times \bar{H}_b) \cdot \hat{n}\ dS = \pi w_o^{\ 2} A_o R_m \{\Gamma(p+1)\}^2 \left[1 + j\left\{1 + Q\frac{\omega_o}{\omega}\left(\frac{\omega}{\omega_o} - \frac{\omega_o}{\omega}\right)\right\}\right]$$

$$- j\omega_o\varepsilon_o(\varepsilon_r - 1)\int_{2V'} \bar{E}_a \cdot \bar{E}_b dV \tag{5.71}$$

Let $\omega = \omega_o + \delta\omega - \frac{\omega}{2Q}$. Then

$$\frac{\omega}{\omega_o} - \frac{\omega_o}{\omega} = \frac{\omega_o + \delta\omega - \omega/2Q}{\omega_o} - \frac{\omega_o}{\omega_o + \delta\omega - \omega/2Q}$$

$$= \frac{\omega_o^2 + 2\omega_o(\delta\omega - \omega/2Q) + (\delta\omega - \omega/2Q)^2 - \omega_o^2}{\omega_o(\omega_o + \delta\omega - \omega/2Q)}$$

$$\frac{\omega}{\omega_o} - \frac{\omega_o}{\omega} = \frac{2(\delta\omega - \omega/2Q)}{\omega_o} \cdot \frac{1 + (\delta\omega - \omega/2Q)/2\omega}{1 + (\delta\omega - \omega/2Q)/\omega_o} \tag{5.72}$$

The latter expression, when $\left|\frac{\delta\omega - \omega/2Q}{\omega_o}\right|$ is much less than unity, can be approximated by $\frac{2(\delta\omega - \omega/2Q)}{\omega_o}$ with very little error. Equation (5.71) then becomes

$$-\int_{S_a} (\bar{E}_o \times \bar{H}_b)\cdot\hat{n}\, dS = \pi w_o^2 A_o R_m \{\Gamma(p+1)\}^2 (1 + jQ\frac{\delta\omega}{\omega}) - j\omega_o\varepsilon_o(\varepsilon_r - 1)\int_{2V'} \bar{E}_a\cdot\bar{E}_b dV \tag{5.73}$$

In the volume 2V', the variations of $\bar{E}_a = \hat{i}E_{xa}$ and $\bar{E}_b = \hat{i}E_{xb}$ with z are so small that they can be considered as functions of r only and can be written as

$$E_{xb}(r, t) = -\frac{jZ_o w_o}{w_2} L_p^o(\frac{2r^2}{w_2^2}) \exp(-\frac{r^2}{w_2^2}) \sin(kd - \Phi_d) \tag{5.74}$$

$$E_{xa}(r, t) = -\frac{jA_o Z_o w_o}{w_2} L_p^o(\frac{2r^2}{w_2^2}) \exp(-\frac{r^2}{w_2^2}) \sin(kd - \Phi_d) \tag{5.75}$$

Taking a volume element

$$dV = \frac{r^2}{2R_t} \cdot 2\pi r\, dr = \frac{\pi r^3}{R_t} dr \tag{5.76}$$

where R_t is the radius of curvature of the wave front at the interfaces, the volume integral in (5.73) becomes

$$\int_{2V'} \bar{E}_a\cdot\bar{E}_b dV = \frac{2\pi}{R_t}\int_o E_{xa}E_{xb} r^3 dr \tag{5.77}$$

This involves an integral

$$I = \int_0^\infty \left(\frac{w_o}{w_2}\right)^2 \left\{L_p^o\left(\frac{2r^2}{w_2^2}\right)\right\}^2 \exp\left(-\frac{2r^2}{w_2^2}\right) r^3 dr \qquad (5.78)$$

Applying the transformation in (5.67)

$$I = \frac{w_o^2 w_2^2}{8} \int_0^\infty u\{L_p^o(u)\}^2 \exp(-u)du$$

$$= \frac{w_o^2 w_2^2}{8} (2p + 1)\{\Gamma(p + 1)\}^2 \qquad (5.79)$$

Hence

$$\int_{2V'} \bar{E}_a \cdot \bar{E}_b dV = -\frac{\pi t A_o Z_o^2}{\epsilon_r k^2} (2p + 1)\{\Gamma(p + 1)\}^2 \sin^2(kd - \Phi_d) \qquad (5.80)$$

Since $\hat{n} = -\hat{k}$ at the input coupling aperture and $\bar{H}_b = \hat{j}H_{yb}$, we get

$$\bar{E}_o \times \bar{H}_b \cdot \hat{n} = \bar{E}_o \cdot \bar{H}_b \times \hat{n} = -\bar{E}_o \cdot \hat{i}H_{yb} = -E_{ox}H_{yb} \qquad (5.81)$$

Thus only the x-component of $\bar{E}_o$ is needed. We assume this to be uniform over the coupling aperture. We also assume $a_o << w_m$, w_m being the beam radius at the mirrors, so that H_{yb} is also uniform over the coupling aperture, having the value

$$\frac{w_o}{w_m} L_p^o(0) = \frac{w_o}{w_m} \Gamma(p + 1) \qquad (5.82)$$

We then find

$$\frac{\pi a_o^2 w_o}{w_m} \Gamma(p + 1)E_{ox} = R_m \pi w_o^2 A_o \{\Gamma(p + 1)\}^2 \left(1 + jQ\frac{\delta\omega}{\omega}\right)$$

$$+ \frac{j\pi t A_o Z_o}{\epsilon_r k} (\epsilon_r - 1)(2p + 1)\{\Gamma(p + 1)\}^2 \sin^2(kd - \Phi_d) \qquad (5.83)$$

or

$$A_o = \frac{a_o^2}{w_o w_m \Gamma(p+1)} \frac{E_{ox}}{R_m\left(1 + jQ\frac{\delta\omega}{\omega}\right) + \frac{jtZ_o}{\varepsilon_r k w_o^2}(\varepsilon_r - 1)(2p+1)\sin^2(kd - \Phi_d)} \tag{5.84}$$

It can be seen from (5.84) that resonator modes are excited by the external source and the polarization current. Unless degeneracy occurs, energy will be conserved in the resonator. However, the polarization current causes a shift in the resonant frequency which is represented by the second term in the denominator in (5.84). This agrees with the result obtained in §4.7. Thus the effect of plane dielectric surfaces on the measurement of loss tangent is quite small since a small change in resonant frequency will not affect the result very much. If the error involved in neglecting this frequency shift is found to be large, the measured loss tangent can be corrected by applying correction to the measured resonant frequency.

CHAPTER 6

EQUIPMENT

6.1 The Open Resonator

6.1.1 Electromagnetic Design

The open resonator is characterized by the folowing four dimensions:

R_o, the radius of curvature of the mirrors,

D, the distance of separation between the mirrors,

a_m, the radius of the mirrors,

a_o, the radius of the coupling apertures.

The mirror curvature R_o and the mirror separation D determine the mode spectrum of the resonator. They also determine the beam radius w for a given frequency. In order to satisfy the assumed condition $k^2w_o^2 >> 1$, the ratio D/R_o can be chosen from the curve in Fig. 3.3 to give a large w_o/w_{oc} value. The choice of R_o is somewhat arbitrary. However, too large a value of R_o, although it gives a large beam radius, requires inconveniently large mirror diameter and dielectric sample. As a compromise, the radius of curvature R_o was chosen to be 127.0 cm.

The mirror separation D also affects the frequency shift $\frac{\delta\omega}{\omega}$ in (4.76) and the factor $F = \dfrac{\Delta t + d}{\Delta t + \sin 2(kd - \phi_d) \,/\, 2k(1 - 2/n^2k^2w_t^2)}$ in (5.45) when a dielectric sheet of known thickness is to be measured. Based on these two equations, the variations of $\frac{\delta\omega}{\omega}$ and F with D/2t can be plotted for the worst case, i.e. when $\sin(kd - \phi_d) = 1$, as shown in Fig. 6.1. To obtain accurate results, $\frac{\delta\omega}{\omega}$ should be as small as possible. This requires a large mirror separation. If low-loss material is to be measured, it is also necessary that F should be very close to 1 in order that a

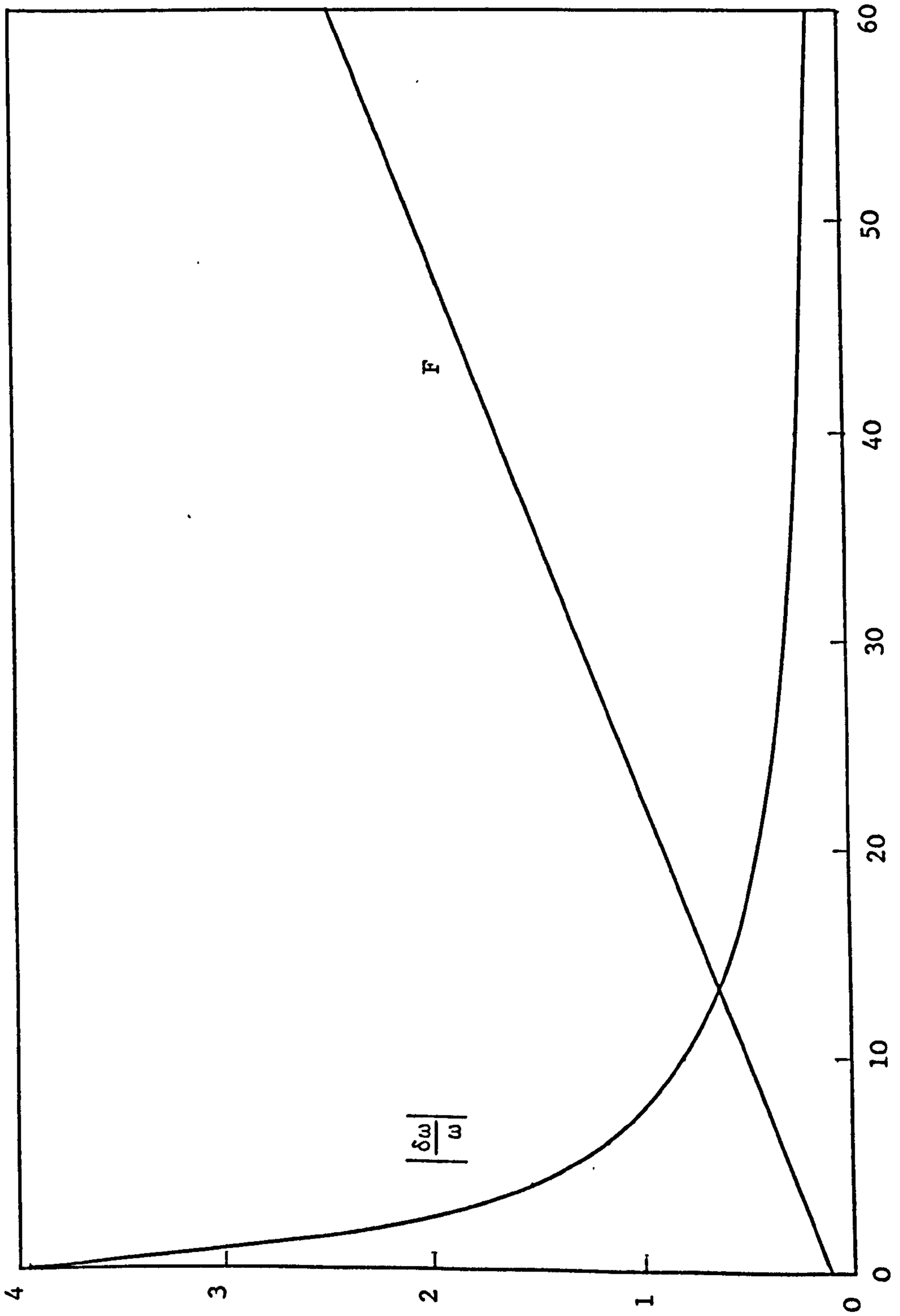

FIG. 6.1 $\left|\frac{\delta\omega}{\omega}\right|$ and F against d/t for $\varepsilon_r = 2.54$

considerable change in Q is detected when the resonator is purturbed by the insertion of the dielectric sample. This can be achieved by using a small separation. In view of these facts, a range of mirror separations varying from 50 cm to 70 cm was chosen giving a ratio D/R_o of between 0.39 and 0.55.

The higher order modes most likely to be excited are those with circular symmetry. For degeneracies to be avoided, the first few even multiples of the factor $\frac{1}{\pi}\cos^{-1}(1 - D/R_o)$ should not lie too close to an integer. Since this factor has a value of between 0.35 and 0.29, trouble from degeneracy in the empty resonator is unlikely. However, degeneracies or near degenercies might occur when the dielectric sample is inserted. This can be seen from the theoretical resonant frequencies of the fundamental and the TEM_{lo} modes listed in Table 6.1. These frequencies have been calculated based on (4.27) and (4.28) for various thicknesses of the dielectric sample and for $\epsilon_r = 2.56$, $R_o = 127.0$ cm and $D = 70.0$ cm.

TABLE 6.1

Resonant frequencies of TEM_{oo} and TEM_{lo} modes

	TEM_{oo}		TEM_{lo}	
2t (cm)	f_a	f_s	f_a	f_s (GHz)
0	9.92559	10.13972	10.07627	10.29041
0.1	9.92544	10.11799	10.07600	10.26873
0.2	9.92482	10.09907	10.07523	10.24922
0.3	9.92320	10.08437	10.07344	10.23436
0.4	9.91999	10.07391	10.07002	10.22380
0.5	9.91448	10.06702	10.06423	10.21684
0.6	9.90591	10.06285	10.05530	10.21261
0.7	9.89358	10.06062	10.04251	10.21032
0.8	9.87722	10.05964	10.02563	10.20927
0.9	9.85753	10.05937	10.00547	10.20889
1.0	9.83644	10.05928	9.98407	10.20867

When 2t = 0.5 cm, the resonant frequency of the symmetrical TEM_{oo} mode lies very close to that of the asymmetrical TEM_{1o} mode, the frequency separation being about 3 MHz. For the measurement of low-loss material, Q_L is usually quite high. This means the bandwidth of the resonance curve is narrow. Since TEM_{1o} mode is only weakly excited, the chance of getting degeneracy seems very small. In practice, if degeneracy should happen affecting the measured loss tangent, a second measurement using a sample of different thickness is recommended.

The radius of the mirror a_m affects the upper limit of the unloaded Q, but as long as $a_m >> w_m$, the beam radius at the mirrors, the losses due diffractional spillover are small in comparison with the other losses in the resonator. From (3.20) and (3.21), it is found for λ = 3.00 cm and D = 70.0 cm, w_o = 7.37 cm and w_m = 8.59 cm. The mirror radius was arbitrarily chosen to be 18.4 cm. The theoretical diffraction loss per pass is estimated from the fraction of the Gaussian beam not intercepted by the mirror. In our case, this has the value

$$\alpha = \exp -\left(\frac{2a_m^2}{w_m^2}\right) = 10.5 \times 10^{-4}$$

This corresponds to a diffraction-limited Q of 1.4×10^6. The conductivity limited Q is about 4.4×10^5. Thus an upper limit for the unloaded Q is about 3.3×10^5.

Because of coupling losses, the radius of the coupling apertures a_o affects the Q of the empty resonator. Two sizes of coupling holes, e.g. $2a_o$ = 6.4 mm and 8.0 mm, were used giving a Q_o of about 180,000 and 80,000 respectively. The former size is particularly suitable for the measurement of low-loss dielectric such as polystyrene and the latter,

for high-loss material such as perspex.

To summarize the above, the resonator has the following characteristics:

(i) Radius of curvature of the mirrors R_o = 127.0 cm

(ii) Distance of separation of the mirrors D = 50 - 70 cm

(iii) Radius of the mirror apertures a_m = 18.4 cm

(iv) Radius of the coupling aperture a_o = 3.2 and 4.0 mm

6.1.2 Mechanical Design

The mirrors were turned from 19 mm thick duralumin disc. The surface finish of the concave part of the mirrors is better than 100 μm. As shown in Plate 6.1, the mirrors are rigidly fixed to 1.3 cm thick duralumin back plates which are in turn fixed to compound slides consisting of vertical slides with swivels and cross slides. One of the compound slide is secured to the left end of a 3.5 ft lathe bed and the other one is supported by a movable carriage. The separation between the mirrors is variable from 25 to 70 cm by moving the carriage along the bed. The aperture planes of the mirrors can be adjusted for perpendicularity to the axis of the resonator by means of the swivels. Alignment of the mirrors in the axial direction can be made by adjusting the vertical and the cross slides. Waveguides can be connected to the two mirrors with the help of specially designed flanges. Coupling from the waveguides to the resonator takes place at the centre of each mirror through coupling holes of 8.0 mm diameter which can be reduced, when required, to 6.4 mm using adapters.

A mounting frame holding the dielectric sample is fixed to a rotary table which is then supported by another movable carriage.The rotary table allows the sample to be turned at any angle and the movable carriage provides accurate axial movement of the sample.

PLATE 6.1 The open resonator

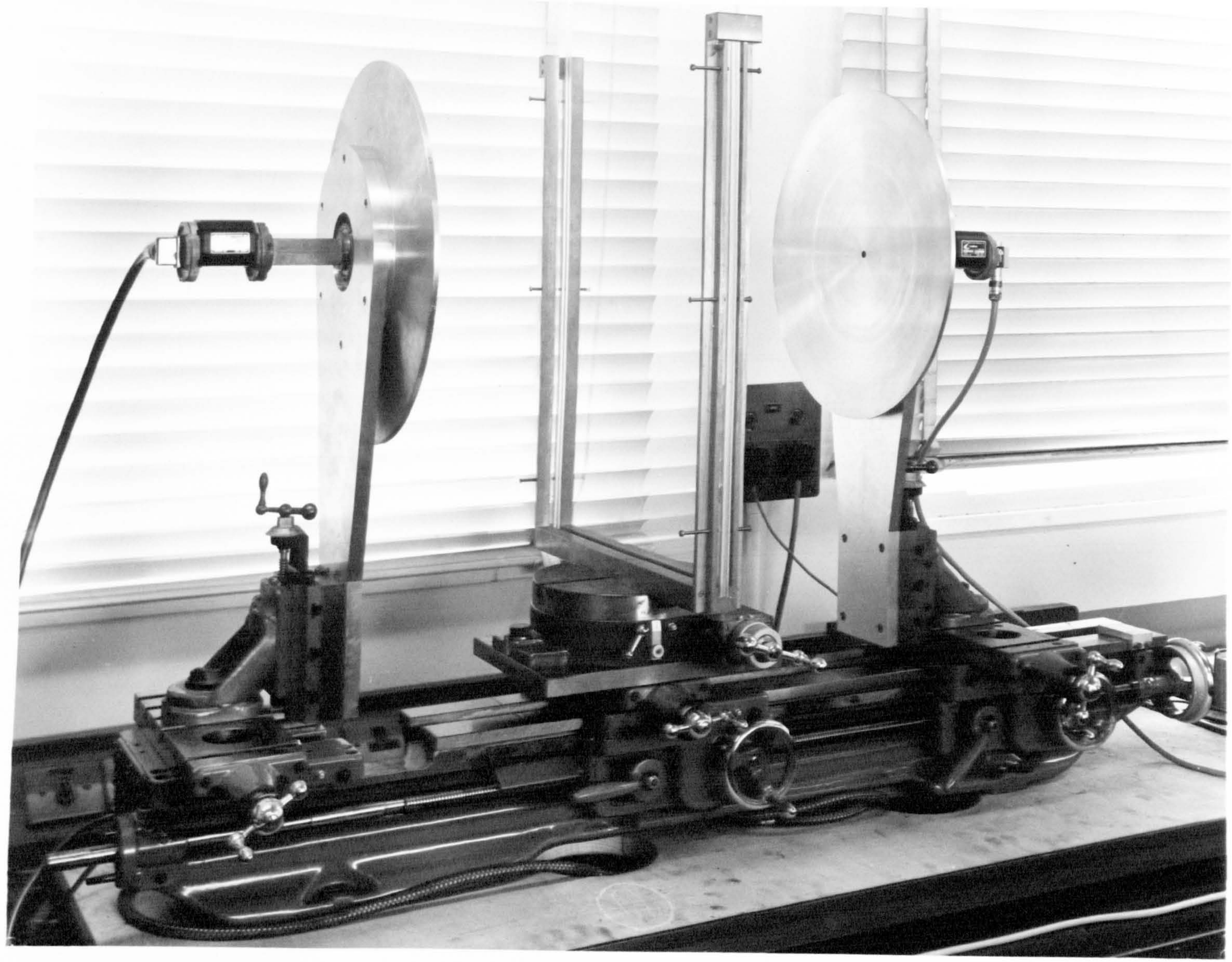

6.2 Mode Spectrum

The electrical performance of the mirrors in this resonator has been verified at a separation of 80 cm.[37] It has been found that the experimental transverse field distribution in the central plane of symmetry of the resonator is Gaussian in form, and that the theoretical and experimental mode spacings agree very well with each other. The latter shows that the separation between the mirrors can be measured electrically using (3,23).

The mode spectrum of the resonator can be obtained experimentally by connecting a microwave sweep oscillator to the input of the resonator and recording the output of the resonator using an X-Y recorder. The resonant frequencies can be measured by means of an electronic counter with a 8-18 GHz frequency converter having an accuracy of about 1 part in 10^8. The block diagram of the experimental set-up is shown in Fig. 6.2 and two typical mode spectra for the resonator with and without the dielectric are shown in Fig. 4.2. The mode spectrum of an empty resonator comprises a set of major resonances. For coupling holes of 8.0 mm diameter, minor resonances at TEM_{1o} frequencies have been detected, but for holes of 6.4 mm diameter they can hardly be oberved. Both the axial and the azimuthal mode spacings are functions of mirror separation. Table 6.2 gives their values for three mirror separations.

TABLE 6.2

Axial and azimuthal mode spacings

Mirror separation (cm)	Axial mode spacing (MHz)	Azimuthal mode spacing (MHz)
70.00	214.13	75.34
60.00	249.83	80.72
50.00	299.79	87.74

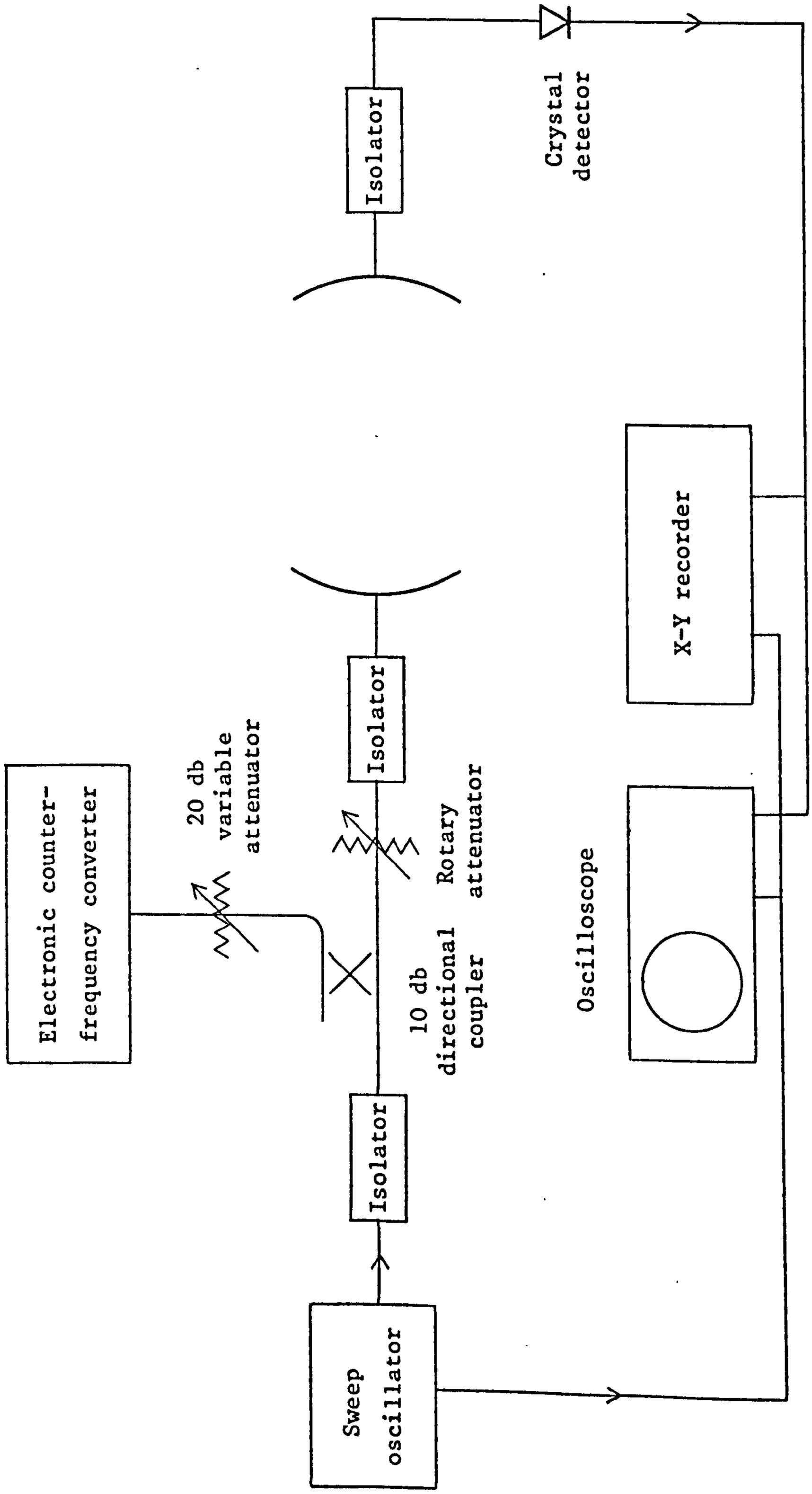

FIG. 6.2 Arrangement for mode spectrum and bandwidth measurements

6.3 Measurement of Q

The range of Q to be measured varies from a fraction of a million for the empty resonator with small coupling holes to a few thousands when high-loss material such as perspex is to be measured. It is impossible to use a single method to cover such wide range of Q-measurement without affecting its accuracy. Two methods, e.g. the decrement method and the bandwidth method, have been employed for this purpose, the former being used when $Q > 25{,}000$ and the latter being used when $Q < 25{,}000$.

6.3.1 Decrement Method

This method is based on measuring the time rate of decay of microwave energy stored in the resonator and is particularly suited to the measurement of high Q-factors. Let Δt be the time interval during which the energy decays to a level A db lower than its value at the beginning of the interval. Then the Q can be determined from

$$Q = 27.3 f \Delta t / A \qquad (6.1)$$

For a 3 db power level change, this becomes

$$Q = 9.1 f \Delta t \qquad (6.2)$$

The experimental set-up is shown in Fig. 6.3. A microwave sweep oscillator operating in the unlevelled cw mode is pulse modulated by applying rectangular voltage pulses of 5 μsec duration and 10 kHz repitition rate to the diode modulator. Forced oscillations are exponentially built up in the resonator during the onset of the rf power and the energy then decays exponentially when the pulse is over.

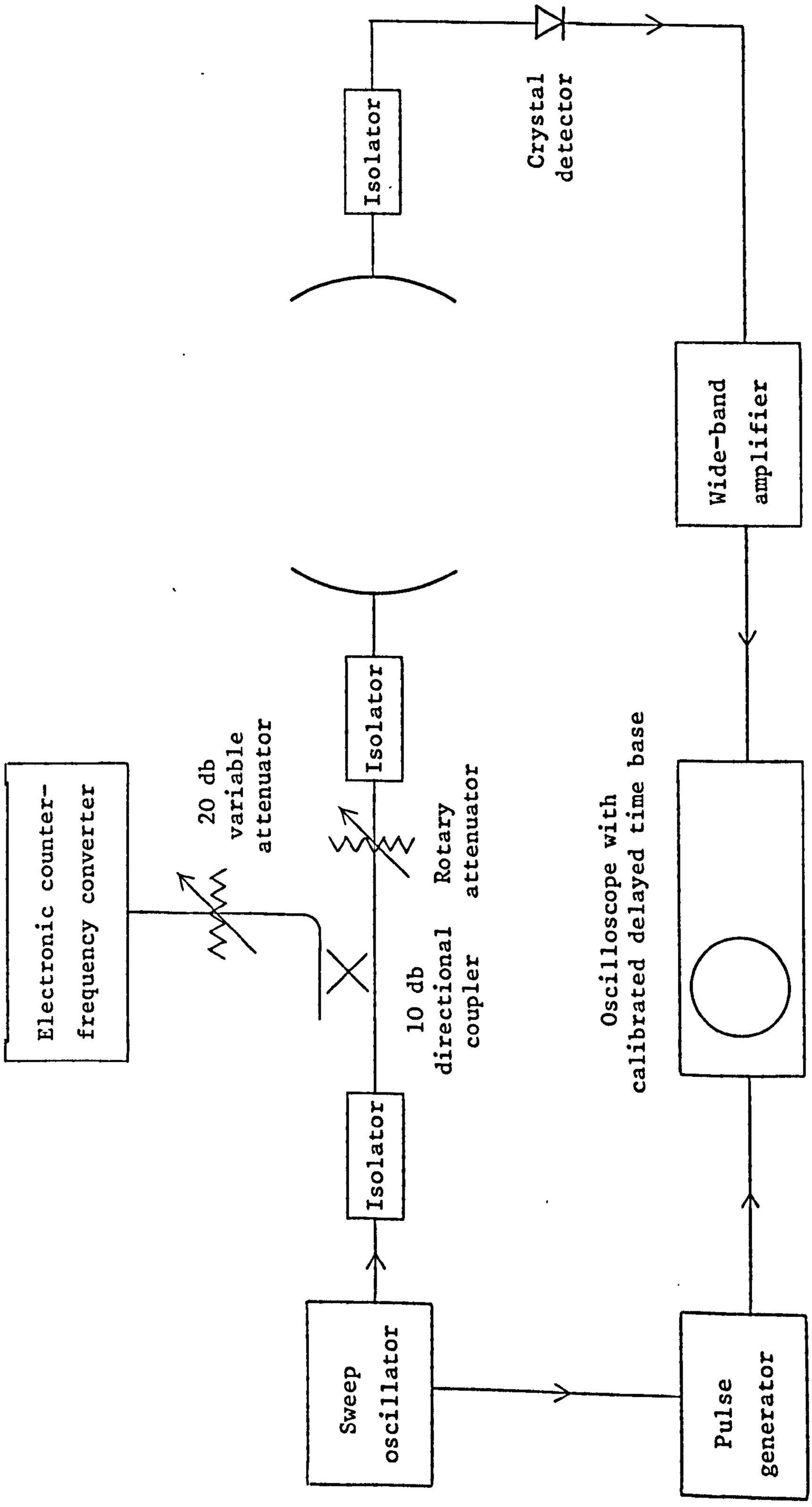

FIG. 6.3 Decrement method of measuring Q

The pulse generator also sends a synchronizing pulse to initiate the horizontal sweep of the oscilloscope.

The decay of energy is observed by means of a crystal detector coupled to the resonator. After passing through a wide-band amplifier, the transient build-up and decay is displayed on an oscilloscope with a vertical amplifier having 10 MHz bandwidth. Plate 6.2 shows such a trace taken when a Q of about 180,000 was measured. The decay time is measured by means of the calibrated time base in the oscilloscope. Delay accuracy of the time base is 1% of full scale reading, and delay time linearity is within 0.2% of full scale of delay. The rotary attenuator is used to determine the half power point in the decay curve.

PLATE 6.2 Transient buildup and decay of energy in the resonator

Decrement measurements are not affected by the residual FM in the sweep oscillator because small fluctuations of the source frequency about a mean value have very little effect on the level of energy buildup and on the rate of energy decay in the resonator. It can be seen from (6.2) that as the Q increases so does the time interval Δt, so that, on this account, the precision of the measurement tends to increase, provided the frequency stability is adequate.

Before attempting to measure dielectric loss tangents, this method has been tried out to measure the Q-factor of the empty resonator with several mirror separations at the resonant frequencies of 10.00 GHz and 9.50 GHz. The results are shown in Fig. 6.4. It can be seen from these curves that Q_o increases at first linearly with D until it reaches the peak where diffraction losses start to predominate. After the peak, Q_o decreases rapidly with further increase of D. This is not unexpected since the beam radius at the mirrors, which has an exponential effect on the diffraction losses, increases continuously with D in a manner as shown in Fig. 3.3. As the coupling losses are not known, theoretical values of Q_o are not available for comparison.

6.3.2 Bandwidth method

Observation of the power transmitted through the resonator as a function of frequency affords a particularly simple and potentially accurate method of measuring low Q-factors. In this method, the bandwidth Δf between the half-power frequencies is measured and the Q is calculated by

$$Q = \frac{f}{\Delta f} \tag{6.3}$$

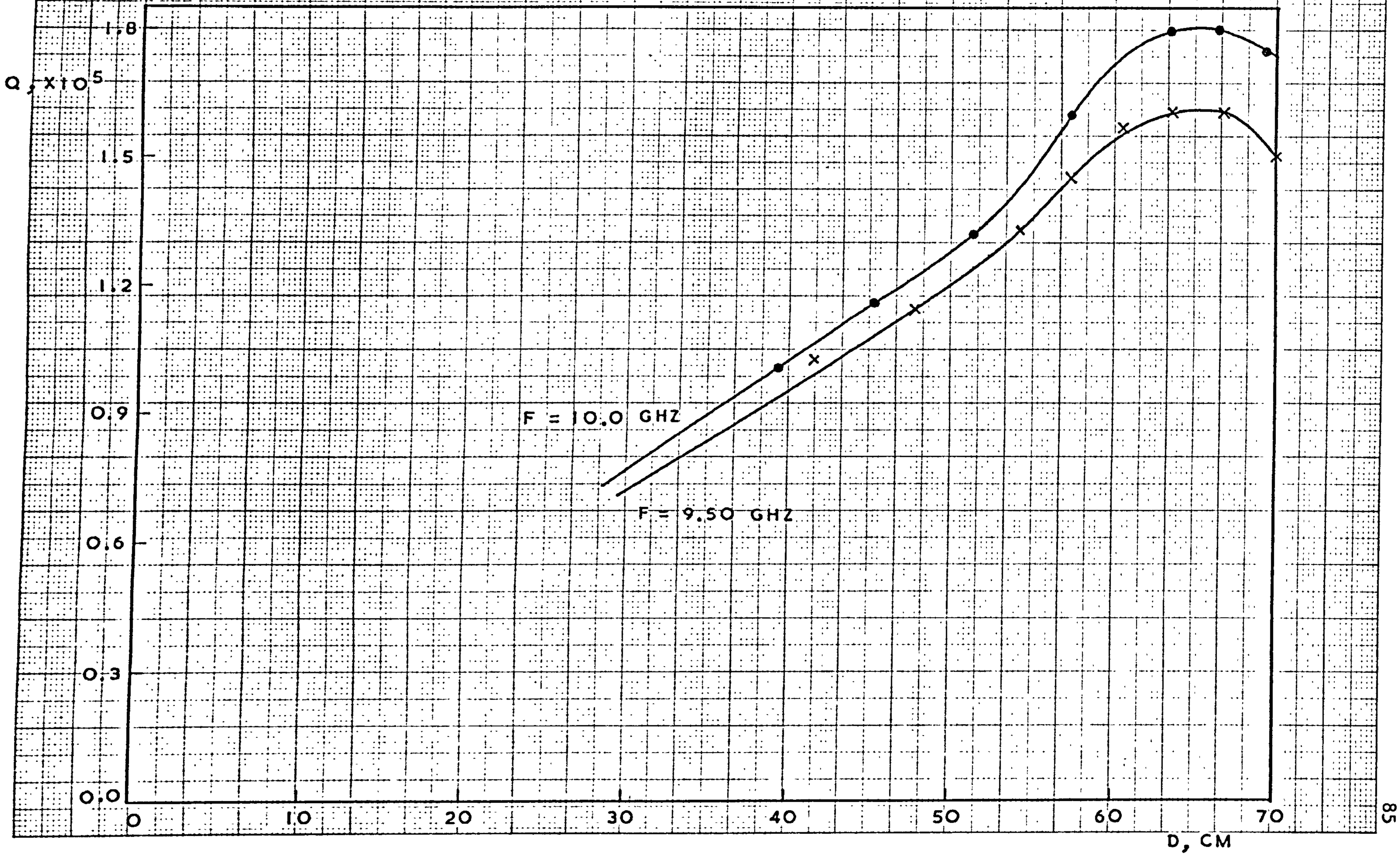

FIG. 6.4 VARIATIONS OF Q-FACTOR OF THE EMPTY RESONATOR WITH DISTANCE OF SEPARATION

The measurement set-up is the same as illustrated in Fig. 6.3. The sweep oscillator is operated in the symmetrical sweep mode in which the frequency sweeps about a pre-set centre frequency. The width of the sweep can be adjusted independently. A synchronized saw-tooth sweep is also applied to the horizontal input of the oscilloscope giving a steady display of the transmitted power versus frequency on the oscilloscope screen. This trace is then recorded by means of an X-Y recorder using a much slower sweeping rate. The resonant frequency and the bandwidth of the trace are then measured. Thus Δf can be deduced from this bandwidth and Q can be calculated using (6.3).

With the limited frequency stability and the inherent residual frequency modulation of the sweep oscillator, the accurate measurement of the half-power bandwidth for high-Q circuit is very difficult. Thus this method is more suitable for low-Q measurements.

CHAPTER 7

EXPERIMENTS AND RESULTS

7.1 Measuring Procedures

The experimental set-up is shown in Plate 7.1. The separation between the mirrors is first adjusted to an arbitrary value. The Q of the empty resonator is measured using the decrement method and the axial mode spacing is noted from which the mirror separation D can be found. The dielectric sheet is then inserted at the centre of the resonator normal to the resonator axis. The centre position is ensured by noting the resonant frequency of the symmetrical mode f_s is a minimum and that of the adjacent lower-frequency asymmetrical mode f_a is a maximum. These two frequencies and Q_L of the perturbed resonator are measured. The dielectric constant and the loss tangent can then be related to f_s, f_a, Q_o, Q_L, D and the thickness of the dielectric sheet 2t by the formulas given in Chapters 4 and 5.

7.2 Dielectric Constant of Polystyrene Sheets

Dielectric constants of polystyrene sheets of various thicknesses have been measured following the procedures given above at five mirror separations of 70.1124, 65.0266, 60.0254, 55.0206 and 50.0180 cm. Table 7.1 gives the results at $f_s \approx 10$ GHz, obtained by solving (4.27) for n. The repeatability of the results is extremely good. If we exclude the value 2.567 for 2t = 7.95 mm and D = 65.0266 cm, which is probably due to some human error in the measurement, the maximum deviation from the average value is 0.28%. When the measured dielectric constants are compared with the quoted value of 2.54,[38] the agreement is excellent.

PLATE 7.1 The experimental set-up

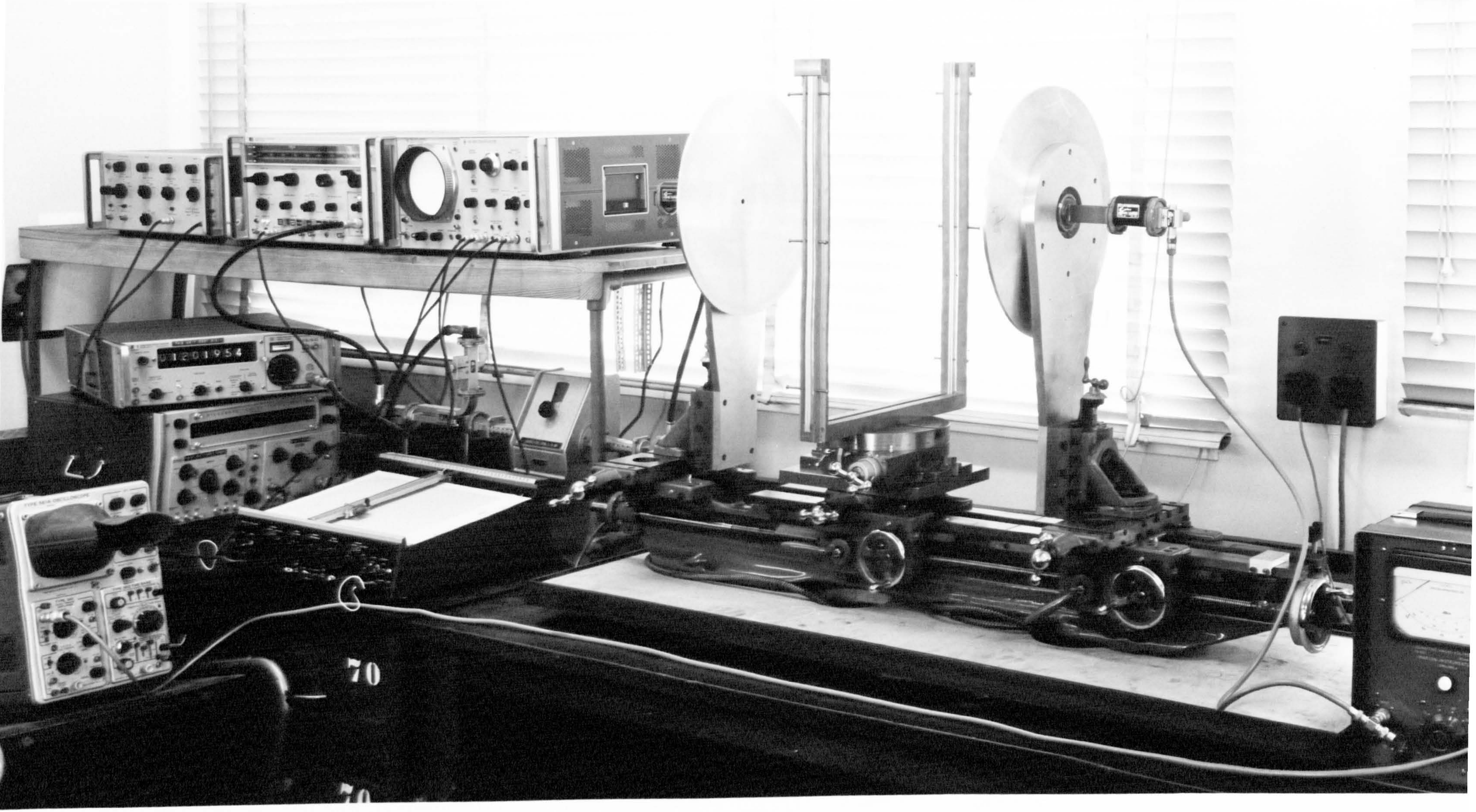

TABLE 7.1

Dielectric constants obtained by solving

the transcendental equation

2t (mm) \ D (cm)	70.1124	65.0266	60.0254	55.0206	50.0180	average over all D
5.97	2.545	2.550	2.549	2.549	2.549	2.548
6.96	2.541	2.548	2.543	2.546	2.548	2.545
7.95	2.539	2.567	2.542	2.546	2.547	2.548
8.84	2.540	2.552	2.542	2.548	2.547	2.546
9.96	2.539	2.544	2.541	2.547	2.541	2.542

average value = 2.546

The measured dielectric constants given in Table 7.1 were then corrected to account for the error introduced by the plane dielectric surfaces. The frequency correction $\frac{\delta\omega}{\omega}$ in (4.76) was applied to the measured resonant frequency f as follows:

$$f_{corr} = f(1 + \frac{\delta\omega}{\omega}) \tag{7.1}$$

f_{corr} being the corrected value of f. Substitution of the corrected data into (4.27) yielded the results in Table 7.2.

TABLE 7.2

Corrected values of the dielectric constants

2t (mm) \ D (cm)	70.1124	65.0266	60.0254	55.0206	50.0180	average over all D
5.97	2.544	2.549	2.547	2.548	2.548	2.547
6.96	2.540	2.547	2.543	2.545	2.547	2.544
7.95	2.539	2.567	2.542	2.545	2.547	2.548
8.84	2.540	2.552	2.542	2.548	2.547	2.546
9.96	2.539	2.544	2.541	2.547	2.541	2.542

average value = 2.545

The differences between the original and the corrected values are very small. This is because the thicknesses of the samples were between $\frac{\lambda}{4}$ and $\frac{\lambda}{2}$, and with such thicknesses the dielectric surfaces were subjected to low field intensity for symmetrical mode. For thinner sheets, the differences will be much bigger.

From the measured data, the two sets of approximate formulas (4.37), (4.40) and (4.46), (4.47) gave similar results. Table 7.3 lists the more accurate set of results obtained by substituting the corrected data into (4.46) and (4.47). The maximum deviation from the average value is 0.6%.

TABLE 7.3

Dielectric constants calculated by using

the approximate formulas

D (mm) / 2t (mm)	70.1124	65.0266	60.0254	55.0206	50.0180	average over all D
2.88	2.539	2.543	2.537	2.540	2.539	2.540
4.92	2.529	2.529	2.533	2.530	2.531	2.530
5.97	2.525	2.529	2.527	2.527	2.527	2.527
6.96	2.517	2.523	2.518	2.521	2.520	2.520

average value = 2.529

It is observed that the measured values vary with the thickness of the sample, and become very poor as the thickness approaches $\frac{\lambda}{2}$. This is understandable because of the tangent and the cotangent terms involved in the formulas. The estimated accuracy is ±0.5% if samples near an integral number of half wavelengths thick are avoided.

This shows that the approximate formulas are very useful when a computer is not available. In any case, knowing ε_r approximately can help to select the right answer from the computer solutions.

Results obtained by solving (4.27) and (4.28) simultaneously are less accurate, because d is variable in the calculation, and are omitted.

7.3 Loss Tangent of Polystyrene Sheets

Table 7.4 gives the measured loss tangents of polystyrene sheets of 5.97, 6.96, 7.95, 8.84 and 9.96 mm thick, obtained from the measured Q_o and Q_L following the procedures given above. The average value is 0.00053

TABLE 7.4

Measured loss tangents, $\times 10^{-4}$

D (cm) / 2t (mm)	70.1124	65.0266	60.0254	55.0206	50.0180	average over all D
5.97	6.6	6.0	5.7	5.4	4.8	5.7
6.96	5.3	5.1	5.8	5.3	4.9	5.3
7.95	5.8	5.2	6.0	5.7	4.8	5.5
8.84	4.9	5.4	5.6	5.2	4.9	5.2
9.96	4.5	3.6	4.8	5.0	4.9	4.6

and the maximum deviation is 32%. These poor results are mainly due to the inaccuracy in the measured values of Q_L which are around 70,000. These values were found too low to be measured with the decrement method and too high with bandwidth method, and were eventually measured by using the former one. As the accuracy of the loss tangent measurement is limited mostly by the accuracy of Q measurements, it is expected that more elaborate instrumentation for measuring Q will give better results.

To justify the method used here, loss tangents have also been measured by measuring Q_o and Q_L at constant resonant frequency and slightly different mirror separations. Table gives the results which are extremely close to those in Table 7.4.

TABLE 7.5

Measured tanδ at constant resonant frequency

D = 65.0266 cm when the sample is inserted

2t (mm)	tanδ , × 10^{-3}
5.97	6.1
6.96	5.2
7.95	5.2
8.84	5.4
9.96	3.7

7.4 Dielectric Constant and Loss Tangent of Perspex Sheets

In order to test the suitability of the method in measuring high-loss dielectric materials, the dielectric constants and loss tangents of perspex sheets of 3.14 and 6.17 mm thick have been measured. Extremely low output was found with the 6.4 mm diameter coupling holes. Larger holes with 8.0 mm diameter were then used. The measured dielectric constants calculated from (4.27) and from the approximate formulas (4.46) and (4.47) are tabulated in Tables 7.6 and 7.7. The measured loss tangents are given in Table 7.8. The results are extremely consistent, particularly those in Table 7.6, and are in good agreement with the quoted values, e.g. $\varepsilon_r = 2.59$ and $\tan\delta = 0.0067$ at 10 GHz.[38] This shows that the method here can be used for measuring low-loss as well as high-loss materials.

TABLE 7.6

ε_r of perspex sheets obtained by solving

the transcendental equation

2t (mm) \ D (cm)	70.1124	65.0266	60.0254	55.0206	50.0180	average over all D
3.14	2.630	2.630	2.631	2.629	2.628	2.630
6.17	2.627	2.628	2.628	2.627	2.626	2.627

average value = 2.629

maximum deviation = 0.12%

TABLE 7.7

ε_r of perspex sheets calculated by using

the approximate formulas

2t (mm) \ D (cm)	70.1124	65.0266	60.0254	55.0206	50.0180	average over all D
3.14	2.628	2.627	2.626	2.626	2.626	2.627
6.17	2.659	2.664	2.660	2.666	2.652	2.660

average value = 2.644

maximum deviation = 0.83%

TABLE 7.8

$\tan\delta$ of perspex sheets, $\times 10^{-3}$

2t (mm) \ D (cm)	70.1124	65.0266	60.0254	55.0206	50.0180	average over all D
3.14	7.4	7.2	7.1	7.2	7.2	7.2
6.17	7.9	7.6	7.5	7.3	7.3	7.5

average value = 7.4×10^{-3}

maximum deviation = 6.8%

CHAPTER 8

ESTIMATION OF ERRORS

8.1 Errors in Measured Dielectric Constant

8.1.1 Errors in ϵ_r Due to Errors in Measured f, d and t

The measured values of frequency f, distance from the interface to the mirror d and the thickness of the dielectric sample 2t, which are required in the evaluation of the dielectric constant ϵ_r using the formulas given in Chapter 4, are susceptible to errors. Let these errors be δf, δd and δt. The error in ϵ_r is then given by

$$\delta\epsilon_r = \frac{\partial\epsilon_r}{\partial f}\delta f + \frac{\partial\epsilon_r}{\partial d}\delta d + \frac{\partial\epsilon_r}{\partial t}\delta t \qquad (8.1)$$

In terms of relative errors, (8.1) can be written as

$$\frac{\delta\epsilon_r}{\epsilon_r} = \frac{\delta\epsilon_{r1}}{\epsilon_r} + \frac{\delta\epsilon_{r2}}{\epsilon_r} + \frac{\delta\epsilon_{r3}}{\epsilon_r} \qquad (8.2)$$

where

$$\frac{\delta\epsilon_{r1}}{\epsilon_r} = \frac{\partial\epsilon_r}{\partial f}\frac{f}{\epsilon_r}\frac{\delta f}{f}$$

$$\frac{\delta\epsilon_{r2}}{\epsilon_r} = \frac{\partial\epsilon_r}{\partial d}\frac{d}{\epsilon_r}\frac{\delta d}{d} \qquad (8.3)$$

$$\frac{\delta\epsilon_{r3}}{\epsilon_r} = \frac{\partial\epsilon_r}{\partial t}\frac{t}{\epsilon_r}\frac{\delta t}{t}$$

which can be obtained, based on (4.37), as follows.

Putting $S = k_s d - \Phi_d$, $A = K_a d - \Phi_d$ and $k_1 = k_s - k_a$, (4.37) can be written as

$$\epsilon_r = -\frac{\cot S - (k_s - k_a)t\cot^2 S}{\tan A - (k_s - k_a)t} \qquad (8.4)$$

Let k_a be fixed. Since Φ_d is not a function of frequency, differentiating with respect to k_s, we obtain

$$\frac{\partial \varepsilon_r}{\partial k_s} = \frac{1}{\tan A - k_1 t} \{d \csc^2 S(1 - 2k_1 t \cot S) + t(\cot^2 S - \varepsilon_r)\} \qquad (8.5)$$

Using (8.3), we find

$$\frac{\delta \varepsilon_{r1}}{\varepsilon_r} = \frac{k_s}{\varepsilon_r(\tan A - k_1 t)} \{d \csc^2 S(1 - 2k_1 t \cot S) + t(\cot^2 S - \varepsilon_r)\} \frac{\delta f_s}{f_s}$$

$$= F_f \frac{\delta f_s}{f_s} \qquad (8.6)$$

where $F_f = \frac{k_s}{\varepsilon_r(\tan A - k_1 t)} \{d \csc^2 S(1 - 2k_1 t \cot S) + t(\cot^2 S - \varepsilon_r)\}$

To find the error in ε_r due to the error in d, we consider first

$$\Phi_2(t) = \tan^{-1}\left(\frac{2t}{n^2 k w_o^2}\right) \qquad (4.24)$$

$$\Phi_2(d + t) = \tan^{-1}\left[\frac{2}{k w_o^2}(d + t/n^2)\right] \qquad (4.25)$$

$$k w_o^2 = 2\sqrt{(R_o - d - t/n^2)(d + t/n^2)} \qquad (4.15)$$

Differentiating (4.25) with respect to d, we obtain

$$\frac{\partial}{\partial d}\{\Phi_2(d + t)\} = \frac{1}{k w_o^2} \qquad (8.7)$$

Similarly, differentiating (4.24), we find

$$\frac{\partial \Phi_2(t)}{\partial d} = -\frac{t}{n^2 k w_t^2}\left(\frac{2}{k w_o^2}\right)^2 (R_o - 2d - 2t/n^2) \qquad (8.8)$$

Since $\frac{\partial \Phi_2(t)}{\partial d} << \frac{\partial}{\partial d}\{\Phi_2(d + t)\}$, we can write

$$\frac{\partial \Phi_d}{\partial d} = \frac{1}{kw_o^2} \tag{8.9}$$

Differentiating (8.4) with respect to d and applying the relationship in (8.3), the relative error is

$$\frac{\delta \varepsilon_{r2}}{\varepsilon_r} = \frac{d}{\tan A - k_1 t}\left\{\frac{1}{\varepsilon_r}\left(k_s - \frac{1}{kw_o^2}\right)\csc^2 S(1 - 2k_1 t \cot S) + \left(k_a - \frac{1}{kw_o^2}\right)\sec^2 A\right\}\frac{\delta d}{d}$$

$$= F_d \frac{\delta d}{d} \tag{8.10}$$

where $F_d = \frac{d}{\tan A - k_1 t}\left\{\frac{1}{\varepsilon_r}\left(k_s - \frac{1}{kw_o^2}\right)\csc^2 S(1 - 2k_1 t \cot S) + \left(k_a - \frac{1}{kw_o}\right)\sec^2 A\right\}$

By analogous operations, we have

$$\frac{\partial \Phi_d}{\partial t} = \frac{1}{n^2 kw_o^2} \tag{8.11}$$

Differentiating (8.4) with respect to t and using (8.3), the relative error in ε_r due to the error in t is

$$\frac{\delta \varepsilon_{r3}}{\varepsilon_r} = \frac{t}{\varepsilon_r(\tan A - k_1 t)}\left[\frac{1}{\varepsilon_r kw_o^2}\{\csc^2 S(2k_1 t \cot S - 1) - \varepsilon_r \sec^2 A\}\right.$$

$$\left. + k_1(\cot^2 S - \varepsilon_r)\right]\frac{\delta t}{t}$$

$$= F_t \frac{\delta t}{t} \tag{8.12}$$

where $F_t = \frac{t}{\varepsilon_r(\tan A - k_1 t)}\left[\frac{1}{\varepsilon_r kw_o^2}\{\csc^2 S(2k_1 t \cot S - 1) - \varepsilon_r \sec^2 A\}\right.$

$$\left. + k_1(\cot^2 S - \varepsilon_r)\right]$$

Consider the factors F_f, F_d and F_t. Fig. 8.1 shows the experimental curves of their variations with the thickness of the dielectric sheet 2t,

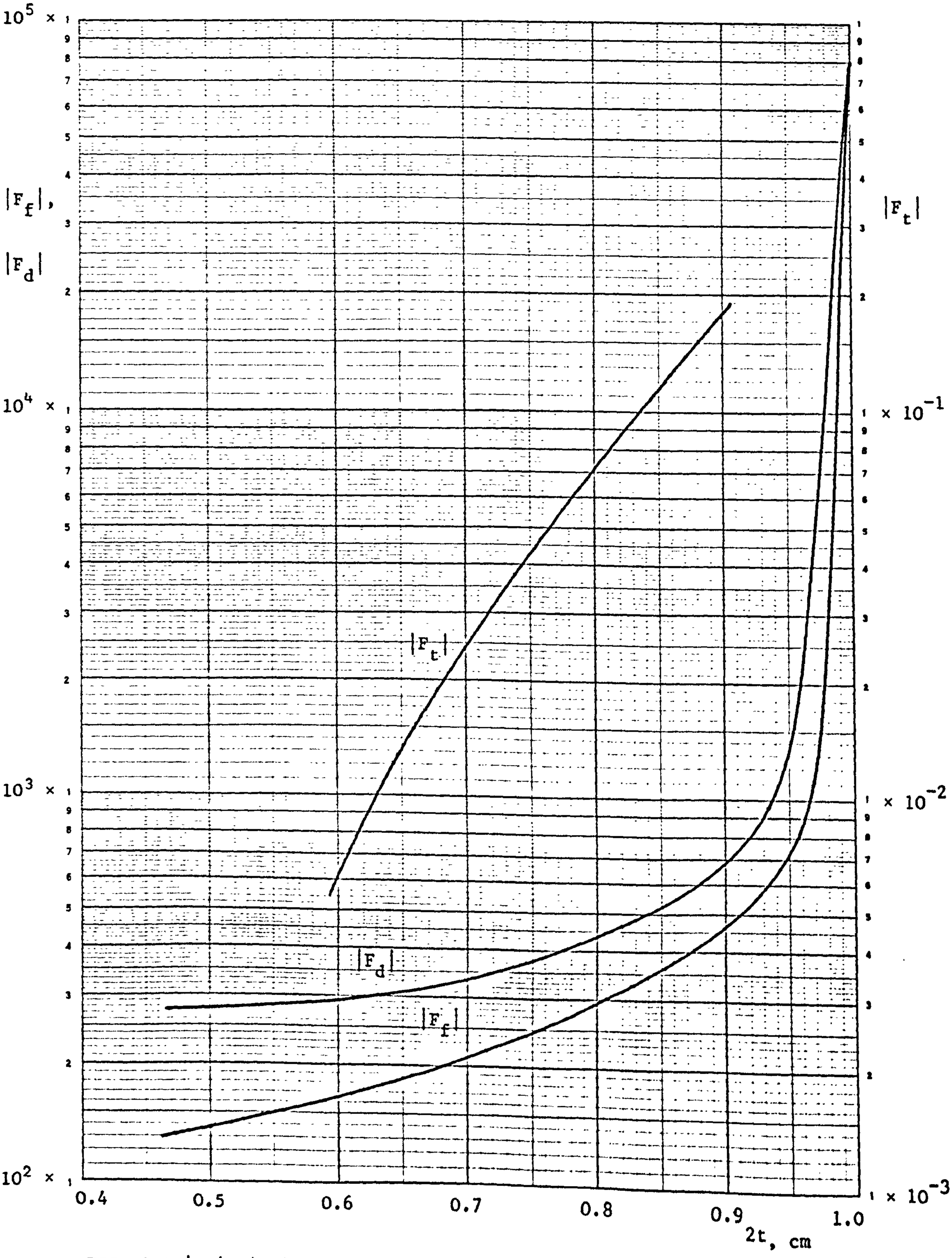

FIG. 8.1 $|F_f|$, $|F_d|$ and $|F_t|$ against thickness of the dielectric sheet

for D = 65.0266 cm and $f_s \simeq 9.5$ GHz. It can be seen that the errors in ε_r, due to errors in f, d and t, vary with the thickness of the dielectric. They are quite small for sheet of around 5 mm thick, but become very large as the thickness approaches $\frac{\lambda}{2}$. This accounts for the poor dielectric constant results for sheets of nearly $\frac{\lambda}{2}$ thick, calculated by using the approximate formulas.

Errors in ε_r, which is obtained by solving the transcendental equation (4.27), depend very little on the thickness of the dielectric, and the proportional factors F_f, F_d and F_t have now the values of around 100, 100 and 1 respectively, varying slowly with the sample thickness.

8.1.2 Error in ε_r Due to Axial Displacement of the Sample

In the analysis in Chapter 4, it has been assumed that the sample is placed at the centre of the resonator normal to the resonator axis. This condition may not be fulfilled in practice. If the sample is slightly displaced from its central position, an error will be introduced to the resonant frequency. Let $\delta\ell$ be the small axial displacement, and V_1 and V_1' be the perturbed volumes. The amount of frequency error can be calculated using (4.68), which can now be written as

$$\frac{\delta\omega}{\omega} = -\frac{\int_{V_1} \bar{E}\cdot\bar{D}'dV - \int_{V_1'} \bar{E}\cdot\bar{D}'dV}{\int (\bar{E}\cdot\bar{D} - \bar{H}\cdot\bar{B})dV} \qquad (8.13)$$

$$2V_o$$

In the perturbed volumes, the electric field has the value

$$E_1 = \frac{A_1 w_o}{w_1} \exp\left(-\frac{r^2}{w_1^2}\right) \begin{matrix}\cos\\ \sin\end{matrix}(nkz - \Phi_1) \qquad (8.14)$$

where the cosine and the sine functions are for the symmetrical and the asymmetrical modes respectively.

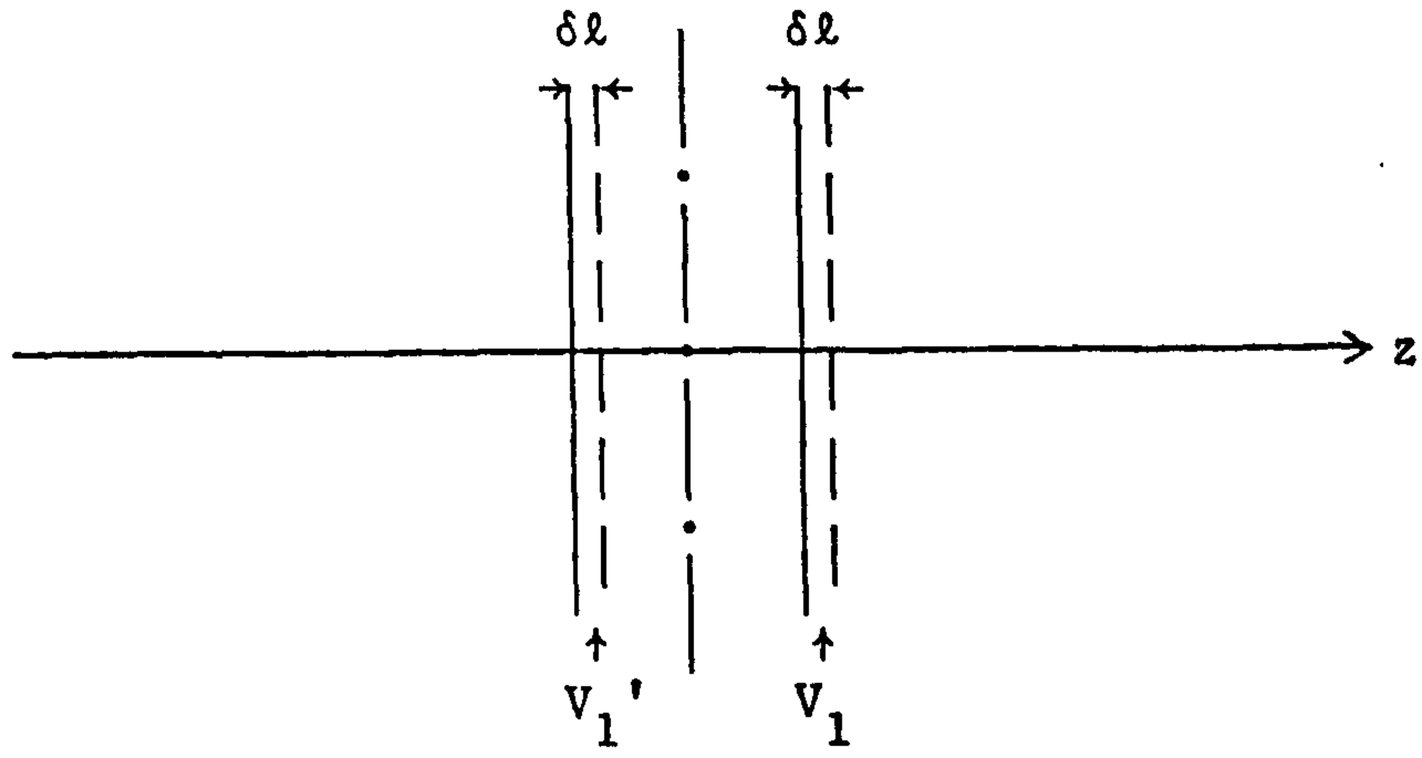

FIG. 8.2 Dielectric sample displaced axially from centre

The volume element may be written as $dV = 2\pi r\, dr\, dz$. Equation (8.13) then becomes

$$\frac{\delta\omega}{\omega} = -\frac{2\pi|A_1|^2\varepsilon_o(\varepsilon_r - 1)\left[\int_t^{t+\delta\ell}\int_o^{\infty}|E_1|^2 r\,dr\,dz - \int_{t-\delta\ell}^{t}\int_o^{\infty}|E_1|^2 r\,dr\,dz\right]}{\int_{2V_o}(\bar{E}\cdot\bar{D} - \bar{H}\cdot\bar{B})dV} \qquad (8.15)$$

Substituting (8.14) into (8.15) and performing the r-integration, we have

$$\frac{\delta\omega}{\omega} = -\frac{|A_1|^2\pi w_o^2\varepsilon_o(\varepsilon_r - 1)\left[\int_t^{t+\delta\ell}\begin{matrix}\cos^2\\ \sin^2\end{matrix}(nkz - \Phi_1)dz - \int_{t-\delta\ell}^{t}\begin{matrix}\cos^2\\ \sin^2\end{matrix}(nkz - \Phi_1)dz\right]}{2\int_{2V_o}(\bar{E}\cdot\bar{D} - \bar{H}\cdot\bar{B})dV} \qquad (8.16)$$

The first integral in the numerator on the left-hand side of (8.16) can be written as

$$I_1 = \frac{1}{2}\int_t^{t+\delta\ell}\{1 \pm \cos 2(nkz - \Phi_1)\}dz \qquad (8.17)$$

Integrating by parts and neglecting higher order terms as in Section 5.1.1, this becomes

$$I_1 = \frac{\delta\ell}{2} \pm \frac{1}{2}\left[\frac{\sin 2\{nk(t + \delta\ell) - \Phi(t + \delta\ell)\}}{2\{nk - 2/nkw^2(t + \delta\ell)\}} - \frac{\sin 2(nkt - \Phi_t)}{2(nk - 2/nkw_t^2)}\right] \tag{8.18}$$

Similarly, the second integral in the numerator in (8.16) can be written as

$$I_2 = \frac{\delta\ell}{2} \pm \frac{1}{2}\left[\frac{\sin 2(nkt - \Phi_t)}{2(nk - 2/nkw_t^2)} - \frac{\sin 2\{nk(t - \delta\ell) - \Phi(t - \delta\ell)\}}{2\{nk - 2/nkw^2(t - \delta\ell)\}}\right] \tag{8.19}$$

If $\delta\ell << t$, it can be assumed $\Phi(t + \delta\ell) \simeq \Phi(t - \delta\ell) \simeq \Phi_t$ and $w(t + \delta\ell) \simeq w(t - \delta\ell) \simeq w_t$. Subtraction of (8.19) from (8.18) gives

$$\begin{aligned} I_1 - I_2 &= \pm \frac{1}{4(nk - 2/nkw_t^2)} [\sin 2\{nk(t + \delta\ell) - \Phi_t\} + \sin 2\{nk(t - \delta\ell) - \Phi_t\} \\ &\qquad - 2\sin 2(nkt - \Phi_t)] \\ &= \pm \frac{\sin 2(nkt - \Phi_t)}{2(nk - 2/nkw_t^2)}(\cos 2nk\delta\ell - 1) \end{aligned} \tag{8.20}$$

Equation (8.16) then becomes

$$\frac{\delta\omega}{\omega} = \mp \frac{|A_1|^2 \pi w_o^2 \varepsilon_o(\varepsilon_r - 1)(\cos 2nk\delta\ell - 1)\sin 2(nkt - \Phi_t)}{4(nk - 2/nkw_t^2)\int_{2V_o} (\bar{E}\cdot\bar{D} - \bar{H}\cdot\bar{B})dV} \tag{8.21}$$

From (4.75) and (5.40), the integral in the denominator can be written as

$$\int_{2V_o} (\bar{E}\cdot\bar{D} - \bar{H}\cdot\bar{B})dV = \pi w_o^2 \varepsilon_o(\Delta t + d) \tag{8.22}$$

Substitution of (5.32), (5.36), (5.38) and (8.22) into (8.21) yields

$$\frac{\delta\omega}{\omega} = \frac{(\varepsilon_r - 1)(1 - \cos 2nk\delta\ell)\sin 2(kd - \Phi_d)}{4k\varepsilon_r(1 - 2/n^2k^2w_t^2)(\Delta t + d)} \tag{8.23}$$

This is the required formula for the frequency error and is valid for both symmetrical and asymmetrical modes. Fig. 8.3 shows the theoretical and experimental curves of the variation of $\left|\frac{\delta\omega}{\omega}\right|$ with $\delta\ell$ for polystyrene sheets of 4.92 and 9.78 mm thick when D = 70.1124 cm and the unperturbed resonant frequency f ≃ 9.5 GHz. It can be seen that the change in resonant frequency due to a small displacement of the sample from the centre is extremely small. The error so introduced in the measured dielectric constant is, therefore, negligible.

8.1.3 Errors in ε_r Due to Tilting of the Sample

If the sample is not exactly normal to the axis of the resonator, a shift in the resonant frequency will also be resulted. In Fig. 8.4 the experimental values of the frequency shift $\left|\frac{\delta\omega}{\omega}\right|$ are plotted against the small tilt angle $\delta\theta$ for polystyrene sheets. These curves are for parallel polarization. For perpendicular polarization, much the same results have been obtained.

In practice, the dielectric sample can usually be adjusted for perpendicularity to the resonator axis to within 0.1^o by observing the frequency minimum for the symmetrical mode and the frequency maximum for the asymmetrical mode. For such a small angle of tilt, the frequency shift $\frac{\delta\omega}{\omega}$ is very small. Thus the error in ε_r due to this cause is negligible.

In addition to the errors discussed above, energy stored in the coupling holes may cause a shift in the resonant frequency. As the holes are very thin, this frequency shift can also be neglected.

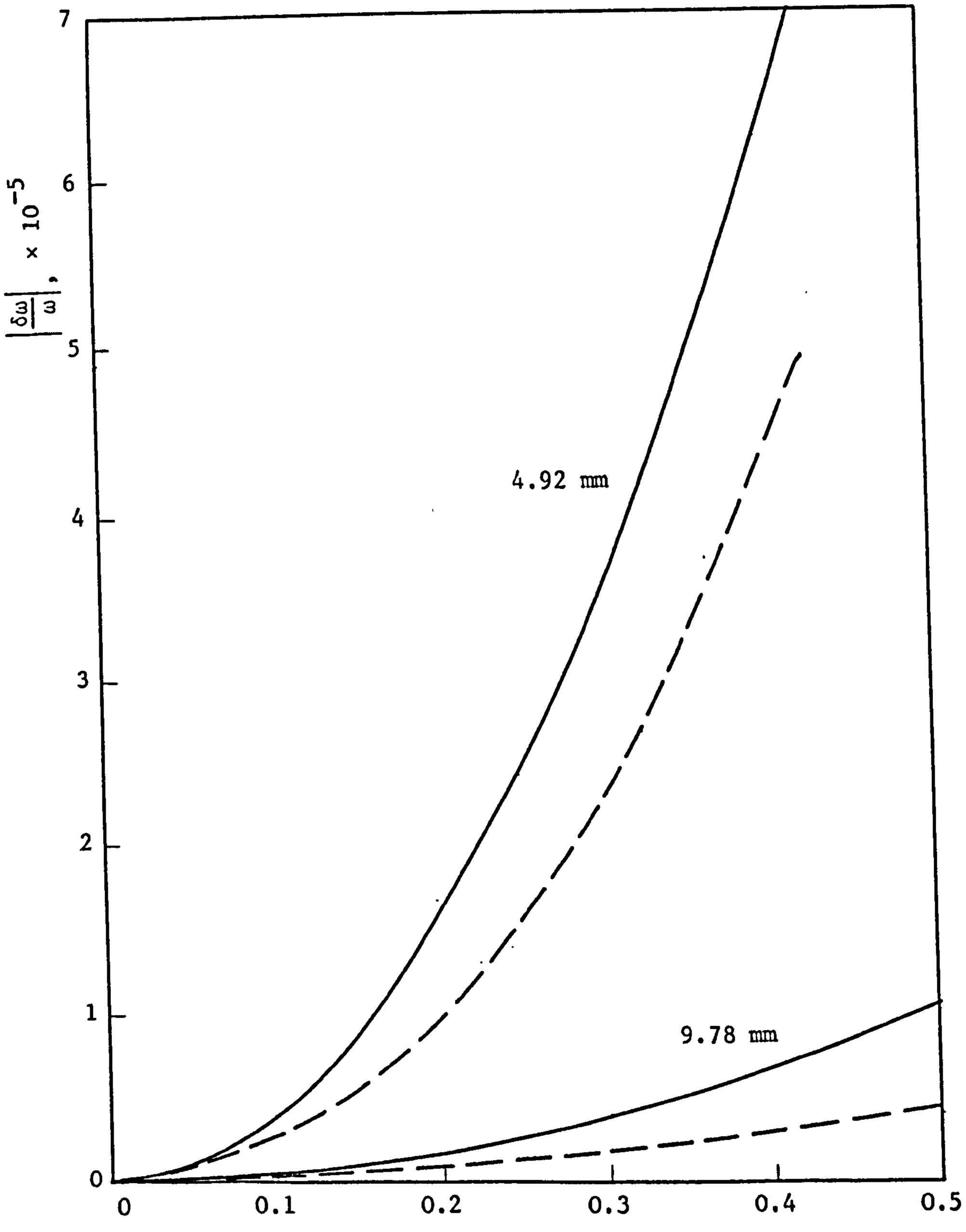

FIG. 8.3 Variation of $\left|\frac{\delta\omega}{\omega}\right|$ with $\delta\ell$

D = 70.1124, f ≃ 9.5 GHz

——————— Theoretical

— — — — Experimental

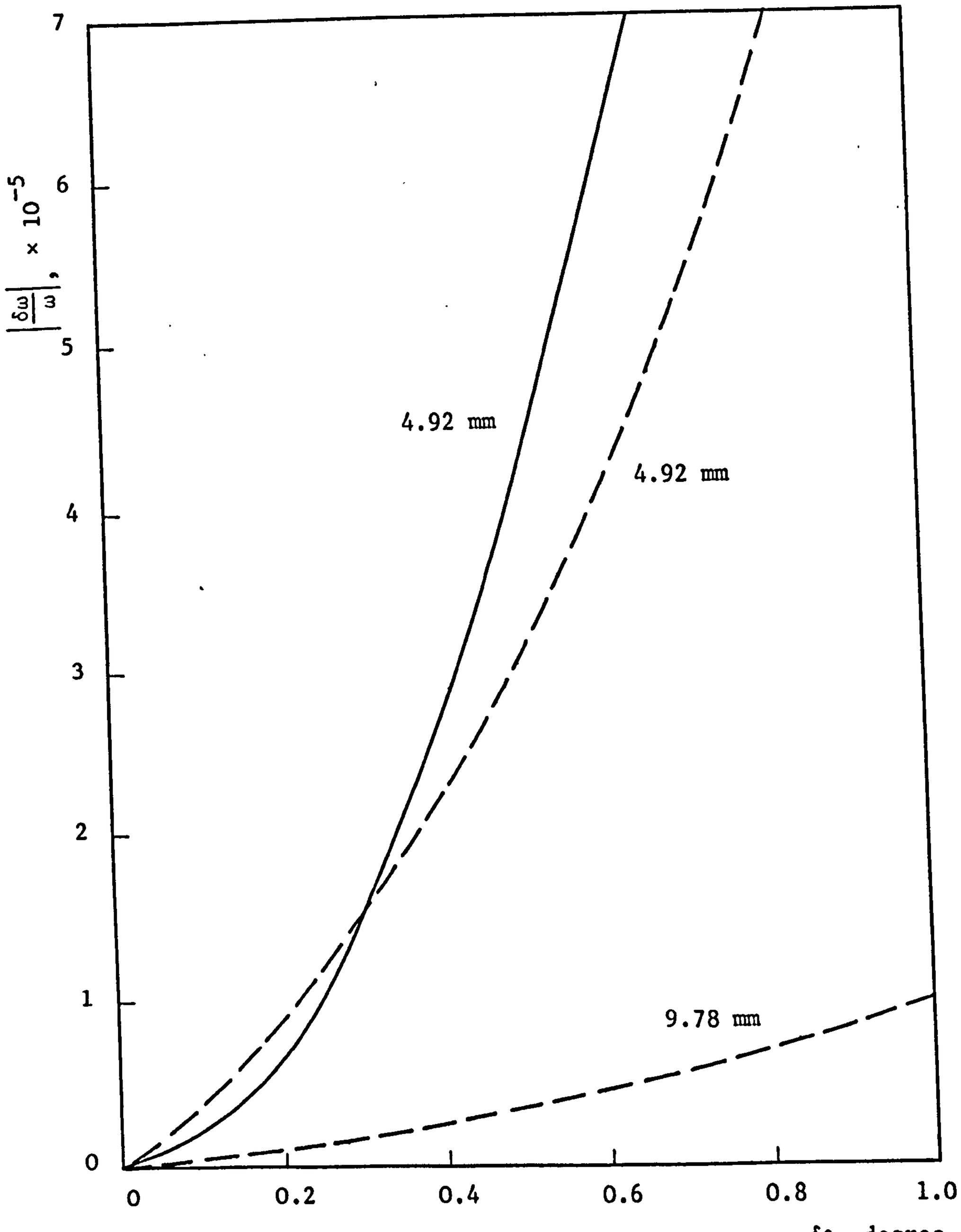

FIG. 8.4 Variation of $\left|\frac{\delta\omega}{\omega}\right|$ with $\delta\theta$

D = 70.1124 cm, f ≈ 9.5 GHz

——————— Symmetrical mode

— — — — Asymmetrical mode

8.2 Errors in Measured Loss Tangent

Since the accuracy in measuring loss tangent is not so high as that in measuring dielectric constant, small errors in measured resonant frequency, separation between the mirrors and the thickness of the dielectric sheet have little effect on the loss tangent results.

In Figs. 8.5 and 8.6, the experimental curves of the variation of $\frac{\delta Q_L}{Q_L}$ with the axial displacement $\delta\ell$ and with the angle of tilt $\delta\theta$ are shown for polystyrene sheets. It is observed that Q_L is nearly constant for small values of $\delta\ell$ and $\delta\theta$. As the loss tangent is proportional to $(1/Q_L - 1/Q_o)$, the errors in tanδ so introduced are extremely small.

The measured loss tangent has errors which are inherent in those involved in the measurement of Q. Thus the precision to which Q is measured determines the accuracy of the loss tangent.

8.3 Accuracy

The resonant frequency and the mirror separation can be measured to an accuracy of better than 1 part in 10^6, and variations in dielectric sheet thickness can be controlled to 1 part in 10^4. When the dielectric constant is obtained by solving the transcendental equation, the errors in ε_r due to these deviations amount to 2 parts in 10^4. Another probable source of error comes from the resonator theory used in which the second derivative $\frac{\partial^2\psi}{\partial z^2}$ has been neglected, by assuming $k^2 w_o^2 >> 1$, when deriving the beam wave equation (3.3). Judging from the high precision of the experimental results, the error due to this source is quite small. It is on these results that an accuracy of ±0.25% is claimed.

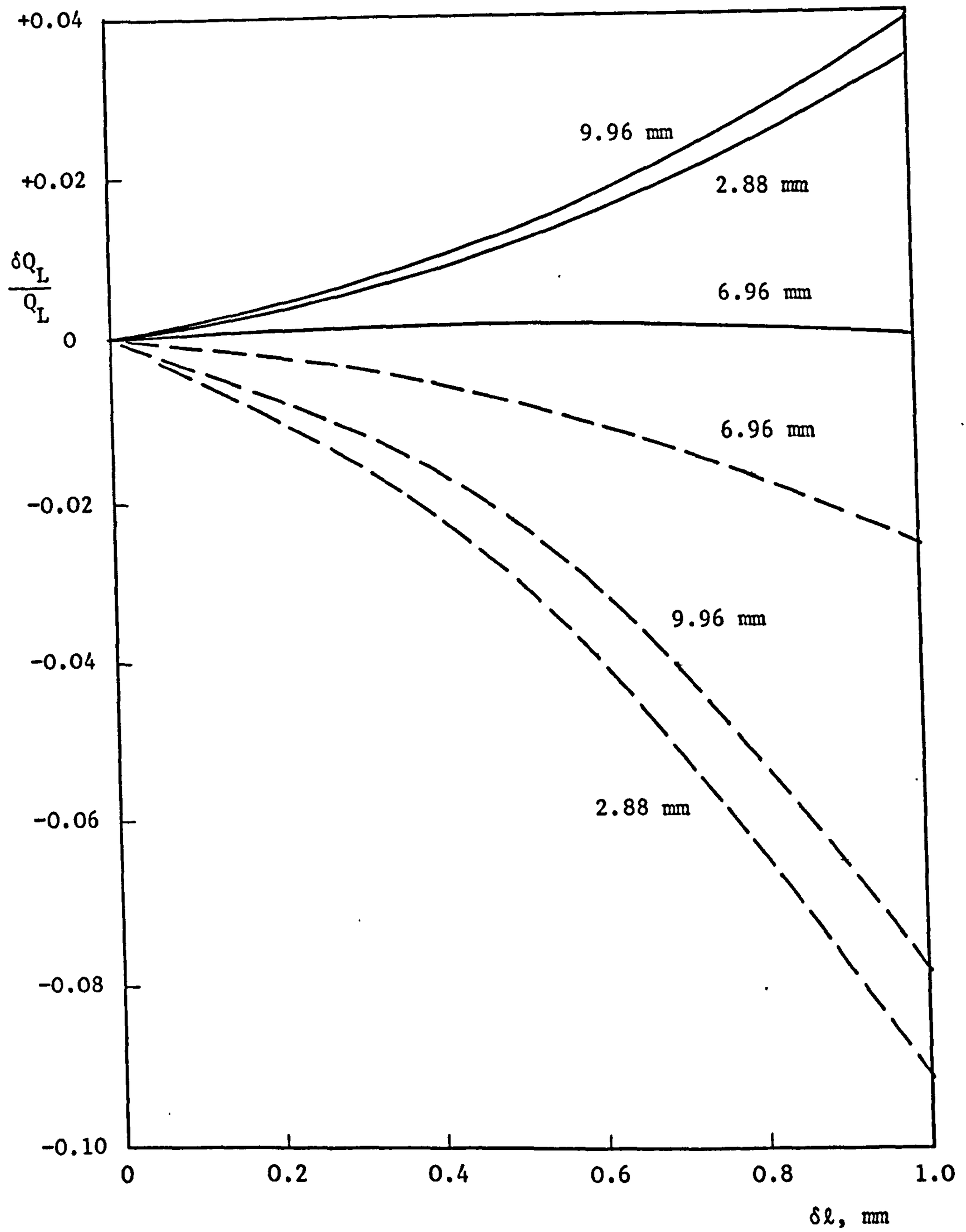

FIG. 8.5 Variation of $\delta Q_L/Q_L$ with $\delta\ell$

D = 70.1124 cm, f ≃ 9.5 GHz

———— Symmetrical mode

— — — — Asymmetrical mode

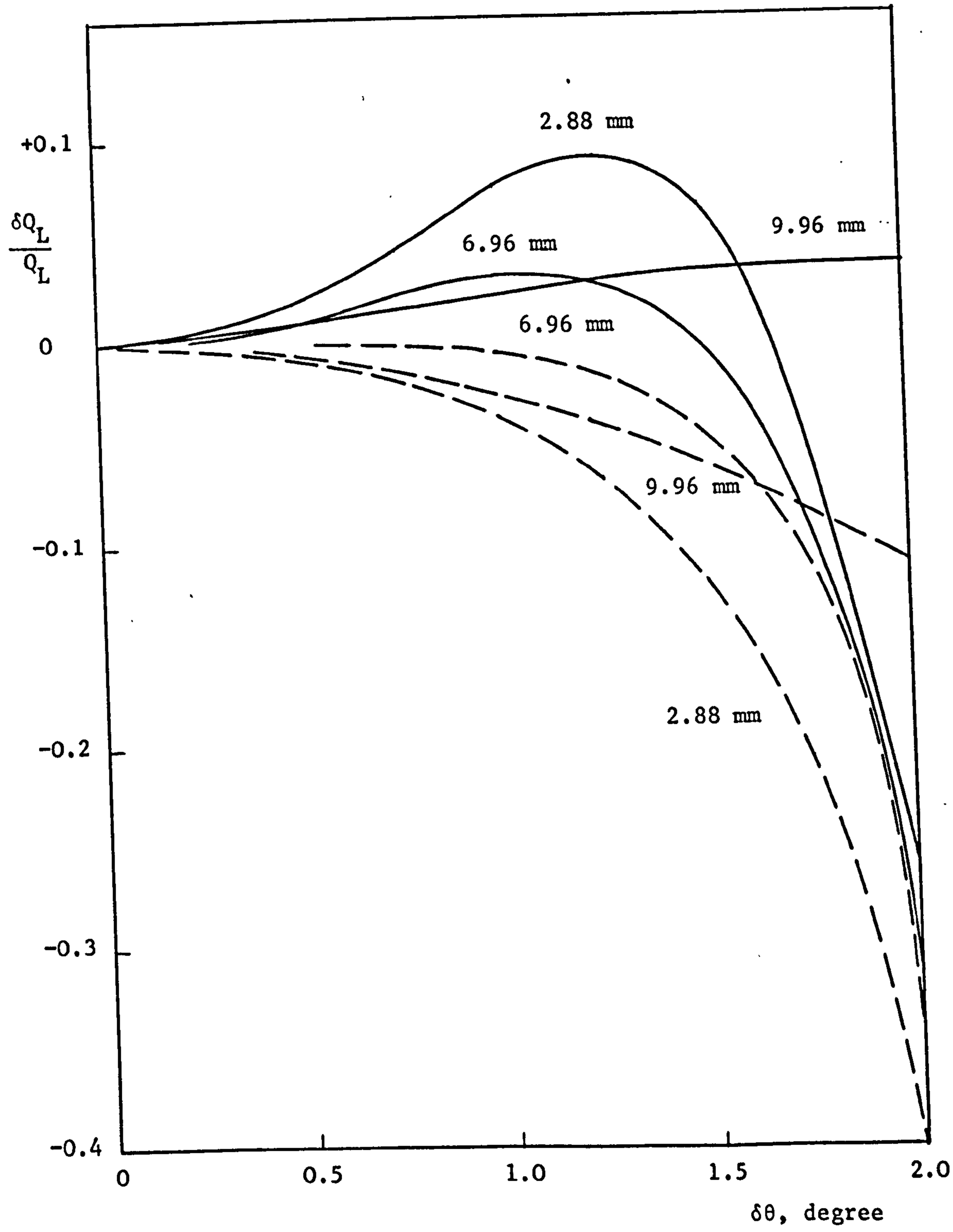

FIG. 8.6 Variation of Q_L/Q_L with δθ

D = 70.1124 cm, f ≈ 9.5 GHz

———— Symmetrical mode

—·—·— Asymmetrical mode

When the approximate formulas are used to determine the dielectric constant, the errors in the result depend on the thickness of the dielectric sheet. Provided samples of nearly an integral number of half wavelengths thick are avoided, the accuracy of this method is estimated to be ±0.5%.

The accuracy of the loss tangent measurement is limited by the accuracy of the Q measurements. The loss tangent results for perspex sheets are quite satisfactory. This is because Q_L, having a value of around 5,000, was low enough to be measured quite accurately by using the bandwidth method. Poor loss tangent results for polystyrene sheets were due to inaccurate Q_L measurements which were in turn due to the high input noise level of the wide-band amplifier affecting the sharpness of the energy decay curve on the oscilloscope. As it is difficult to read the oscilloscope trace to better than 10%, the accuracy of the loss tangent measurement for low-loss materials is estimated to be about ±10%. For high-loss materials, the accuracy of the method is about ±5%.

CHAPTER 9

CONCLUSIONS

A method for measuring dielectric constants and loss tangents of both low-loss and high-loss materials in sheet form has been described and has been found very satisfactory at X-band frequencies. It could also be used at higher frequencies and would give more accurate results owing to the increase of the factor $k^2w_o^2$ which is required to be much bigger than one in the theory.

By measuring the resonant frequencies of the perturbed and the unperturbed resonator, it was possible to measure the dielectric constant of polystyrene and perspex quite accurately. The dielectric constant deduced from the transcendental equation for symmetrical mode and that deduced from the approximate formulas are probably accurate to within ±0.25% and ±0.5% respectively. In the latter case, the accuracy reduces as the thickness of the sample approaches a multiple of half wavelengths. The accuracy of the loss tangent measurement is estimated to be about ±10%.

The principal advantages and disadvantages of the method are as follows.

Advantages of the method

(i) This method is applicable to the measurements of both low-loss and high-loss materials and becomes more accurate at higher frequencies.

(ii) The experimental procedures are simple and straight forward involving no mechanical movement of any part of the resonator.

(iii) When the dielectric constant is determined by using the approximate formulas, its accuracy is comparatively unaffacted by the error in the measured thickness of the sample.

(iv) The dimensions of the sample do not need to have any specified values, as long as its surface area is bigger than that of the mirrors.

(v) The sample can be inserted and removed from the resonator easily.

Disadvantages of the method

(i) When the approximate formulas are used for the determination of the dielectric constant, a reduction in precision occurs for certain unfavourable ranges of sample thickness.

(ii) In order to obtain accurate results, variations in sample thickness must be accurately controlled.

(iii) Relatively large sample is required.

To obtain increased accuracy a number of lines of attack are possible. Besides increasing the operating frequencies, the accuracy of the dielectric constant measurement could be improved by using mirrors of larger radius of curvature at shorter distance of separation. The assumed condition $k^2w_o^2 >> 1$ would then be more justifiable and the error in the dielectric constant due to the deviation in the measured frequency would be reduced.

The accuracy of the loss tangent measurement depends on the precision to which Q is measured. The latter could be improved by employing more elaborate instrumentation, including the use of a

stabilized oscillator system, a crystal detector with flat frequency response and high sensitivity, and a wide-band amplifier with very low input noise level, for measuring Q.

The flexibility of the open resonator method is very great. With improved instrumentation for measuring Q and by reducing further losses due to metal absorption and coupling to maximize the Q of the empty resonator, very low-loss materials having loss tangent of the order of 10^{-5} could be measured.

APPENDIX I

CONDITION FOR NEGLECTING THE SECOND DERIVATIVE

The condition for neglecting the second derivative $\frac{\partial^2\psi}{\partial z^2}$ in the beam wave equation (3.3) can be obtained by comparing it with the term $2jk\frac{\partial\psi}{\partial z}$.

Consider first the derivatives

$$\frac{\partial}{\partial z}\left(\frac{1}{R}\right) = -\frac{1}{R^2}\frac{\partial}{\partial z}\left[z\left\{1 + \left(\frac{kw_o^2}{2z}\right)^2\right\}\right] = \frac{4}{k^2w_o^2} - \frac{1}{R^2} \tag{I.1}$$

$$\frac{\partial\Phi}{\partial z} = \frac{\partial}{\partial z}\left\{\tan^{-1}\left(\frac{2z}{kw_o^2}\right)\right\} = \frac{2}{kw_o^2} \tag{I.2}$$

$$\frac{\partial w^2}{\partial z} = \frac{\partial}{\partial z}\left[w_o^2\left\{1 + \left(\frac{2z}{kw_o^2}\right)^2\right\}\right] = \frac{8z}{k^2w_o^2} = \frac{2w^2}{R} \tag{I.3}$$

$$\frac{\partial w}{\partial z} = \frac{1}{2w}\frac{\partial w^2}{\partial z} = \frac{w}{R} \tag{I.4}$$

$$\frac{\partial}{\partial z}\left(\frac{1}{w}\right) = -\frac{1}{w^2}\frac{\partial w}{\partial z} = -\frac{1}{wR} \tag{I.5}$$

$$\frac{\partial}{\partial z}\left(\frac{1}{w^2}\right) = -\frac{2}{w^3}\frac{\partial w}{\partial z} = -\frac{2}{w^2R} \tag{I.6}$$

where w, R and Φ are given in (3.6), (3.7) and (3.8).

Let

$$g = \frac{1}{w^2} + \frac{jk}{2R} = \frac{1}{w_o w}\exp(j\Phi) \tag{I.7}$$

then

$$\frac{\partial g}{\partial z} = \frac{\partial}{\partial z}\left\{\frac{1}{w_o w}\exp(j\Phi)\right\} = \frac{2jg^2}{k} \tag{I.8}$$

Equation (3.4) can then be written as

$$\psi = \frac{w_o}{w} \exp(-gr^2 + j\Phi) \tag{I.9}$$

The first derivative of ψ is

$$\frac{\partial\psi}{\partial z} = \frac{1}{2jk} (4g^2r^2 - 4g)\psi \tag{I.10}$$

The second derivative of ψ is

$$\frac{\partial^2\psi}{\partial z^2} = \frac{4g^2}{k^2} (-g^2r^4 + 4gr^2 - 2)\psi \tag{I.11}$$

Using (I.7), (I.10) and (I.11) can be written as

$$2jk\frac{\partial\psi}{\partial z} = -4\left[\frac{1}{w_o w}\exp(j\Phi) - \frac{r^2}{w_o^2 w^2} \exp(j2\Phi)\right]\psi \tag{I.12}$$

$$\frac{\partial^2\psi}{\partial z^2} = -\frac{4}{k^2 w_o w}\left[\frac{2}{w_o w} \exp(j2\Phi) - \frac{4r^2}{w_o^2 w^2} \exp(j3\Phi) + \frac{r^4}{w_o^3 w^3} \exp(j4\Phi)\right]\psi \tag{I.13}$$

In order that the second derivative $\frac{\partial^2\psi}{\partial z^2}$ is negligible in comparison with $2jk\frac{\partial\psi}{\partial z}$, we must have

$$k^2 w_o^2 >> 1 \tag{I.14}$$

This is the condition required.

APPENDIX II

COMPUTER PROGRAMMES

```
//JOB              USER=IX4,TIME=50,PAGES=50
C
C
C                  CALCULATION OF DIELECTRIC CONSTANT BY
C                  SOLVING A TRANSCENDENTAL EQUATION
C
C
C                  F0  K0  YL
C
      REAL K4, K5, K, KWTSG, KNTSG, K1
      COMMON B, D, T, K4, K5
      EXTERNAL FCT1, FCT2
      READ (5,1000) LIMT, LINE
 1000 FORMAT (2I10)
      DO 30 I = 1, LIMT
      READ (5,1001) DD, TT
 1001 FORMAT (2F10.0)
      WRITE (6,1002) DD, TT
 1002 FORMAT (/2X,'DD =',F10.6, 3X, 'CM', 6X, 'TT =',F10.6, 3X, 'CM'//
     1     3X, 'F1 (GHZ)', 3X, 'F2 (GHZ)', 8X, 'TSR', 15X, 'E', 15X, 'N',
     2       13X, 'EPSILON 1', 8X, 'EPSILON 2'/)
      T = TT / 2.
      D = DD / 2. - T
      DO 30 J = 1, LIMF
      READ (5, 1004) FA, FS
 1004 FORMAT (2F10.0)
      KA = 6.28318 * FA / 29.979
      KS = 6.28318 * FS / 29.979
      F = 127.
      CALL RTMI (1., F, FCT1, 1.E-3, 2.E-3, 1.E-5, 200, IER)
      EPS = N ** 2
      WRITE (6,1003) FA,      IER, F, N, EPS
 1003 FORMAT (1F16.5,22X, I4, 5X, 1PE16.6)
      CALL RTMI (1., F, FCT2, 1.E-3, 2.E-3, 1.0E-5, 200, IER)
      EPS = N ** 2
      WRITE (6,1004)      FS, IER, F, N, EPS
 1004 FORMAT (16X,F16.4,5X,I4,5X, 1PE16.5, 16X, 1PE16.5)
      K1 = KS - KA
      PHIDA = ATAN(SQRT(D / (R - D)))
      A = K4 * D - PHIDA
      C = K5 * D - PHIDA
      EPS = COS(A) * COS(C) / (K1 * T * SIN(K1 * D) - SIN(A) * SIN(C))
      WRITE (6, 1007) EPS
 1007 FORMAT (112X, 1PE16.6)
   30 CONTINUE
      STOP
      END
```

```
      FUNCTION FCT1(N)
      REAL K1, N, KW**2
      COMMON R, D, T, K1, K2
      TDN = T / N
      TDN2 = TDN / N
      KW**2 = 2.0*SQRT((R - D - TDN2) * (D + TDN2))
      PHIT = ATAN(2.0 * TDN / KW**2)
      PHID = ATAN((D + TDN2) * 2.0 / KW**2) - ATAN(2.0 * TDN2/KW**2)
      FCT1 = 1 / TAN(N * K1 * T - PHIT) + 1.0 / TAN(K1 * D - PHID)
      RETURN
      END
```

```
      FUNCTION FCT2(N)
      REAL KS, N, KWOSQ
      COMMON T, D, T, KA, KS
      TON = T / N
      TONSQ = TON / N
      KWOSQ = 2.0*SQRT((S - D  - TONSQ) * (D  + TONSQ))
      PHIT = ATAN(T / (2.0 * TON / KWOSQ)
      PHID = ATAN((D + TONSQ) * 2.0 / KWOSQ) - ATAN(2.0 * TONSQ/KWOSQ)
      FCT2 = 1.0 / TAN(1. * KS * T - PHIT) - N * TAN(KS * D - PHID)
      RETURN
      END
```

```
      SUBROUTINE RTMI(X,F,FCT,XLI,XRI,EPS,IEND,IER)
C
C
C     PREPARE ITERATION
      IER=0
      XL=XLI
      XR=XRI
      X=XL
      TOL=X
      F=FCT(TOL)
      IF(F)1,15,1
    1 FL=F
      X=XR
      TOL=X
      F=FCT(TOL)
      IF(F)2,15,2
    2 FR=F
      IF(SIGN(1.,FL)+SIGN(1.,FR))25,3,25
C
C     BASIC ASSUMPTION FLFR LESS THAN 0 IS SATISFIED.
C     GENERATE TOLERANCE FOR FUNCTION VALUES.
    3 I=0
      TOLF=10.**EPS
C
C
C     START ITERATION LOOP
    4 I=I+1
C
C     START BISECTION LOOP
      DO 13 K=1,IEND
      X=.5*(XL+XR)
      TOL=X
      F=FCT(TOL)
      IF(F)5,15,5
    5 IF(SIGN(1.,F)+SIGN(1.,FR))7,6,7
C
C     INTERCHANGE XL AND XR IN ORDER TO GET THE SAME SIGN IN F AND FR
    6 TOL=XL
      XL=XR
      XR=TOL
      TOL=FL
      FL=FR
      FR=TOL
    7 TOL=F-FL
      A=F*TOL
      A=A+A
      IF(A-FR*(FR-FL))9,9,9
    8 IF(I-IEND)13,13,9
    9 XR=X
      FR=F
C
C     TEST ON SATISFACTORY ACCURACY IN BISECTION LOOP
      TOL=EPS
      A=ABS(XR)
      IF(A-1.)11,11,10
   10 TOL=TOL*A
```

```
      11 IF(ABS(X2-XL)-TOL)12,12,13
      12 IF(ABS(F2-FL)-TOLF)14,14,13
      13 CONTINUE
C        END OF BISECTION LOOP
C
C        NO CONVERGENCE AFTER IEND ITERATION STEPS FOLLOWED BY IEND
C        SUCCESSIVE STEPS OF BISECTION OR STRICTLY INCREASING FUNCTION
C        VALUES AT RIGHT BOUNDS. ERROR RETURN.
         IER=1
      14 IF(ABS(FR)-ABS(FL))16,16,15
      15 X=XL
         F=FL
      16 RETURN
C
C        COMPUTATION OF ITERATED X-VALUE BY INVERSE PARABOLIC INTERPOLATION
      17 A=FR-F
         DX=(X-XL)*FL*(1.+FR*(F-TOL)/(A*(FR-FL)))/TOL
         XM=X
         FM=F
         X=XL-DX
         TOL=X
         F=FCT(TOL)
         IF(F)18,16,18
C
C        TEST ON SATISFACTORY ACCURACY IN ITERATION LOOP
      18 TOL=EPS
         A=ABS(X)
         IF(A-1.)20,20,19
      19 TOL=TOL*A
      20 IF(ABS(DX)-TOL)21,21,22
      21 IF(ABS(F)-TOLF)16,16,22
C
C        PREPARATION OF NEXT BISECTION LOOP
      22 IF(SIGN(1.,F)+SIGN(1.,FL))24,23,24
      23 XR=X
         FR=F
         GO TO 4
      24 XL=X
         FL=F
         XR=XM
         FR=FM
         GO TO 4
C        END OF ITERATION LOOP
C
C
C        ERROR RETURN IN CASE OF WRONG INPUT DATA
      25 IER=2
         RETURN
         END

*ENTRY
```

```
//JOB             UCEE01X7,TIME=60,PAGES=50
C
C
C
C               CALCULATION OF DIELECTRIC CONSTANT BY SOLVING
C               TWO TRANSCENDENTAL EQUATIONS FOR N AND D
C
C
C               P. K. YU
C
      IMPLICIT REAL*8(A-H, O-Z)
      REAL*8 KA, KS, N
      COMMON B, T, KA, KS
      DIMENSION X(2), E(2)
      PI = 3.14159265D0
      CC = 29.9792500
      DO 30 I = 1, 93
      READ (5, 100) FA, FS, DD, TT
  100 FORMAT (4F10.0)
      T = TT / 2.
      D = DD / 2. - T
      KA = 2. * PI * FA / CC
      KS = 2. * PI * FS / CC
      F = 127.
      ESCALE = 1000.
      IPRINT = 2
      ICON = 1
      MAXIT = 50
      N = 1.6
      X(1) = N
      X(2) = D
      F(1) = 1.D-4
      F(2) = 1.D-4
      CALL M4D4A (X, E, 2, F, ESCALE, IPRINT, ICON, MAXIT)
      EPS = X(1) ** 2
      DDD = 2. * (X(2) + T)
      WRITE (6, 300) EPS, DDD, DD, TT, FA, FS
  300 FORMAT (/2X, 'EPSILON =', 1PD14.6, 2X, 'DDD =', 1PD14.6, 2X,
     1      'DD =', 1PD14.6, 2X, 'TT =', 1PD14.6, 2X, 'FA =', 1PD14.6,
     2       2X, 'FS =', 1PD14.6/)
   30 CONTINUE
      STOP
      END
```

```
      SUBROUTINE CALCFX (M, X, F)
      IMPLICIT REAL*8(A-H, O-Z)
      REAL*8 KA, KS, I, KWOSQ
      COMMON R, T, KA, KS
      SQRT(X) = DSQRT(X)
      ATAN(X) = DATAN(X)
      TAN(X) = DTAN(X)
      DIMENSION X(2)
      N = X(1)
      D = X(2)
      TON = T / N
      TONSQ = TON / N
      KWOSQ = 2. * SQRT((R - D - TONSQ) * (D + TONSQ))
      PHIT = ATAN(2. * TON / KWOSQ)
      PHID = ATAN((D + TONSQ) * 2. / KWOSQ) - ATAN(2. * TONSQ / KWOSQ)
      FCT1 = N / TAN(N * KA * T - PHIT) + 1. / TAN(KA * D - PHID)
      FCT2 = 1. / TAN(N * KS * T - PHIT) - N * TAN(KS * D - PHID)
      F = FCT1 ** 2 + FCT2 ** 2
      RETURN
      END
```

```
      SUBROUTINE VA04A(X,E,N,F,ESCALE,IPRINT,ICON,MAXIT)
      IMPLICIT REAL*8 (A-H,O-Z)
      REAL*8 DMIN1,DMAX1
      DIMENSION W(2000),X(40),E(40)
      ABS(X)=DABS(X)
      SQRT(X)=DSQRT(X)
      SIGN(X,Y)=DSIGN(X,Y)
      DDMAG=0.1D0*ESCALE
      SCER=0.05D0/ESCALE
      JJ=N*N+1
      JJJ=JJ+N
      K=N+1
      NFCC=1
      ITD=1
      ITN=1
      DO 1 I=1,N
      DO 2 J=1,N
      W(K)=0.0D0
      IF(I-J)4,3,4
    3 W(K)=ABS(E(I))
      W(I)=ESCALE
    4 K=K+1
    2 CONTINUE
    1 CONTINUE
      ITERC=1
      ISCRAD=2
      CALL CALCFX(N,X,F)
      FKEEP=ABS(F)+ABS(F)
    5 ITONE=1
      FF=F
      SUM=0.0D0
      IXP=JJ
      DO 6 I=1,N
      IXP=IXP+1
      W(IXP)=X(I)
    6 CONTINUE
      IDIRN=N+1
      ILINE=1
    7 DMAX=W(ILINE)
      DACC=DMAX*SCER
      DMAG=DMIN1(DDMAG,0.1*DMAX)
      DMAG=DMAX1(DMAG,20.*DACC)
      DLMAX=10.0D0*DMAG
      GO TO (70,70,71),ITONE
   70 DL=0.0D0
      D=DMAG
      FFREV=F
      IS=5
      FA=F
      DA=DL
    8 DD=D-DL
      DL=D
   58 K=IDIRN
      DO 9 I=1,N
      X(I)=X(I)+DD*W(K)
      K=K+1
```

```
      9 CONTINUE
        CALL CALCFX(N,X,F)
        NFCC=NFCC+1
        GO TO (10,11,12,13,14,96),IS
     14 IF(F-FA)15,16,24
     16 IF(ABS(D)-DMAX)17,17,18
     17 D=F+D
        GO TO 8
     18 PRINT 19
     19 FORMAT(5X,44HVALUE OF MAXIMUM CHANGE DOES NOT ALTER FUNCTION)
        GO TO 20
     15 FB=F
        DB=D
        GO TO 21
     24 FB=FA
        DB=DA
        FA=F
        DA=D
     21 GO TO (83,23),ISGRAD
     23 D=DA+DB-DA
        IS=1
        GO TO 8
     83 D=0.5D0*(DA+DB-(FA-FB)/(DA-DB))
        IS=4
        IF((DA-D)*(D-DB))25,8,8
     25 IS=1
        IF(ABS(D-DA)-DDMAX) 8,8,26
     26 D=DB+SIGN(DDMAX,DA-DA)
        IS=1
        DDMAX=DDMAX+DDMAX
        DDMAG=DDMAG+DDMAG
        IF(DDMAX-DMAX)8,8,27
     27 DDMAX=DMAX
        GO TO 8
     13 IF(F-FA)28,23,23
     28 FC=FB
        DC=DB
     29 FB=F
        DB=D
        GO TO 30
     12 IF(F-FB)28,28,31
     31 FA=F
        DA=D
        GO TO 30
     11 IF(F-FB)32,10,10
     32 FA=FB
        DA=DB
        GO TO 29
     71 DA=1.0D0
        DDMAX=5.0D0
        FA=FB
        DA=-1.0D0
        FB=FHOLD
        DB=0.0D0
        D=1.0D0
     10 FC=F
```

```
      DC=D
   30 A=(DB-DC)*(FA-FC)
      B=(DC-DA)*(FB-FC)
      IF((A+B)*(DA-DC))33,33,34
   33 FA=FB
      DA=DB
      FB=FC
      DB=DC
      GO TO 25
   34 D=(.500*(A*(DB+DC)+B*(DA+DC))/(A+B)
      DI=DB
      FI=FB
      IF(FB-FC)44,44,43
   43 DI=DC
      FI=FC
   44 GO TO (36,36,85),ITONE
   85 ITONE=2
      GO TO 45
   86 IF(ABS(D-DI)-DACC) 41,41,93
   93 IF(ABS(D-DI)-0.0300*ABS(D)) 41,41,45
   45 IF ((DA-DC)*(DC-D)) 47,46,46
   46 FA=FB
      DA=DB
      FB=FC
      DB=DC
      GO TO 25
   47 IS=2
      IF ((DB-D)*(D-DC)) 48,8,8
   48 IS=3
      GO TO 8
   41 F=FI
      D=DI-DL
      DD=SQRT((DC-DB)*(DC-DA)*(DA-DB)/(A+B))
      DO 49 I=1, N
      X(I)=X(I)+D*W(IDIRN)
      W(IDIRN)=DD*W(IDIRN)
      IDIRN=IDIRN+1
   49 CONTINUE
      W(ILINE)=W(ILINE)/DD
      ILINE=ILINE+1
      IF(IPRINT-1)51,50,51
   50 PRINT 52,ITERC,NFCC,F,(X(I),I=1,N)
   52 FORMAT ( 1X,9HITERATION,I5,I15,16H FUNCTION VALUES,
     1 11(X,3HF =,G21.14,2G24.14))
      GO TO(51,53),IPRINT
   51 GO TO (55,38),ITONE
   55 IF (FPREV-F-SUM) 94,95,95
   95 SUM=FPREV-F
      JJ=ILINE
   94 IF (IDIRN-JJ) 7,7,84
   84 GO TO (92,72),IND
   92 FIELD=F
      IS=6
      IXP=JJ
      DO 59 I=1,N
      IXP=IXP+1
```

```
219           W(IXP)=X(I)-W(IXP)
220        50 CONTINUE
221           DD=1.0D0
222           GO TO 53
223        96 GO TO (112,37),IND
224       112 IF (FP-F) 37,37,91
225        91 D=2.0D0*(FP+F-2.0D0*FHOLD)/(FP-F)**2
226           IF (D*(FP-FHOLD-SUM)**2-SUM) 87,37,37
227        87 J=JIL*N+1
228           IF (J-JJ) 60,60,61
229        60 DO 62 I=J,JJ
230           K=I-N
231           W(K)=W(I)
232        62 CONTINUE
233           DO 97 I=JIL,N
234           W(I-1)=W(I)
235        97 CONTINUE
236        61 IDIRN=IDIRN-N
237           ITONE=3
238           K=IDIRN
239           IXP=JJ
240           AAA=0.0D0
241           DO 65 I=1,N
242           IXP=IXP+1
243           W(K)=W(IXP)
244           IF (AAA-ABS(W(K)/E(I))) 66,67,67
245        66 AAA=ABS(W(K)/E(I))
246        67 K=K+1
247        65 CONTINUE
248           DMAG=1.0D0
249           W(N)=ESCALE/AAA
250           ILINE=N
251           GO TO 7
252        37 IXP=JJ
253           AAA=0.0D0
254           F=FHOLD
255           DO 99 I=1,N
256           IXP=IXP+1
257           X(I)=X(I)-W(IXP)
258           IF (AAA*ABS(E(I))-ABS(W(IXP))) 98,99,99
259        98 AAA=ABS(W(IXP)/E(I))
260        99 CONTINUE
261           GO TO 72
262        38 AAA=AAA*(1.0D0+DI)
263           GO TO (72,106),IND
264        72 IF (IPRINT-2) 53,50,50
265        53 GO TO (109,88),IND
266       109 IF (AAA-0.1D0) 89,89,76
267        89 GO TO (20,116),ICON
268       116 IND=2
269           GO TO (100,101),INN
270       100 INN=2
271           K=JJJ
272           DO 102 I=1,N
273           K=K+1
274           W(K)=X(I)
```

```
      X(I)=X(I)+10.*E(I)
  102 CONTINUE
      FKEEP=F
      CALL CALCFX (N,X,F)
      NFCC=NFCC+1
      DDIAG=0.0D0
      GO TO 103
   76 IF (F-FF) 35,78,78
   78 PRINT 80
   80 FORMAT (5X,37HVA04A ACCURACY LIMITED BY ERRORS IN F)
      GO TO 20
   88 IPR=1
   35 DDIAG=0.4D0*SQRT(FP-F)
      ISCRAD=1
  108 ITERC=ITERC+1
      IF (ITERC-MAXIT) 5,5,81
   81 PRINT 82,MAXIT
   82 FORMAT(I5,30H ITERATIONS COMPLETED BY VA04A)
      IF (F-FKEEP) 20,20,110
  110 F=FKEEP
      DO 111 I=1,N
      JJJ=JJJ+1
      X(I)=W(JJJ)
  111 CONTINUE
      GO TO 20
  101 JIL=1
      FF=FKEEP
      IF (F-FKEEP) 105,78,104
  104 JIL=2
      FF=F
      F=FKEEP
  105 IXP=JJ
      DO 113 I=1,N
      IXP=IXP+1
      K=IXP+N
      GO TO (114,115),JIL
  114 W(IXP)=W(K)
      GO TO 113
  115 W(IXP)=X(I)
      X(I)=W(K)
  113 CONTINUE
      JIL=2
      GO TO 92
  106 IF (AA-0.1D0) 20,20,107
   20 RETURN
  107 IPR=1
      GO TO 35
      END

#ENTRY
```

REFERENCES

1. Degenford, J. E. and Colman, P. D.:'A quasi-optics perturbation technique for measuring dielectric constants', Proc. IEEE, 1966, 54, pp. 520-522.

2. Degenford, J. E.:'A quasi-optic technique for measuring dielectric loss tangents', IEEE Trans., 1968, IM-17, pp. 413-417.

3. Breeden, K. H. and Langley, J. B.:'Fabry-Perot cavity for dielectric measurements', The Review of Scientific Instruments, 1969, 40, pp. 1162-1163.

4. Yuba, Y., Ohota, I. and Makimoto, T.:'Measurement of complex dielectric constant by Fabry-Perot resonator', Electronics and Communications in Japan, 1967, 50, pp. 268-276.

5. Kogelnik, H. and Li, T.:'Laser beams and resonators', Proc. IEEE, 1966, 54, pp. 1312-1329.

6. Barlow, H. M. and Cullen, A. L.:'Microwave measurements' (Constable, 1966).

7. Sucher, M. and Fox, J.:'Handbook of microwave measurements' (Polytechnic Press, 1963), Vol. II.

8. Hershberger, W. D.:'Absorption of microwaves by gases. I', J. Appl. Phys., 1946, 17, p. 495.

9. Hershberger, W. D.:'Absorption of microwaves by gases. II', ibid., 1946, 17, p. 814.

10. Roberts, S. and Von Hippel, A. R.:'A new method for measuring dielectric constant and loss in the range of centimeter waves', ibid., 1946, 17, p. 610.

11. Surber, W. H., Jr. and Crough, G. E. Jr.:'Dielectric measurement methods for solids at microwave frequencies', ibid., 1948, 19, No. 12.

12. Redheffer, R. M., Wildman, R. C. and O'Gorman, V.:'The computation of dielectric constants', ibid., 1952, 23, No. 5.

13. Oliner, A. A. and Altschuler, H. M.:'Methods of measuring dielectric constants based upon a microwave network viewpoint', ibid., 1955, 26, No. 2.

14. Clarricoats, P. J. B.:'A new waveguide method for measuring permittivity', Proc. IEE, 1962, 109, pp. 858-862.

15. Bell, R. O. and Rupprecht, G.:'Measurement of small dielectric losses in material with a large dielectric constant at microwave frequencies', IRE Trans., 1961, MTT-9, p. 239.

16. Birnbaum, G. and Franean, J.:'Measurement of the dielectric constant and loss of solids and liquids by a cavity perturbation method', (letter), J. Appl. Phys., 1949, 20, No. 8.

17. Saito, S.:'Measurement at 9,000 mc of the dielectric constant of air containing various quantities of water vapor', (letter), Proc. IRE, 1955, 43, No. 8.

18. Horner, F., Taylor, T. A., Dunsmuir, R., Lamb, J. and Jackson, W.: 'Resonance methods of dielectric measurement at centimetre wavelengths', Journal IEE, 1946, 93, Part III, p. 53.

19. Lamb, J.:'Dielectric measurement at wavelengths around 1 cm by means of an H_{o1} cylindrical-cavity resonator', ibid., 1946, 93, Part IIIA, p. 1447.

20. Penrose, R. P.:'Some measurements of the permittivity and power factor of low loss solids at 25,000 Mc/s', Symposium on dielectrics, The Faraday Society, 1946, p. 108.

21. Sinha, J. K. and Brown, J.:'A new cavity-resonator method for measuring permittivity', Proc. IEE, 1960, 107B, p. 522.

22. Bethe, H. A. and Schwinger, J.:'Perturbation theory for cavities', N.R.D.C. Report DI-117, Radiation Laboratory, MIT (march 1943).

23. Casimir, H. B. G.:'On the theory of electromagnetic waves in resonant cavities', Philips Research Reports, 1951, 6, p. 162.

24. Hakki, B. W. and Coleman, P. D.:'A dielectric resonator method of measuring inductive capacities in the millimeter range', IRE Trans., 1960, MTT-8, pp. 402-410.

25. Culshaw, W. and Anderson, M. V.:'Measurement of permittivity and dielectric loss with a millimetre-wave Fabry-Perot interferometer', Proc. IEE, 1962, 109, Part B supplement No. 23, pp. 820-826.

26. Dicke, R. H.:'Molecular amplification and generation systems and methods', U. S. Patent 2851652, 1958.

27. Prokhorov, A. M.:'Molecular amplifier and generator for sub-millimetre waves', JETP (USSR), 1958, 34, pp. 1658-1659; Sov. Phys. JETP, 1958, 7, pp. 1140-1141.

28. Schawlow, A. L. and Townes, C. H.,:'Infrared and optical masers', Phys. Rev., 1958, 29, pp. 1940-1949.

29. Fox, A. G. and Li, T.:'Resonant modes in an optical maser', Proc. IRE (Correspondence), 1960, 48, pp. 1904-1905; 'Resonant modes in a maser interferometer', Bell Sys. Tech. J., 1961, 40, pp. 453-488.

30. Boyd, G. D. and Gordon, J. P.:'Confocal multimode resonator for millimeter through optical wavelength masers', ibid., 1961, 40, pp. 489-508.

31. Boyd, G. D. and Kogelnik, H.:'Generalized confocal resonator theory', Bell Sys. Tech. J., 1962, 41, pp. 1347-1369.

32. Goubau, G. and Schwering, F.:'On the guided propagation of electromagnetic wave beams', IRE Trans., 1961, AP-9, pp. 248-256.

33. McCumber, D. E.:'Eigenmodes of a symmetrical cylindrical confocal laser resonator and their perturbation by output-coupling apertures', Bell Sys. Tech. J., 1965, 44, pp. 333-363.

34. IBM System/360 Scientific Subroutine Package (360-CM-03X) Version III Programmer's Manual, 1968.

35. Powell, M. J. D.: Computer Journal, 1964, 7, pp. 135-162.

36. Morse, P. M. and Feshbach, H.:'Methods of theoretical physics', Part I, p. 785.

37. Cullen, A. L. and Kumar, A.:'The absolute determination of extinction cross-sections by the use of an open resonator', Proc. Roy. Soc. Lond., 1970, A. 315, pp.217-230.

38. Von Hippel, A. R.:'Dielectric materials and applications' (Wiley, 1954).